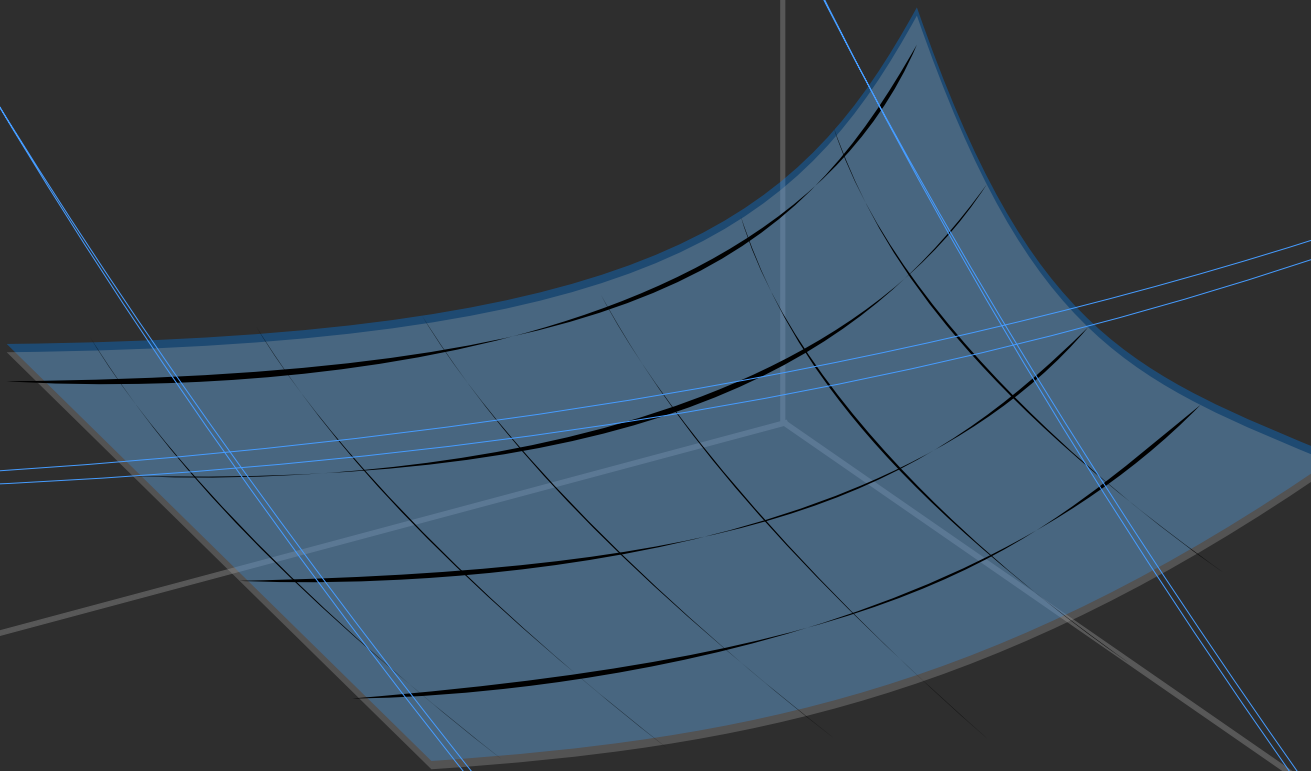


Mathematical Modelling of the Hydrolysis

Process of Waste Activated Sludge in a Novel

Cascade System



GRADUATION REPORT

Master of Science in Environmental Engineering

Mathematical Modelling of the Hydrolysis Process of Waste Activated Sludge in a Novel Cascade System

by Sebastian Jérôme Durry, 4920767

Daily Supervisor:

Dr.ir Hongxiao Guo

Main Supervisor:

Prof.dr.ir Jules van Lier

Thesis Committee:

Prof.dr.ir Jules van Lier (Chair, TU Delft)

Prof.dr.ir Merle de Kreuk (TU Delft)

Assoc. prof.dr.ir. Robbert Kleerebezem (TU Delft)

Dr.ir Hongxiao Guo (TU Delft)

Dr.ir André Visser (Royal Haskoning DHV)

A thesis submitted in fulfilment of the requirements
for the degree of Master of Science in Environmental Engineering at the
Faculty of Civil Engineering and Geosciences, Sanitary Engineering Research Group,
Department of Water Management

15 April 2022



DECLARATION OF AUTHORSHIP

I, Sebastian Jérôme DURRY, declare that this thesis titled, “Mathematical Modelling of the Hydrolysis Process of Waste Activated Sludge in a Novel Cascade System” and the work presented in it are my own. I confirm that:

- This work was done wholly in candidature for a research degree at Technical University Delft.
- Where any part of this thesis has previously been submitted for a degree or any other qualification at this University or any other institution, this has been clearly stated.
- Where I have consulted the published work of others, this is always clearly attributed.
- Where I have quoted from the work of others, the source is always given. With the exception of such quotations, this thesis is entirely my own work.
- I have acknowledged all main sources of help.
- Where the thesis is based on work done by myself jointly with others, I have made clear exactly what was done by others and what I have contributed myself.



Sebastian Durry

Delft, 15 April 2022

ACKNOWLEDGEMENTS

The last year of my thesis has been a rollercoaster with countless lessons on a professional and personal level. This report would not have been written without all the support and constructive feedback that I received. Therefore, I would like to thank all people that helped me graduate and conduct my research.

Firstly, I would like to thank my main Supervisors, namely my daily supervisor Dr.ir. Hongxiao Guo for the motivation and support that he gave me during the first months of the project. The close supervision changed half-way through the project to Prof.dr.ir. Jules van Lier (chair of committee) and Prof.dr.ir. Merle de Kreuk. Thank you for your sympathies and the time you invested in so many meetings to bring me back on track.

Furthermore, I would like to thank the committee members Robbert Kleerebezem and André Visser (Royal Haskoning DHV) for their honest interest and participation and their constructive feedback. Your feedback helped me to see my work in the bigger picture and to stay critical.

This work would not have been finalized without the emotional support of my family and friends. I would like to thank my parents Gaby and Roger for their warmth and constant support throughout my study years, supporting me during all my decisions. Thanks also go to my older brother Philipp who manages so well to cheer me up and makes me see more clearly when I am stressed. I am grateful to have such a kind and empathetic family.

Many warm thanks go to my good friends Manu and Kinan who made me feel like having family also in the Netherlands. Furthermore, I would like to thank my good friend Rob for all the uplifting bouldering sessions we had, and my friends and roommates Jon and Stijn for pulling through the pandemic times together. Our discussions and house evenings helped me to keep the spirits up during the difficult period of isolation. The same is true for my friends Ben, Floor, Roos and Jet who taught me the Dutch way of living in South Africa. Thanks also go to Zoe for constantly trying to keep me motivated. Also, it is good to have a fellow German to share all the struggles and speak your mother tongue with.

Special thanks, go to my beloved partner Katharina who helped me so much during this last year of my studies. Without you this report would not have been finished. Thank you for always believing in me and being so open-hearted.

Sebastian Durry

Delft, 15 April 2022

iii

ABSTRACT

The hydrolysis of sludge solids especially for difficultly degradable sludges such as WAS is not fully understood, yet. The first-order hydrolysis rate was shown to function well for most easily degradable sludges and soluble substrates. This description for substrate hydrolysis in the context of anaerobic digestion has the benefit of being very simple and therefore applicable for many engineering applications where little data is available. On the other hand, in the last decades many studies reported that the first-order hydrolysis would need a modification to better describe the degradation of difficultly degradable solids. Guo et al. (2021) developed a cascade system for anaerobic digestion of WAS that does not seem to follow first-order hydrolysis kinetics when lowering the applied SRTs from 22 to 15 and 12 days, respectively. Based on observations by Guo et al. (2021) and a statistical analysis of the cascade system performed in the study at hand it seems that the first order hydrolysis rate constant is in fact a coefficient and that the first-order hydrolysis rate is not solely dependent on sludge characteristics and substrate concentrations. This hypothesis is tested in the thesis at hand. In Guo et al.'s study the cascade system was always compared to a reference system. To test this hypothesis and understand the kinetics of the cascade system in more detail a statistical analysis was performed for both systems from which an empirical hydrolysis model was derived. This model was implemented in ADM1 to replace the existing hydrolysis rate expression and was tested for the mentioned cascade system and the reference system. The empirical model was compared to the results of the standard ADM1 which uses a first-order hydrolysis expression. The empirical model assumed a dependency of the hydrolysis rate based on load and residence time along the cascade system to achieve a change in hydrolysis rate coefficients along the cascade system. The models were compared based on visual inspection and quantitative analysis of the simulated results. Both models showed low R^2 values which is likely due to the high level of detail implemented in ADM1 that does not fit to the resolution of the experimental data. However, calculated RMSE values agreed with the standard deviations of the experimental results. Therefore, the overall predictive capability for both models is given. The ADM1 managed to model the reference system with reasonable agreement to the experimental data. The performance of the empirical model for the reference was comparable. For the cascade system however the ADM1 could not fully describe the experimental at the applied low SRTs of 15 and 12 days. The empirical model in this case showed better predictive capabilities. This is an indication that a hydrolysis rate which is made dependent on system characteristics such as load and residence time might indeed have its justification and be better applicable to anaerobic digestion systems that show a concentration profile along the reactor as it is in the case with plug-flow and cascade systems.

CONTENTS

ABSTRACT	iv
LIST OF FIGURES	vii
LIST OF TABLES	viii
LIST OF ABBREVIATIONS.....	x
1 Introduction	1
1.1 Background.....	1
1.2 Problem Statement	3
1.3 Research Objective	5
1.4 Research Questions.....	5
2 LITERATURE REVIEW	6
2.1 WAS Degradation and Pre-treatment	6
2.2 Two-stage/Multiple Stage Systems compared to Single-Stage Systems	7
2.3 Types of Hydrolysis Kinetics	8
2.4 Modelling of AD.....	10
2.5 Approaches of Modelling PFR and Multiple CSTR-Configuration.	11
3 Theory and Data.....	13
3.1 Model Structure of the Standard ADM1	13
3.2 Description of Guo et al.'s (2021) Cascade System.....	16
3.3 Description of Provided Data	17
4 METHODS.....	20
4.1 Data Cleaning	20
4.2 Parameter Identifiability Analysis (Sensitivity Analysis) for ADM1	21
4.3 Development of Empirical Model Structure	22
4.3.1 Statistical Analysis	22
4.3.2 Cascade System Analysis	23
4.4 Structures of Implemented Hydrolysis Models.....	23
4.4.1 First-Order Hydrolysis Model as in ADM1.....	24
4.4.2 Empirical Hydrolysis Model in Combination with Simplified ADM1	24
4.5 Calibration Procedure.....	25
4.5.1 Calibration of General First-Order Model and ADM1 with one k_{hyd}	27
4.5.2 Calibration of Empirical Hydrolysis Rate Model and simplified ADM1	27

4.6 Model Implementation in Aquasim®	28
4.6.1 Implementation of Reactors in Aquasim®	28
4.6.2 Implementation of Equations in Aquasim®	29
4.7 Analysis of Modelled Output.....	30
5 RESULTS AND DISCUSSION.....	31
5.1 Sensitivity Analysis	31
5.2 Proposed Changes to ADM1 based on Parameter Identifiability Analysis.....	32
5.3 Results of Statistical and Cascade System Analysis.....	34
5.3.1 Linear Regression for VS/TS.....	34
5.3.2 Linear Regression for gCOD/gVS	34
5.3.3 Linear Regression for Specific Hydrolysis Rates against Enzymatic Activity	35
5.3.4 Linear Regression for HRsp OLR and Load.....	36
5.4 Results of Cascade Systems Analysis.....	37
5.5 Modelled Results of ADM1.....	41
5.5.1 Results of ADM1 for Cascade System.....	41
5.5.2 Results of ADM1 for Reference System	43
5.6 Results of Empirical Hydrolysis Model	45
5.6.1 Results of Empirical Model for Cascade System	45
5.6.2 Results of Empirical Model for Reference System	47
5.9 Results of Quantitative Model Analysis (R^2 and RMSE)	48
6 GENERAL DISCUSSION.....	51
7 CONCLUSIONS AND RECOMMENDATIONS.....	53
7.1 Conclusions.....	53
7.2 Recommendations.....	54
A References	55
B APPENDIX – Data Overview	57
C Appendix – Additional Figures	63
Modelled Outputs	63
ADM1 – Results for Cascade System.....	63
Modified First-Order Model (Empirical) – Results for Cascade System	65
ADM1 – Results for Reference System.....	67
Modified First-Order Model (Empirical) – Results for Reference System.....	69
D Appendix – ADM1 Overview.....	71
E Appendix - Python Script for Quantitative Model Analysis	74

LIST OF FIGURES

Figure 1 - Calculated specific hydrolysis rates for both reactor systems. The columns represent the calculated specific hydrolysis rates based on measured methane flow, VFA and VS concentrations. The dots represent the corrected specific hydrolysis rate for the cascade reactor which was calculated based on the stabilised sludge fraction in the fourth reactor, figure retrieved from Guo et al. (2021).	4
Figure 2 - General pathways of AD, image retrieved from (Batstone 1999).....	14
Figure 3 - Scheme of cascade system, image modified after Guo et al. (2021).....	16
Figure 4 - Concept of the Absolute Relative Sensitivity function, (Reichert 1998)	22
Figure 5 - SensAR function for tCOD (reactor 1 - 4 of the cascade system) with respect to the hydrolysis rate parameters k _{hyd} : (black for carbohydrates, green for proteins and red for lipids).....	31
Figure 6 - SensAR function for methane (reactor 1 - 4 of the cascade system) with respect to the hydrolysis rate parameters k _{hyd} : (black for carbohydrates, green for proteins and red for lipids).....	32
Figure 7- Linear regression for VS and TS, the dots represent average values of each reactor at different applied SRTs.	34
Figure 8 - Linear regression for tCOD and VS, the dots represent average values of each reactor at different applied SRTs.	35
Figure 9 - Linear regression of specific hydrolysis rates and total enzymatic activity. The dots represent average values of each reactor at different applied SRTs.....	35
Figure 10 - Linear correlations between OLR and the HR _{sp} for reactors 1 - 3 (R1-R3; blue) of the cascade and reactor 4 (R4, red) of the cascade and the Reference (Ref, red). The dots represent average values of each reactor at different applied SRTs.	36
Figure 11 - Linear correlations between specific hydrolysis rates and the load for the cascade the Reference. The dots represent average values of each reactor at different applied SRTs.....	37
Figure 12 - Cascade system analysis with respect to specific hydrolysis rates, the individual dots in the graphic represent the HR _{sp} plotted against total SRT (or flow) and against the SRT _c (residence time in the system).	38
Figure 13 - Modelled results of the standard ADM1 hydrolysis model for the cascade system for the variables methane flow, tCOD, pH and acetate and plotted with the experimental data of Guo et al. (2021), The R ² values and RMSE values in the title refer to reactor	42
Figure 14 - Modelled results of ADM1 for the reference system for the variables methane flow, tCOD, pH and acetate and plotted with the experimental data of Guo et al. (2021), The R ² values and RMSE values in the title refer to reactor one to four (from left to right).....	44
Figure 15 - Modelled results of the empirical hydrolysis model for the cascade system for the variables methane flow, tCOD, pH and acetate and plotted with the experimental data of Guo et al. (2021), The R ² values and RMSE values in the title refer to reactor one to four (from left to right).	46
Figure 16 - Modelled results of the empirical model for the reference system for the variables methane flow, tCOD, pH and acetate and plotted with the experimental data of Guo et al. (2021), The R ² values and RMSE values in the title refer to reactor one to four (from left to right).	47

LIST OF TABLES

Table 1 - Examples for kinetic hydrolysis models; Symbols modified after original publications to match: k_{hyd} refers to the hydrolysis rate coefficient, S is the substrate concentration, K_s is the saturation concentration, X refers to the hydrolytic biomass, α is the non-degradable fraction, S_0 refers to the initial substrate concentration and, and β the equilibrium constant for adsorption and desorption of biomass to the substrate	9
Table 2 - Biochemical rate coefficients ($v_{i,j}$) and kinetic rate equations (ρ_j) for soluble components ($i = 1 - 3$ and 12 , $j = 1 - 4$), modified after Batstone et al. (2002); for a full description of ADM1 see Appendix D.	15
Table 3: Biochemical rate coefficients ($v_{i,j}$) and kinetic rate equations (ρ_j) for particulate components ($i = 13 - 16$ and 24 , $j = 1 - 4$), modified after Batstone et al. (2002); for a full description of ADM1 see Appendix D.	15
Table 4 - Overview over experimental Phases, corresponding days and applied SRTs	17
Table 5 - Overview of provided measured variables by Guo et al. (2021). For a full list of the data see Appendix F. EA: average values were provided for cell-attached and free protease and cellulase respectively, EA was measured for each reactor for all experimental phases; Specific Hydrolysis Rates: were calculated based on the methane production, sCOD and the mass of VS in the reactor.....	18
Table 6 - mean values for total COD, cleaned from outliers and reactor phases..	18
Table 7 - mean values for methane flow, cleaned from outliers and instable reactor phases.....	19
Table 8 - mean values for total VFA concentrations, cleaned from outliers and reactor phases.....	19
Table 9- mean values for pH, cleaned from outliers and reactor phases.	19
Table 10 - measured sludge characteristics for WAS with respect to the VS fraction, * result of statistical analysis (see Section 5.3.1).....	26
Table 11 - calculated and calibrated parameters for both models (the general first-order hydrolysis model and the empirical hydrolysis model in combination with the simplified ADM1).....	26
Table 12 - k_{hyd} values that were used for model calibration of the empirical model, the specific hydrolysis rates were calculated by Guo et al. (2021)	28
Table 13 – Applied changes to the standard ADM1 (Batstone, 2002) for this study; Biochemical rate coefficients ($v_{i,j}$) and kinetic rate equations (ρ_j) for particulate components ($i = 13 - 16$ and 24 , $j = 1 - 2$), for a full overview of ADM1 see Appendix D	33
Table 14 - Applied changes to the standard ADM1 (Batstone, 2002) for this study; Biochemical rate coefficients ($v_{i,j}$) and kinetic rate equations (ρ_j) for particulate components ($i = 1 - 3$, $j = 1 - 2$), for a full overview of ADM1 see Appendix D.....	33
Table 15 - Logarithmic regression for specific hydrolysis rates with respect to load and SRTc.....	39
Table 16 - R^2 and RMSE values for the cascade system. Green cells mean that the respective model performed better than the other tested model.....	48
Table 17 - R^2 and RMSE values for the reference system. Green cells mean that the respective model performed better than the other tested model.....	49
Table 18 - Mean values of total enzymatic activity for each reactor and all tested SRTs.....	57
Table 19 - Mean values of specific hydrolysis rates for each reactor and all tested SRTs.	57
Table 20 - Mean values of tCOD for each reactor and all tested SRTs.....	58
Table 21 - Mean values of sCOD for each reactor and all tested SRTs.	58
Table 22 - Mean values of particulate COD for each reactor and all tested SRTs.....	58

Table 23 - Mean values of methane flow for each reactor and all tested SRTs..... 59
Table 24 - Mean values of pH for each reactor and all tested SRTs..... 59
Table 25 - Mean values of total VFA concentrations for each reactor and all tested SRTs. 59
Table 26 - Mean values of acetate for each reactor and all tested SRTs. 60
Table 27 - Mean values of propionate for each reactor and all tested SRTs. 60
Table 28 - Mean values of ammonia for each reactor and all tested SRTs. 60
Table 29 - Mean values of phosphate for each reactor and all tested SRTs. 61
Table 30 - Mean values of alkalinity for each reactor and all tested SRTs..... 61
Table 31 - Mean values of volatile solids for each reactor and all tested SRTs. 61
Table 32 - Mean values of total solids for each reactor and all tested SRTs..... 62

LIST OF ABBREVIATIONS

AD	Anaerobic Digestion
ADM1	Anaerobic Digestion Model 1
AGS	Activated Granular Sludge
ARS	Absolute Relative Sensitivity
EA	Enzymatic Activity
EPS	Extracellular Polymeric Substances
HRT	Hydraulic Retention Times
HR	Hydrolysis Rate
HR_{sp}	Specific Hydrolysis Rates
IWA	International Water Association
IQR	Interquartile Range
pCOD	Particulate Chemical Oxygen Demand
PS	Primary Sludge
sCOD	Soluble Chemical Oxygen Demand
SRT	Solids Retention Time
SRT_c	Cumulative Solids Retention Time
tCOD	Total Chemical Oxygen Demand
VFAs	Volatile Fatty Acids
VS	Volatile Solids
WAS	Waste Activated Sludge
WWTP	WasteWater Treatment Plants

1 | Introduction

1.1 Background

Sludge is an inevitable waste product of most WasteWater Treatment Plants (WWTP) (Angelidaki et al. 1999). Its disposal is of increasing importance since it can attribute for up to 50% of the plants' operational costs (Appels et al. 2008). Even though various disposal methods are possible such as burning the sludge or using it as fertiliser, sludge treatment by Anaerobic Digestion (AD) is nowadays most applied due to its benefit of reducing the number of Volatile Solids (VS) and at the same time reclaiming valuable biogas in the process. AD can also be used to reduce the number of pathogens when operated at thermophilic conditions, and odour problems can be limited ((Angelidaki et al. 1999), (Appels et al. 2008)). Since the potential of the AD process is widely recognised, the technology is constantly refined to increase digester efficiencies and biogas quality (Appels et al. 2008).

AD is made possible by four successive microbiological steps, i.e. hydrolysis, acidogenesis, acetogenesis and methanogenesis (Angelidaki et al. 1999). The AD process is highly complex since each step involves another bacterial group with different optimum working conditions. These bacteria are reactive to process parameters such as pH, alkalinity, Hydraulic Retention Time (HRT) and their metabolism can easily be inhibited at high concentrations of free ammonia, hydrogen, sodium, potassium, heavy metals, or Volatile Fatty Acids (VFAs) (Appels et al. 2008). During the disintegration and hydrolysis step, the sludge solids are broken down into smaller soluble components by physicochemical dissolution. Proteins, carbohydrates, and lipids are then converted into simpler derivatives by enzymatic reactions ((Angelidaki et al. 1999), (Appels et al. 2008)). In the acidogenesis and acetogenesis steps, amino acids, saccharides, LCFAs, and VFAs are fermented. Finally, methanogenic bacteria convert acetic acid and hydrogen into methane and carbon dioxide ((Angelidaki et al. 1999), (Batstone et al. 2002)).

AD is commonly applied for food waste, silage and Primary Sludge (PS) (Ersahin 2018) but also for more complex sludges such as Activated Granular Sludge (AGS) or Waste Activated Sludge (WAS). (Guo et al. 2020b). The hydrolysis step is recognized as the rate limiting step of the overall AD process in most conventional sludge digestion systems (Appels et al. 2008). This especially applies to the particle degradation of sludges such as AGS and WAS, which require considerably longer retention times compared

to PS due to their high content of difficultly degradable solids such as active biomass (Ersahin 2018) and Extracellular Polymeric Substances (EPS) (Guo et al. 2020a). The kinetics of the hydrolysis step are highly complex and still not fully understood (Vavilin et al. 2008).

To describe the hydrolysis process various mathematical models were proposed over the years. The simplest of those models is the first-order hydrolysis rate which was proposed by Eastman and Ferguson (1981). To describe the hydrolysis process more mechanistically, other mathematical models were introduced, over time. They can be categorized into growth-related and surface-based models (Sanders 2001).

Growth-related models (mostly applied for soluble substrate) are built on the assumption that there is a lack of enzymes compared to the available substrate and therefore the hydrolysis rate depends on the enzymatic activity or the hydrolytic biomass concentration. Surface-based models on the other side are used to describe the hydrolysis of particulate substrate and are based on the premise that enzymes are present in excess to the substrate and therefore the hydrolysis rate is made dependent on the available substrate surface (Sanders 2001). A model that is increasingly applied for the hydrolysis of solids is the so called Contois-model (Vavilin et al. 1996). Even though it yielded good results in some cases (Nelson and Holder 2009) its application for the description of solids hydrolysis should be seen critically since it is more a growth-related model type due to its close relation to the Monod and Michaelis-Menten type kinetics (Vavilin et al. 1996).

Each mathematical model has its limitations and boundary conditions. The first order hydrolysis model was proven to be well applicable for food waste and most easily degradable sludge types ((Eastman and Ferguson 1981), (Vavilin et al. 1996) (Ersahin 2018)), however for substrates that are more complex and not as easily degradable, this mathematical description might need a modification. For models with high or fluctuating organic loading rates, hydrolysis kinetics that include growth of biomass were shown to achieve good results. The surface-related two-phase model and the Contois model (often applied as surface-related model) were able to fit data of the digestion of a broad range of organic wastes ((Vavilin et al. 2008), (Nelson and Holder 2009)), however it must be considered that both models approach first-order kinetics at a high biomass to substrate concentration (Vavilin et al. 2008). They can therefore be seen as more general models, but a first-order model might give as good results for specific cases. Therefore, the model choice depends strongly on the application and the scenario that is modelled.

1.2 Problem Statement

Single-stage AD reactors with a low applied SRT or operating at high organic loading rates can result in VFA accumulation, acidify and consequently fail (Angelidaki et al. 1999). In a laboratory study at TU Delft, Guo et al. (2021) (see end of Appendix) showed that lowering the Solids Retention Time (SRT) from 22 to 15 and lastly to 12 days led to an increase in Specific Hydrolysis Rates (HR_{sp}) for two different anaerobic digestion systems digesting WAS, i.e. a single CSTR and a cascade system (described in Section 3.23.2

Description of Guo et al.'s (2021) Cascade System). Only the cascade system remained stable at the SRT of 12 days with a Total Chemical Oxygen Demand (tCOD) reduction of 40-42%, whereas the single CSTR (Reference) only achieved a tCOD reduction of 31% and struggled with overall process performance.

Both systems had the same total reactor volume (22 L) and were operated with the same applied SRTs/HRTs (no solids liquid separation) under mesophilic conditions (35°C). The sludge feed composition and concentration can be considered constant over all tested SRTs. Reactor one to three of the cascade system experience a gradual change in conditions along the cascade reactor. Along the cascade reactor a gradual decrease of all concentrations (except ammonia increased), specific hydrolysis rates, as well as enzymatic activity was observed. A recycle stream of 10% of the inflow was implemented from Reactor three to Reactor one. Reactor four of the cascade system and the Reference CSTR had very comparable environmental conditions (pH, alkalinity, ammonia, phosphate, and other concentrations).

With lowering the SRT, Guo et al. (2021) found that the Enzymatic Activity (EA) as well as the Specific Hydrolysis Rate (HR) (see Figure 1) increased in all reactors but decreasing along the cascade. Guo et al. (2021) indicated that the hydrolysis in the cascade system might have been surface limited due to a higher increase in enzymatic activity compared to the specific hydrolysis rates. Thus, the hydrolysis kinetics for the cascade system were theorized to be more complex than the first-order model which is often assumed for AD. The challenge in modelling this system lies therein that the active biomass cannot be distinguished from the substrate. Both are part of the measured VS.

Since the hydrolysis rate is increasing with a lowered SRT, but inflowing substrate concentrations were kept constant in all experimental phases the hydrolysis kinetics might indeed be more complex than the standard first-order hydrolysis model which assumes that the only two dependencies of the hydrolysis rate are with respect to substrate concentration in the reactor and a sludge dependent hydrolysis rate constant. Historically this model has been shown to function well for conventional anaerobic digesters. With the uprising of new sludge types and new reactor technologies, sometimes other models work better

to explain the hydrolysis process in these systems or for these sludges. Therefore, modifications of the first-order model have been proposed.

Currently, it seems that the standard first-order model cannot fully describe the hydrolysis process of WAS in the cascade system of Guo et al. (2021). This thesis aims to mathematically model Guo et al's (2021) cascade system to increase understanding of the hydrolysis kinetics for this type of reactor and to reveal some of the underlying processes.

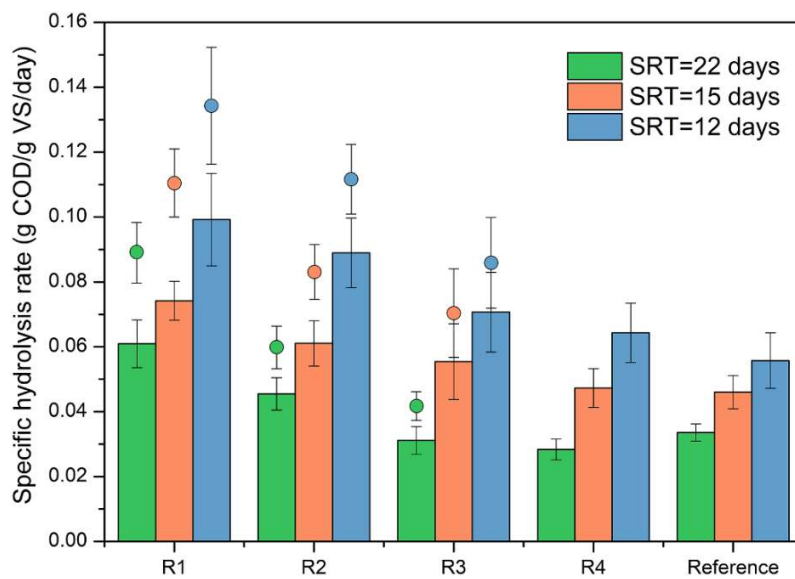


Figure 1 - Calculated specific hydrolysis rates for both reactor systems. The columns represent the calculated specific hydrolysis rates based on measured methane flow, VFA and VS concentrations. The dots represent the corrected specific hydrolysis rate for the cascade reactor which was calculated based on the stabilised sludge fraction in the fourth reactor, figure retrieved from Guo et al. (2021).

1.3 Research Objective

Modelling is a useful tool to investigate complex processes such as AD that are difficult or too costly to examine in the laboratory. A good computational or mathematical model can be used to save time and money when answering research questions that would require many experimental samples or are highly time-intensive due to slow growth rates of anaerobic bacteria. Furthermore, mathematical models can provide insights that might prevent process failure or help to optimise a system which in consequence saves investment and operational costs (Batstone et al. 2002).

A functioning model able to describe the experimental results of Guo et al. (2021) could prove itself useful for future research in the field of AD. The study at hand aims to explore the Guo et al.'s (2021) cascade system mechanistically and to describe the hydrolysis kinetics of the system mathematically.

1.4 Research Questions

1. What relationships can be found in the experimental data of Guo et al. (2021) that could potentially explain an increased hydrolysis rate with shortened SRT?
2. Which type of hydrolysis kinetics can describe Guo et al.'s (2021) cascade system? Does the first-order hydrolysis model as implemented in ADM1 or a modified first order model based on Guo et al.'s (2021) experimental data represent the cascade system better in terms of data fit (measured by R^2) and qualitative model analysis?

2 | LITERATURE REVIEW

2.1 WAS Degradation and Pre-treatment

Anaerobic digestion is commonly applied for the treatment of manures, silages, food wastes, Primary Sludge (PS) and Waste Activated Sludge (WAS) ((Appels et al. 2008); (Guo et al. 2020b)). Due to the increasing amounts of sludge volumes that are produced by municipal sewage treatment plants, understanding the digestion of complex municipal sludges such as WAS is of economic and ecological importance since AD contributes to the independency and climate neutrality of Wastewater treatment plants (Guo et al. 2020b).

Whereas PS is mainly composed of smaller particles, WAS has a higher overall percentage of bigger particles. Usually, WAS consists of large particulate organics, composed of proteins, carbohydrates, lignocellulosic matters, and fats (Guo et al. 2020a). The hydrolysis of these sludge solids is the rate-limiting step in the sludge digestion ((Vavilin et al. 2008); (Odnell et al. 2016)).

To achieve a sufficient state of degradation for WAS most conventional anaerobic digestion systems (single CSTRs) are operated at long retention times (around 20 days). These long retention times lower the efficiency of the sludge treatment (Guo et al. 2020b). The HRT in the Activated Sludge (AS) Process highly influences the biomethane potential and biodegradability during AD (Bolzonella et al. 2005). Mixed sludges and PS can relatively easily be degraded compared to WAS due to their lower content of complex particulate matter. Volatile solids removal for AS is significantly lower (13 – 27%) compared to mixed sludges (50%) (Bolzonella et al. 2005). Therefore, the biomethane potential of PS is much higher than the methane potential of WAS (Guo et al. 2020a).

WAS contains large amounts of Extracellular Polymeric Substances (EPS) which make up most of the carbohydrates. These EPS are reported to slow down the hydrolysis of the sludge particles (Guo et al. 2020a) and make them considerably more difficult to degrade than PS. During the hydrolysis of WAS tightly bound EPS are converted into loosely bound EPS (Guo et al. 2020a). Sludge pre-treatment prior to AD can break up the EPS-structure and enhance the sludge digestion (Zhen et al. 2017).

Different methods for pre-treatment of difficultly degradable sludges such as WAS were shown to function well in terms of enhancement of the hydrolysis process. These methods range from mechanical and thermic sludge pre-treatment over enzymatic pre-treatment methods to catalytic enhancement by addition of zero-valent ions (Zhen et al. 2017). However, these methods are most often not economical viable choices (Guo et al. 2020a).

2.2 Two-stage/Multiple Stage Systems compared to Single-Stage Systems

The efficient operation of single stage CSTRs is challenging due to the inevitable requirement of adjusting the operation such that the bacterial groups with different optimal working conditions, that are involved in AD, are not only maintained in the reactor but also not inhibited by intermediate products. Separation of this process in two stages was shown to improve AD performance due to the possibility of better overall controllability of the process (Gosh et al. 1975).

Gosh et al. (1975) achieved VS reductions of 40 % for Activated Sludge in a two-stage system. Whereas operation of the compared single stage system resulted in VS reduction of only 33 %. Gosh (1987) showed that two-phase AD was able to operate at higher efficiencies for municipal sludge than a single CSTR, at various tested loading rates, HRTs and VS concentrations. The two-stage system achieved higher methane yields and showed to be more stable than the single CSTR. Both systems were continuously fed with mixed PS and AS, completely mixed and operated at mesophilic conditions. The two-stage system however was operated with solids recycle.

Maspolim et al. (2015) as well, compared a two-stage system and a single stage CSTR. The overall results agree with Gosh et al. (1975) and Gosh (1987). Maspolim et al. (2015) found the two-stage system to be significantly more efficient and operation was more stable than in the single CSTR. Differently, from Gosh et al. (1975) significant methanogenic activity was found in the acidogenic phase of the systems. Furthermore, it was reported that VS reduction not only took place in the acidogenic reactor but also in the methanogenic reactor, which was reported differently by Gosh et al. (1975). Maspolim et al. (2015) mentions that for the tested HRTs of 30, 20 and 10 days, significant microbial community adaption only occurred at the HRT of 30 days.

Guo et al. (2021) studied a cascade system based on the theory that smaller reactors in front of a larger reactor can enhance the conversion rate of substrates since smaller reactors in the beginning of the cascade system can be operated at higher intermediate hydrolysis rates. Guo et al (2021) achieved the

theorized increase in hydrolysis rates for WAS. The results of this multistage system study agree with the overall results of Maspolim et al. (2015). Guo et al. (2021) as well, observed significant methanogenic activity in the first three reactors of the multistage system. Volatile sludge solids were also hydrolysed in the post-digester which is comparable to the methanogenic reactor of two-stage systems. Differently from Maspolim et al. (2015), Guo et al. (2021) reported signs of significant microbial community adaption even at low HRTs such as 12 days which was possibly linked to an increase in reported specific hydrolysis rates.

2.3 Types of Hydrolysis Kinetics

With processes that are composed of multiple consecutive steps, the overall process is limited by the slowest reaction, also referred to as the rate-limiting step. In anaerobic digestion the rate-limiting step is generally considered to be the hydrolysis of sludge solids (Vavilin et al. 2008). Organic polymers are hydrolysed by the three main types of extra cellular hydrolases, namely cellulases, proteinases and lipases (Batstone et al. 2002). In the Anaerobic Digestion Model 1 (ADM1) the hydrolysis of sludge solids is represented in this way by means of three hydrolysis reactions, one for carbohydrates, one for proteins and one for lipids respectively (Batstone et al. 2002). The applied differential equations in ADM1 are of first-order type which is considered the most general hydrolysis model (Batstone et al. 2002). Generally, all cumulative effects of all the microbial processes involved in AD were combined in a first-order model for the substrate degradation ((Eastman and Ferguson 1981). The applicability of first order kinetics was shown in several studies. Therefore, the IWA task group recommends the use of first order kinetics due to its simplicity but good output performance. However, in conditions where biomass concentration compared to substrate is low, the Contois-growth model (see Table 1) could give a better fit than first order kinetics (Batstone et al. 2015).

Vavilin et al. (2008) mentions that the first-order kinetics are not applicable to all circumstances and that an in depth understanding of the underlying microbiological processes is required to develop models that can accurately describe the hydrolysis process. Recently, other types of models such as growth related, and surface-related models gained increasing interest for the description of the hydrolysis of sludge (Vavilin et al. 2008).

Fernandez et al. (2001) showed that the hydrolysis step might depend on the biomass concentration and activity. Therefore, it might be necessary to integrate a hydrolysis rate which considers the limitation by

biomass concentration and by substrate concentration together with the impact of substrate accessibility and slowly biodegradable material content.

Batstone et al. (2002) mentions that two conceptual models can be considered for the hydrolysis of sludge particles. In the first, organism secrete enzymes to the bulk liquid which adsorb to sludge solids and consequently degrade the solids. The second model assumes that the biomass attaches to the sludge solids and excrete enzymes in its direct proximity, directly profiting from soluble products.

Vavilin et al. (1996) modelled the digestion of swine waste, sewage sludge, cattle manure and cellulose with a surface-related two-phase model (surface colonisation and subsequent degradation of sludge particles, see Table 1). The modelled results were in good agreement with the experimental data. Vavilin et al. (2008) claims that the first-order model should be modified for complex substrate to consider the hydrolysis of hardly degradable material (see Table 1). Furthermore, they mentioned that models in which the hydrolysis is coupled to the growth of hydrolytic bacteria would work well to describe systems that are operated at high or fluctuating loading rates. The Contois-growth model was shown to describe experimental data as good as the surface-related two-phase model. Both showed good fit to a broad range of substrates (Vavilin et al. 2008).

Table 1 - Examples for kinetic hydrolysis models; Symbols modified after original publications to match: k_{hyd} refers to the hydrolysis rate coefficient, S is the substrate concentration, K_S is the saturation concentration, X refers to the hydrolytic biomass, α is the non-degradable fraction, S_0 refers to the initial substrate concentration and, and β the equilibrium constant for adsorption and desorption of biomass to the substrate

Kinetic hydrolysis model	Published by	Rate expression
First-order hydrolysis rate	Eastman and Ferguson (1981)	$k_{hyd} \cdot S$
Contois	Contois (1959); as described in Mairet et al. (2011)	$k_{hyd} \cdot \frac{S \cdot X}{K_S \cdot X + S}$
Degradable fraction	Vavilin et al. (2008)	$k_{hyd} \cdot (S - \alpha S_0)$
Surface-based	Vavilin et al. (1996)	$k_{hyd} \cdot \frac{S \cdot X}{K_S \cdot X + S} \cdot \frac{\beta \cdot X}{1 + \beta \cdot X}$

Nelson and Holder (2009) elaborated that the Contois-growth model was able to describe AD of a wide range of substrates such as wastewater originating from the treatment of olives, solid municipal organic

waste, dairy manure, ice-cream wastewater. Furthermore, it was shown that, the digestion of cattle manure, swine waste, sewage sludge and cellulose could be described with the Contois hydrolysis kinetics.

Mairet et al. (2011) modelled the hydrolysis of microalgae with the Contois-model in which they let the hydrolytic bacteria grow on the produced soluble substrate. Mairet et al. (2011) achieved good data representation with the Contois model. Even though, the Contois model and most surface-related models tend to the general first-order hydrolysis rate model, they can be seen as more general models (Vavilin et al. 2008).

2.4 Modelling of AD

Anaerobic digestion is an intricate process and therefore highly complex to model. One major challenge lies in the difficulty to obtain data for modelling purposes. This is because during reactor operation only a handful of parameters are measured on a regular basis or measured at all which makes it for instance difficult to distinguish active biomass (X) from the substrate (S). This makes it extremely difficult to create verifiable models for long-term dynamic simulations. This lack of data leads to a large variety of modelling approaches resulting in a high variability in the kinetic parameters reported in literature (Donoso-Bravo et al. 2011).

According to Koch and Drewes (2014), the rate of hydrolysis of particulate matter is often estimated by data fitting from batch tests. They describe that, based on results of Eastman and Ferguson (1981), who conducted batch experiments at different loading rates, a batch reactor at the beginning of an experiment would behave similarly to a CSTR which is operated at high organic loading rates and short retention times. Towards the end of the batch experiment the batch reactor behaves like a CSTR with low organic loading rates and long retention times. Koch and Drewes (2014) concludes that, current methods applicable for batch tests might be transferable to CSTRs.

Donoso-Bravo et al. (2011) mentions the following four criteria for a good model:

- simplicity
- causality
- parameter identifiability
- predictive capability

Furthermore, Donoso-Bravo et al. (2011) explains that a model structure must be able to fit the experimental data and have enough degrees of freedom without leading to over parametrization. A unique optimal set of parameters based on the experimental data should be chosen. The latter can either lead to further model simplification or to including additional terms or equations.

Various mathematical models which are applicable for specific applications in the field of AD already exist. Batstone et al. (2002), considers a generic model necessary to create common basis for modelling in the field of AD. Batstone mentions several benefits of a generic model such as the ADM1:

- increased model application for full-scale plant design.
- further development of process optimization and control.
- creating a common basis for further model development and validation for better comparison of study results.
- transferring technology from research to industry

With the ADM1 being a relatively complex model, comprising a variety of biochemical and physical processes, detailed influent and sludge characterization is required (Batstone et al. 2002). Often this information is difficult to obtain from full-scale plants. Due to the difficulty of obtaining dynamic data only few studies in literature exist which investigated the long-term dynamic performance of full-scale anaerobic digesters (Ersahin 2018).

2.5 Approaches of Modelling PFR and Multiple CSTR-Configuration.

According to Nelson and Holder (2009), Plug-Flow Reactors became increasingly more interesting for AD in the last years since they have several competitive advantages in comparison to CSTRs. Donoso-Bravo et al. (2018) states that PFRs make better use of their working volume than CSTR and show a higher capacity to handle overloads. Furthermore, they are more resistant to acidification and create concentration profiles along the reactor. However, PFRs can still suffer from instabilities such as washout of biomass or cascade acidification due to low local retention times of the individual sections in the reactor. Few full-scale applications of PFRs have been reported.

Nelson and Holder (2009) did a steady state analysis of a cascade, consisting of a series of CSTRs without recycling. They found that the stability of the system was a function of the residence time in each reactor of the cascade. The effluent concentration of each reactor was found to be dependent on $1/\tau$ (τ = total

residence time). Alqahtani et al. (2012) and Alqahtani et al. (2013) showed that there is a critical value of total retention time with respect to stability of a cascade system. Below the critical value a settling unit would increase the performance of a cascade reactor with up to 5 reactors, whereas above the critical value the systems performance would decrease with a settling unit. They also modelled that the critical value of total residence time was dependent on recycling ratio and the concentration factor of substrate. Donoso-Bravo et al. (2018) as well, modelled a Plug-Flow Reactor (PFR) by coupling several CSTRs in series. The ADM1 model was then solved for each CSTR where the output of the first one corresponds to the inlet and conditions of the following one, and so on.

Based on the theory the characteristics of a PFR can be achieved by an infinite amount of CSTRs in series (Donoso-Bravo et al. 2018). Guo et al.'s (2021) multi-stage AD setup might be close to a PFR configuration. Guo et al. (2021) showed that the short retention times did not lead to acidification of their multi-stage AD system but to enhancement of the hydrolysis and the overall AD process. The AD remained stable for hydraulic/solid retention times as low as 12 days for the entire system (1.2 days for the acidogenic reactors). A small (10%) recycling stream was implemented in this study which might explain the low achieved retention times as opposed to Nelson and Holder (2009) who modelled cascade systems without recycle stream.

3 | Theory and Data

This section describes the applied frame model for this study, the Anaerobic Digestion Model 1 (ADM1), developed by the International Water Association (IWA), (see Section 3.1). The setup of the cascade system as developed by Guo et al. (2021) is described in Section 3.2. The provided data (Guo et al., 2021) that was used in the modelling study at hand is shortly described in Section 3.3. For a more detailed overview of all measured variables see Appendix B.

3.1 Model Structure of the Standard ADM1

For the modelling study at hand the ADM1 was chosen as a frame for the kinetic hydrolysis models that were developed and tested. The structure of ADM1 follows the basic digestion pathways for AD that are illustrated in Figure 2. The hydrolysis step is the first step in anaerobic digestion. It is an extracellular process in which bacteria excrete enzymes that attach to the substrate (soluble or particulate) and break it down into smaller components. This step is followed by intracellular processes, namely fermentation/acidogenesis, acetogenesis and lastly methanogenesis (see Figure 2).

The ADM1 describes these biochemical processes by means of rate equations. Three main rates can be distinguished: the conversion rates of substrates, uptake rates for the substrates and the growth-related expressions for the biomass. Inhibition factors (pH inhibition, substrate limitation and non-competitive inhibition) are included as additional terms in those rate expressions. Furthermore, physico-chemical processes such as gas exchange between the liquid- and the gas-phase are implemented in the ADM1. The study at hand focusses on the mathematical description of the hydrolysis kinetics. Therefore, only those expressions of ADM1 that target hydrolysis of particles are described here. For a detailed description of all process descriptions, yield factors and stoichiometric factors that are included in the ADM1 Appendix D.

In the ADM1 the hydrolysis of sludge is implemented in the form of the standard first-order hydrolysis rate which is calculated by a sludge dependent hydrolysis rate constant (k_{hyd}) multiplied with the COD concentration of the sludge in the reactor, or in the case of ADM1, the COD concentration of the main sludge components, namely carbohydrates (X_{ch}), proteins (X_{pr}) and lipids (X_{li}). During the hydrolysis step insoluble carbohydrates are broken down and converted into soluble sugars (S_{su}), proteins into amino acids (S_{aa}) and lipids into Long Chain Fatty Acids (LCFAs; ADM1: S_{fa}), (see Figure 2). The produced Soluble COD (sCOD) and the degraded Particulate COD (pCOD) are dependent on the hydrolysis rate, the fraction of pCOD that is converted to the respective sCOD is accounted for with stoichiometric factors (f) (see Table 2 and Table 3).

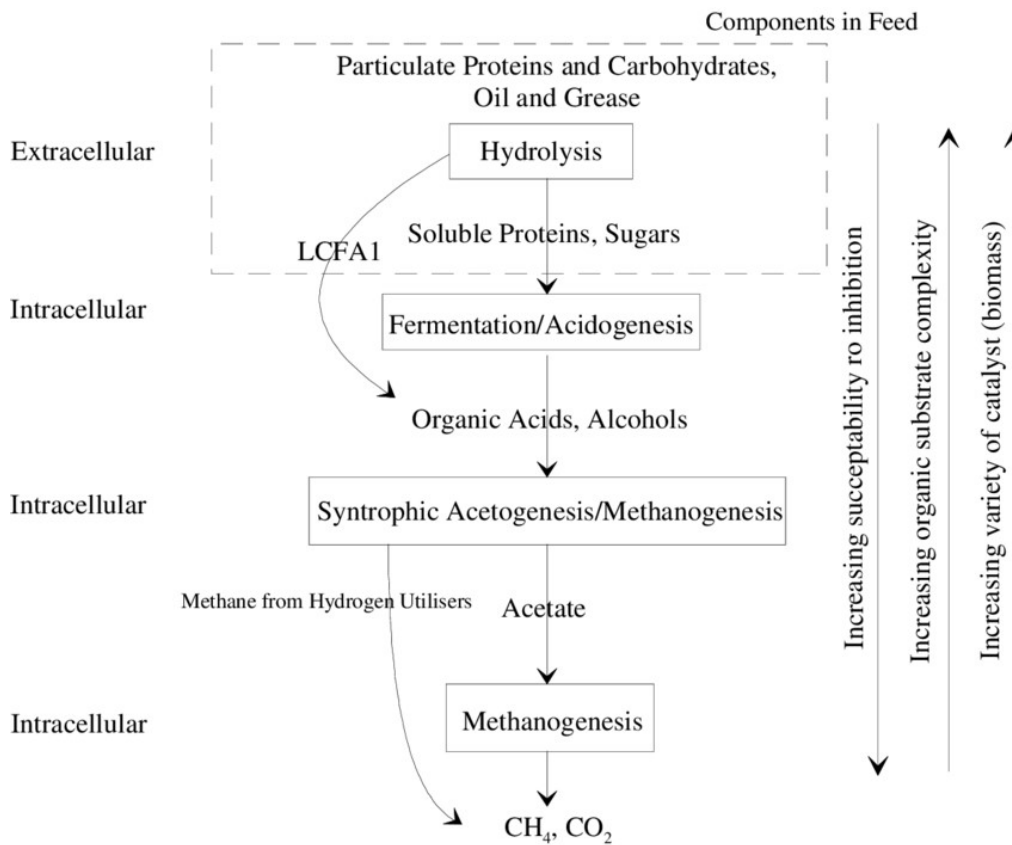


Figure 2 - General pathways of AD, image retrieved from (Batstone 1999).

Table 2 - Biochemical rate coefficients ($v_{i,j}$) and kinetic rate equations (p_j) for soluble components ($i = 1 - 3$ and 12 , $j = 1 - 4$), modified after Batstone et al. (2002); for a full description of ADM1 see Appendix D.

Component →		i	1	2	3	...	12	Rate (ρ_j , kg COD·m ⁻³ ·d ⁻¹)
j	Process ↓		S _{Su}	S _{aa}	S _{fa}	...	S _l	
1	Disintegration					...	f _{sl,xc}	$k_{dis} \cdot X_c$
2	Hydrolysis of Carbohydrates		1			...		$k_{hyd,ch} \cdot X_{ch}$
3	Hydrolysis of Proteins			1		...		$k_{hyd,pr} \cdot X_{pr}$
4	Hydrolysis of Lipids		1 - f _{fa,li}		f _{fa,li}	...		$k_{hyd,li} \cdot X_{li}$
			Monosaccharides (kgCOD·m ⁻³)	Amino acids (kgCOD·m ⁻³)	Long chain fatty acids (kgCOD·m ⁻³)		Soluble inerts (kgCOD·m ⁻³)	

Table 3: Biochemical rate coefficients ($v_{i,j}$) and kinetic rate equations (p_j) for particulate components ($i = 13 - 16$ and 24 , $j = 1 - 4$), modified after Batstone et al. (2002); for a full description of ADM1 see Appendix D.

Component →		i	13	14	15	16	...	24	Rate (ρ_j , kg COD·m ⁻³ ·d ⁻¹)
j	Process ↓		X _c	X _{ch}	X _{pr}	X _{li}	...	X _l	
1	Disintegration		-1	f _{ch,xc}	f _{pr,xc}	f _{li,xc}	...	f _{xl,xc}	$k_{dis} \cdot X_c$
2	Hydrolysis of Carbohydrates			-1			...		$k_{hyd,ch} \cdot X_{ch}$
3	Hydrolysis of Proteins				-1		...		$k_{hyd,pr} \cdot X_{pr}$
4	Hydrolysis of Lipids					-1	...		$k_{hyd,li} \cdot X_{li}$
			Composites (kgCOD·m ⁻³)	Carbohydrates (kgCOD·m ⁻³)	Proteins (kgCOD·m ⁻³)	Lipids (kgCOD·m ⁻³)		Particulate inerts (kgCOD·m ⁻³)	

3.2 Description of Guo et al.'s (2021) Cascade System

Guo et al. (2021) researched a cascade anaerobic digester treating WAS. The cascade system was compared to a single-stage CSTR, from now referred to as reference reactor or shortly reference.

The cascade system in Guo et al.'s (2021) study consisted of a series of four reactors (see Figure 3) with a total volume of 22 L. The fourth reactor contributed with 15.4 L (70 % of V_{total}) the majority to the total volume. The first three reactors in the cascade system are each sized 2.2 L (10 % of V_{total}). A recirculation flow of 10% of the inflow (Q_{in}) was implemented from the third to the first reactor.

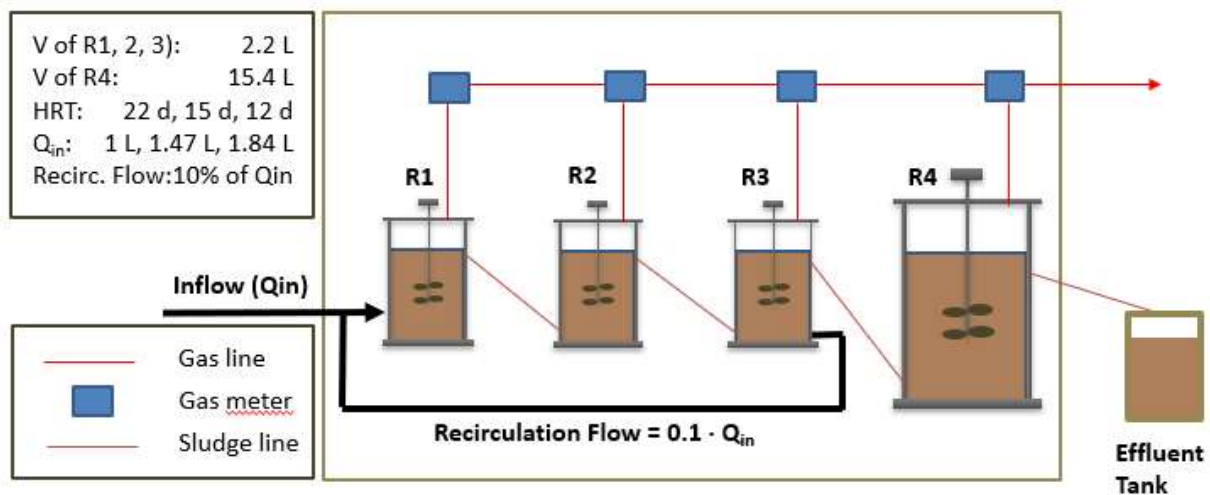


Figure 3 - Scheme of cascade system, image modified after Guo et al. (2021).

The cascade system is compared to a single Continuous-Flow Stirred Tank Reactor (CSTR) with the same total volume of 22L as the cascade system. Both systems were operated with the same sludge type, temperatures, and flows. However, the reference CSTR did not have a recirculation flow. In both systems the terms SRT and HRT can be used interchangeably since there was no solids-liquid separation. Nevertheless, the term SRT will be used to refer to the retention times.

3.3 Description of Provided Data

The experimental data for this modelling study was provided by Guo et al. (2021). Four experimental phases can be distinguished. Phase 1 (days 0 – 72) is the unstable reactor phase (start-up) with a SRT of 22 days, transitioning into a stable experimental phase 2 (days 72 – 152) with a SRT of 22 days. Followed by a shortening of the SRT to 15 days in phase 3 (153 – 259) and to 12 days in phase 4 (days 260 – 330), respectively (see table 4).

Table 4 - Overview over experimental Phases, corresponding days and applied SRTs

Experimental Phase	Time (d)	Applied SRT
Phase 1	0 - 72	22 d
Phase 2	72 - 152	22 d
Phase 3	153 - 259	15 d
Phase 4	260 - 330	12 d

The provided data covers a period of 330 days for both anaerobic digestion systems that are modelled in the study at hand. For an overview of the provided measured variables by Guo et al. (2021) see Table 5. For the average values for tCOD, methane flow, total VFA and pH see Table 6 - Table 9 (next page). For all mean values see Appendix B.

Table 5 - Overview of provided measured variables by Guo et al. (2021). For a full list of the data see Appendix F. EA: average values were provided for cell-attached and free protease and cellulase respectively, EA was measured for each reactor for all experimental phases; Specific Hydrolysis Rates: were calculated based on the methane production, sCOD and the mass of VS in the reactor

Variable	Unit
pH	-
tCOD	g COD/L
sCOD	g COD/L
Particulate COD (tCOD – sCOD)	g COD/L
Volatile Fatty Acids.	mg/L or g/L
Inorganic Nitrogen (NH ₄ ⁺)	mg/L or g/L
Phosphate (PO ₄ ³⁺)	mg/L or g/L
Alkalinity	mg/L or g/L
Total Solids (TS)	wt% or g/L
Volatile Solids (VS)	wt% or g/L
Methane flow	ml/d or L/d
Enzymatic Activities (EA)	(U/L) or (U/g sludge)
Specific Hydrolysis Rates	gCOD/gVS/d

Measured variables were sampled with varying frequency. Some variables such as pH, CODs, methane flow and solids were measured more frequently than ammonia -, phosphate -, and VFA concentrations.

Table 6 - mean values for total COD, cleaned from outliers and reactor phases..

Mean tCOD (g/L) at each tested SRT in each reactor						
	Feed	Reactor 1	Reactor 2	Reactor 3	Reactor 4	Reference
SRT 22 d	50.86	46.41	41.83	39.83	30.45	32.92
Std. dev.	2.35	1.85	1.78	1.28	0.51	0.62
SRT 15 d	50.84	47.44	44.16	41.93	30.75	34.38
Std. dev.	1.97	2.41	2.81	2.55	1.20	1.01
SRT 12 d	52.01	49.14	46.01	43.26	31.00	35.57
Std. dev.	1.02	1.62	1.36	1.57	0.21	1.26

Table 7 - mean values for methane flow, cleaned from outliers and instable reactor phases.

Mean methane flow (L/d) at each tested SRT in each reactor						
	Cascade	Reactor 1	Reactor 2	Reactor 3	Reactor 4	Reference
SRT 22 d	6.54	1.35	1.01	0.72	3.33	5.78
Std. dev.	0.40	0.41	0.23	0.15	0.32	0.36
SRT 15 d	10.29	1.64	1.53	1.33	5.71	9.05
Std. dev.	0.87	0.44	0.23	0.32	0.53	0.76
SRT 12 d	13.30	1.99	1.92	1.54	7.91	10.59
Std. dev.	0.92	0.38	0.27	0.23	1.09	0.59

Table 8 - mean values for total VFA concentrations, cleaned from outliers and reactor phases.

Mean total VFA concentrations (mg COD/L) at each tested SRT in each reactor						
	Feed	Reactor 1	Reactor 2	Reactor 3	Reactor 4	Reference
SRT 22 d	118	282	79	32	6	9
Std. dev.	8	91	25	21	3	4
SRT 15 d	151	365	163	58	6	6
Std. dev.	138	49	15	24	3	4
SRT 12 d	115	518	324	144	6	84
Std. dev.	18	19	43	30	3	13

Table 9- mean values for pH, cleaned from outliers and reactor phases.

Mean pH (-) at each tested SRT in each reactor						
	Feed	Reactor 1	Reactor 2	Reactor 3	Reactor 4	Reference
SRT 22 d	6.46	6.67	6.91	7.01	7.39	7.26
Std. dev.	0.10	0.03	0.02	0.02	0.14	0.10
SRT 15 d	6.34	6.63	6.77	6.85	7.42	7.13
Std. dev.	0.15	0.10	0.09	0.10	0.09	0.10
SRT 12 d	6.41	6.50	6.63	6.74	7.40	7.00
Std. dev.	0.06	0.08	0.07	0.02	0.03	0.09

4 | METHODS

This section describes the general approach and the specific methods that were applied during the study at hand. The setups of the two anaerobic digestion reactors (Cascade system and Reference CSTR), that were introduced in the Problem Statement (see Section 1.2) are described in detail in Section 3.2. The Anaerobic Digestion Model 1 (ADM1), developed by the International Water Association (IWA), is used as a frame for the tested hydrolysis models in this study (see Section 3.1). The process of data cleaning is described in Section 4.1. A parameter identifiability analysis by means of sensitivity analysis was performed to investigate if the hydrolysis rate coefficients of the first-order hydrolysis model in ADM1 can be calibrated meaningfully (see Section 4.2). The experimental data of Guo et al. (2021) was analysed by means of statistical analysis to derive a model structure for the empirical model in this study (see Section 4.3). The developed structures of the general first-order model and the empirical model (based on the experimental data of Guo et al.'s (2021)) are described in Section 4.4. The calibration procedure for both models is discussed in Section 4. The two digestion systems were then implemented in the software Aquasim[®](see Section 4.6). The methods for quantitative analysis of simulated results for the two tested models is described in Section 4.7.

4.1 Data Cleaning

The provided experimental data from Guo et al. (2021) was cleaned prior to the statistical analysis. The data from the experimental phase 1 (days 0 – 71) was excluded from the analysis since both digestion systems (cascade and reference) were not fully stable, yet. Consequently, the data analysis was done for all other experimental phases, i.e. Phase 2 (days 72 – 152), Phase 3 (days 153 – 259), Phase 4 (days 260 – 330). To ensure that only data of stable reactor operation was considered, the first SRT of all experimental phases was excluded from the analysis, as well. Furthermore, the data was cleaned from outliers prior to the statistical analysis. For an overview of the data see Appendix B. Outliers and instable reactor phases were excluded for statistical analysis, models calibration and models validation.

Outliers were identified by applying a lower-range limit and an upper range limit. The lower and upper limits for all data were calculated with Eq. 1.1. 1.1 and Eq. 1.2.

Since very extreme outliers would influence the IQR and consequently shift the lower and upper limits that are applied for selection of outliers, the described method was applied twice to exclude those extreme outliers.

$$\text{Lower range limit} = Q1 - (1.5 \cdot \text{IQR}) \quad \text{Eq. 1.1}$$

$$\text{Higher range limit} = Q3 + (1.5 \cdot \text{IQR}) \quad \text{Eq. 1.2}$$

Where:

- Q1 first quartile
- Q3 third quartile
- IQR Inner Quartile Range = (Q3 – Q1)

4.2 Parameter Identifiability Analysis (Sensitivity Analysis) for ADM1

To identify if the hydrolysis rate coefficients (namely $k_{\text{hyd,ch}}$, $k_{\text{hyd,li}}$, $k_{\text{hyd,pr}}$) in ADM1 can be identified in a meaningful way, a sensitivity analysis was performed. The three variables methane flow, ammonia and tCOD concentrations were tested for their sensitivity to a change in the hydrolysis rate coefficients. Since the modelling was done with the Software Aquasim[®], the sensitivity analysis was performed with the same software. Aquasim[®] has a built-in sensitivity analysis algorithm that allows the user to choose from four different types of linear sensitivity functions. In this specific case the Absolute Relative Sensitivity (SensAR) function was chosen. The concept of the SensAR function is shown in Figure 4. The SensAR measures the absolute change of the tested variable (y) with respect to a 100% (relative) change of the parameter p . The SensAR function is suitable for the identifiability analysis of parameters since its unit is non-dependent on the unit of the parameter (Reichert 1998). The variables methane flow, ammonia and tCOD concentrations were tested (see Eq. 2 **Error! Reference source not found.**) for their sensitivity to a 100% change in the hydrolysis rate coefficients. The SensAR function for all variables were then plotted over time (see Section 5.1).

$$\delta_{y,p}^{a,r} = p \frac{\partial y}{\partial p} \quad \text{Eq. 2}$$

Where:

$\delta_{y,p}^{a,r}$ means absolute relative sensitivity of variable y with respect to a change in parameter p

∂y is the change in variable y

∂p is the change in parameter p

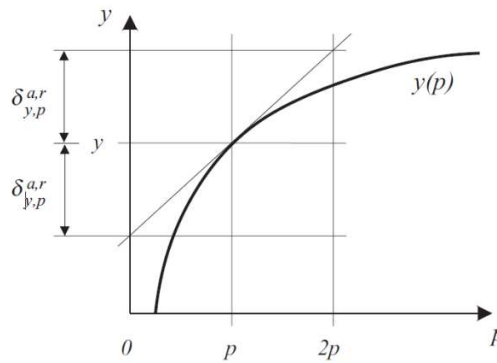


Figure 4 - Concept of the Absolute Relative Sensitivity function, (Reichert 1998)

4.3 Development of Empirical Model Structure

4.3.1 Statistical Analysis

All measured variables of the experimental data were analysed by means of statistical analysis. The method for this analysis consists of a comparison of average values (to smooth out variation in the data) for all reactors at all tested SRTs.

The characteristics of the two reactor systems (cascade and reference) are analysed by means of comparison of averages of the measured variables. Those average values were plotted against each other (or with respect to time, concentration, reactor, or experimental phase). Linear and Logarithmic

Regression based on R^2 -values was used to reveal correlations in the data. For a description of the correlations that were found in the data see Section 5.3. These correlations were used to develop the empirical model structure which is described in Section 4.4.2 and to calibrate both tested models in this study (Section 4.5).

4.3.2 Cascade System Analysis

A series of CSTRs is approximating the behaviour of a plug-flow reactor but with the advantage of better controllability of the overall process. As pointed out in the literature review (see Section 2.5) a CSTR with low loading but a long retention time resembles the end of a batch experiment, whereas a CSTR with high loading and a short retention time resembles the beginning of a batch experiment. Since the cascade systems consists of a series of CSTRs it offers the opportunity to look at the degradation of WAS with time. During the system's analysis this approach was used to describe the cascade system mathematically. Each reactor which each tested SRT was treated as an intermediate step of a batch experiment each with its individual assumed hydrolysis rate coefficient (based on specific hydrolysis rates identified by Guo et al (2021)). The operational parameters that changed during Guo et al's study (2021) were identified and their influence on the specific hydrolysis rate was analysed. A logarithmic regression was applied to derive a formula to calculate the specific hydrolysis rates to apply them in the hydrolysis model.

4.4 Structures of Implemented Hydrolysis Models

In the study at hand, the general first-order hydrolysis model is tested and compared to a hydrolysis model that was based on the experimental data provided by Guo et al. (2021). The structure of the two models is described in this Section 4.4. The general first-order model was used in combination with the standard ADM1 (see section 4.4.1). However, the number of hydrolysis rate constants in ADM1 was reduced from three to one, due to a parameter identifiability problem (discussed in Section 5.1). The empirical model was framed by a simplified version of ADM1 (see Section 5.2). In the simplified ADM1 the number of hydrolysis rate coefficients is reduced to one and the disintegration step is omitted. Instead, the sludge is already theoretically split in degradable (X_d) and inert particulates (X_i) with the loading in the reactor.

4.4.1 First-Order Hydrolysis Model as in ADM1

The general first-order hydrolysis model in combination with the standard ADM1 uses three differential equations (one for each sludge fraction see Eq. 3.1 to 3.3) as described in more detail in Section 3.1. However, differently from the standard ADM1 only one hydrolysis rate constant is applied for all three equations. The first-order hydrolysis rate is linearly proportional to the COD concentration of the sludge fraction (see Eq. 3.1 to 3.3).

$$\frac{dX_{ch}}{dt} = k_{hyd,constant} \cdot X_{ch} \quad \text{Eq. 3.1}$$

$$\frac{dX_{pr}}{dt} = k_{hyd,constant} \cdot X_{pr} \quad \text{Eq. 3.2}$$

$$\frac{dX_{li}}{dt} = k_{hyd,constant} \cdot X_{li} \quad \text{Eq. 3.3}$$

Where:

- $k_{hyd,constant}$ hydrolysis rate constant (d^{-1})
- X_{ch} degradable fraction of carbohydrates ($kg\ COD \cdot m^{-3}$)
- X_{pr} degradable fraction of proteins ($kg\ COD \cdot m^{-3}$)
- X_{li} degradable fraction of lipids ($kg\ COD \cdot m^{-3}$)

4.4.2 Empirical Hydrolysis Model in Combination with Simplified ADM1

For the empirical hydrolysis model Eq 4.1, 4.2 and 4.3 were implemented in a simplified that uses only one hydrolysis rate for the entire sludge instead of three individual expressions for each sludge fraction (i.e. carbohydrates, proteins and lipids). The modifications that were applied to the standard ADM1 and the reasoning behind it are discussed in Section 5.2.

For the empirical model the hydrolysis rate coefficient was made dependent based on load and the residence time along the reactor (named cumulative SRT (SRT_c)) (see Eq. 4.3). The introduced term cumulative SRT refers to the time that the sludge solids spent in the reactor up to a certain position along

the system. The coefficient $k_{\text{hydr, relative}}$ is applied in the hydrolysis model (see Eq. 4.1), in form of an empirically derived logarithmic function (see Eq. 4.2). The empirical formula was derived with the methods in described in Section 4.3 and is discussed in detail in Section 5.4.

$$\frac{dX}{dt} = k_{\text{hydr, relative}} \cdot p\text{COD} \quad \text{Eq 4.1}$$

$$k_{\text{hydr, relative}} = 0.0107 \cdot \ln(x) + 0.0295 \quad \text{Eq 4.2}$$

$$x = \frac{\text{Load}_{p\text{COD}} \left(\frac{\text{gCOD}}{\text{d}} \right)}{\text{SRT}_c \left(\frac{1}{\text{d}} \right)} \quad \text{Eq 4.3}$$

Where:

- $k_{\text{hydr, relative}}$ hydrolysis rate coefficient
- pCOD particulate COD (g COD/L)
- $\text{Load}_{p\text{COD}}$ Massflow of particulate COD (g COD/d)
- SRT_c cumulative SRT (1/d)

4.5 Calibration Procedure

The tested standard ADM1 as well as the empirical hydrolysis model use the same sludge characteristics. The yield values for soluble sugars (S_{su}), amino acids (S_{aa}) and LCFAs (S_{fa}) were derived from experimental data of Guo et al. (2020a). These stoichiometric factors are applied in the hydrolysis rate equations of the two models. For an overview of the values that were used for both models see Table 10. The model simulations were run and calibrated with dynamic input data. The COD content of the sludge fractions (see Table 11) are based on measured values for WAS that are retrieved from Guo et al. (2020a), (see Table 10). The measured characteristics refer to WAS from the same WWTP as in Guo et al. (2021). The COD values used for the calculations (in Table 11) were: 1.5 g-COD/g proteins, 1.07 g-COD/g carbohydrates, 2.88 g-COD/g lipids.

Table 10 - measured sludge characteristics for WAS with respect to the VS fraction, * result of statistical analysis (see Section 5.3.1).

WAS	Unit	WAS
VS/TS	-	0.74*
Degradable fraction of VS	-	0.62
Degradable fraction of WAS	-	0.46
Carbohydrates	mg glucose/g VS	190
Proteins	mg/g VS	389
Protein/Carbohydrates	2	2
Lipids	mg/g VS	35
VFAs	mg/g VS	5.6

Table 11 - calculated and calibrated parameters for both models (the general first-order hydrolysis model and the empirical hydrolysis model in combination with the simplified ADM1).

Parameter	Unit	Value
Yield of S_{su} from X_d	kg COD S · kg COD X^{-1}	COD in carbohydrates + $(1 - f_{fa,li}) \cdot$ COD in Lipids = $0.23 + 0.05 \cdot 0.12$
Yield of S_{aa} from X_d	kg COD S · kg COD X^{-1}	COD in Proteins = 0.65
Yield of S_{fa} from X_d	kg COD S · kg COD X^{-1}	$f_{fa,li} \cdot$ COD in lipids = $0.95 \cdot 0.12$
Uptake rate of acetate (km_{ac})	kg COD S · kg COD $X^{-1} \cdot d^{-1}$	20
Uptake rate of propionate (km_{pro})	kg COD S · kg COD $X^{-1} \cdot d^{-1}$	35

The values for the uptake rates of acetate (km_{ac}) and propionate (km_{pro}) are calculated by first manually fitting them to the methane flow, acetate- and propionate concentrations, respectively. Visual inspection was applied to estimate the goodness of fit. In this way a wide range of values can be tested in a short amount of time. This is done since the calibration algorithm of Aquasim[®] can quickly get stuck in local minima or run for a long time until it reaches a minimum. First manually pre-calibrating can save a significant amount of time. Finally, km_{ac} and km_{pro} were computationally fine-tuned. For the computational calibration the algorithm that is implemented in Aquasim[®] was used. Aquasim[®] uses Eq. 5 to minimize the sum of the squares of the weighted deviations between modelled output and the measurements (Reichert 1998).

$$\chi^2 = \sum_{i=1}^n \left(\frac{y_{meas,i} - y_i(p)}{\sigma_{meas,i}} \right)^2 \quad \text{Eq. 5}$$

4.5.1 Calibration of General First-Order Model and ADM1 with one k_{hyd}

The general first-order hydrolysis rate constant (k_{hyd}) was first manually pre-calibrated by fitting it to the experimental data of the methane flow and particulate COD. Finally, the parameter was computationally calibrated to fine-tune it. For the model calibration, the data of exp. phase 2 and 3 are used, i.e. the variables methane flow, tCOD, acetate and propionate concentrations. Data of experimental phase 4 (days 260 – 330) was reserved for model validation. The calibrated k_{hyd} values for the cascade ($0.21 \cdot d^{-1}$) and the reference ($0.3 \cdot d^{-1}$) were applied to all sludge fractions in ADM1 due to a parameter identifiability issue (discussed in Section 5.1).

4.5.2 Calibration of Empirical Hydrolysis Rate Model and simplified ADM1

The empirical hydrolysis rate model was calibrated with the same procedure as the first-order hydrolysis rate in ADM1 with respect to the parameters listed in Table 10 and Table 11. For the model calibration, the data of experimental phase 2 and 3, i.e. the variables methane flow, tCOD, acetate and propionate concentrations were used. Data of experimental phase 4 (days 260 – 330) was reserved for model validation.

Differently from the first-order model, the empirical model uses a changing hydrolysis rate coefficient for each reactor and with respect to each applied SRT. For the calibration of the hydrolysis rate coefficients the calculated specific hydrolysis rates of Guo et al. (2021) are used (see Table 12). These values of the specific hydrolysis rates were used as a dynamic input for k_{hyd} . After model calibration and for validation, k_{hyd} was implemented as a formula which was derived from the calculated specific hydrolysis rates (see Section 5.4). The logarithmic function (Eq. 4.2), shown in Section 4.4.2 is used for the calculation of k_{hyd} .

Table 12 - k_{hyd} values that were used for model calibration of the empirical model, the specific hydrolysis rates were calculated by Guo et al. (2021)

Specific Hydrolysis Rates (gVS/gCOD/d) used as k_{hyd}					
Time (d)	Cascade System				Reference
	R1	R2	R3	R4	
72 -152	0.061	0.045	0.031	0.028	0.034
153 - 259	0.074	0.061	0.054	0.047	0.046
260 - 330	0.099	0.089	0.071	0.064	0.056

4.6 Model Implementation in Aquasim[®]

4.6.1 Implementation of Reactors in Aquasim[®]

Both digestion systems were implemented in Aquasim[®]. In Aquasim[®] reactors are implemented in form of compartments. In this study all reactors were implemented as *Mixed Reactor Compartments*. The user can specify their volume, inflow, and loading. Furthermore, the user can manually specify the variables, processes and initial conditions that apply for the specific compartment.

All compartments are implemented in the software with the setup described in Section 3.2. For the cascade system all reactors are linked with *Advective Links*. All reactor volumes were set to be constant (outflow = inflow). Each *Mixed Reactor Compartment* is implemented together with its complementary headspace (in Aquasim[®] also defined as *Mixed Reactor Compartment*). The two compartments are linked by means of a *Diffusive Link*. After the implementation of the reactors variables and processes are defined. Variables and processes can be set active for each compartment individually. The same accounts for initial conditions and loadings.

4.6.2 Implementation of Equations in Aquasim[®]

The Aquasim[®] version of the standard ADM1 was modified according to Section 4.4. To implement a model in Aquasim[®] the user must first define all variables. Different types of “variables” can be chosen. In Aquasim[®], real variables are called *State Variables*. These need to be defined before the rate equations can be implemented. The rate equations can then be implemented similarly to a matrix as shown in Table 2 and Table 3 (see Section 3.1). After specifying the rate, the stoichiometric conversion factors for each substance involved in the defined reaction are entered. State Variables change according to the defined stoichiometric factor. When running a simulation Aquasim[®] calculates all State Variables for each specified timestep by solving the differential equation for the change of concentrations (see Eq. 6). In the study at hand, all models’ simulations, calibrations and sensitivity analysis were run with dynamic input loading.

In Aquasim[®], the rate of change of a concentration is defined as the sum of all reaction products times their equivalent stoichiometric coefficients of all process rates that are specified for a compartment. Aquasim[®] calculates the change of concentration over time by means of Eq. 6.

$$\frac{dC_i}{dt} = \frac{I_{in,C_i}}{V_R} - \frac{Q_{in}}{V_R} C_i + r_{C_i} \quad \text{Eq. 6}$$

Where:

- C_i is the substrate concentration (dynamic volume state variable)
- I_{in,C_i} is the loading of the substance, described by the concentration C_i multiplied with the inflow
- V_R is the reactor volume
- Q_{in} is the inflow to the reactor
- r_{C_i} is the sum of all transformation rates of the substance i with the concentration C_i

4.7 Analysis of Modelled Output

The standard ADM1 and the empirical model were both quantitatively analysed in terms of data fit. The R^2 - value as well as the RMSE were calculated for all modelled variables in relation to the experimental data of Guo et al. (2021). The modelled output was compared to the experimental data of the methane flow, COD -, ammonia -, acetate - and propionate concentrations. The modelled data was exported from Aquasim® in form of a “.txt” file. The data files were then analysed with help of a python script (see Appendix E).

To calculate realistic R^2 and RMSE values, the experimental data (Guo et al., (2021)) of the instable reactor phase (days 0 – 71) as well as the first SRT of each experimental phase was excluded for the analysis. Furthermore, outliers were removed from the data by the method as described in Section 4.1.

An interpretation of the model results solely based on R^2 or RMSE values cannot give a clear picture whether the model worked well for the applied case. Therefore, additionally to the quantitative analysis, the results are compared qualitatively in terms of trends that we see in the experimental data of Guo et al. (2021), meaning obvious increases or decreases in concentrations or flows that can visually be observed.

5 | RESULTS AND DISCUSSION

5.1 Sensitivity Analysis

The variables pH, methane flow, ammonia-, acetate-, propionate- and tCOD concentrations were tested for their Absolute Relative Sensitivity to a 100% increase of the hydrolysis rate coefficients ($k_{hyd,ch}$, $k_{hyd,li}$, $k_{hyd,pr}$). The result of the SensAR functions (explained in Section 4.1) was plotted with time. The SensAR curves for the tCOD (kg/m^3) and the methane flow (m^3/d) are shown below (see Figure 5 and Figure 6).

From the SensAR functions for the tCOD concentration and the methane flow one can observe similar curve shapes for all hydrolysis rate coefficients. This indicates a parameter identifiability problem of the tested parameters for the calibration procedure of the model since a positive change in one of the hydrolysis rate coefficients can be balanced out by a negative change in one of the others. Also, for the other variables pH, VFA and ammonia concentrations the same issue presented itself.

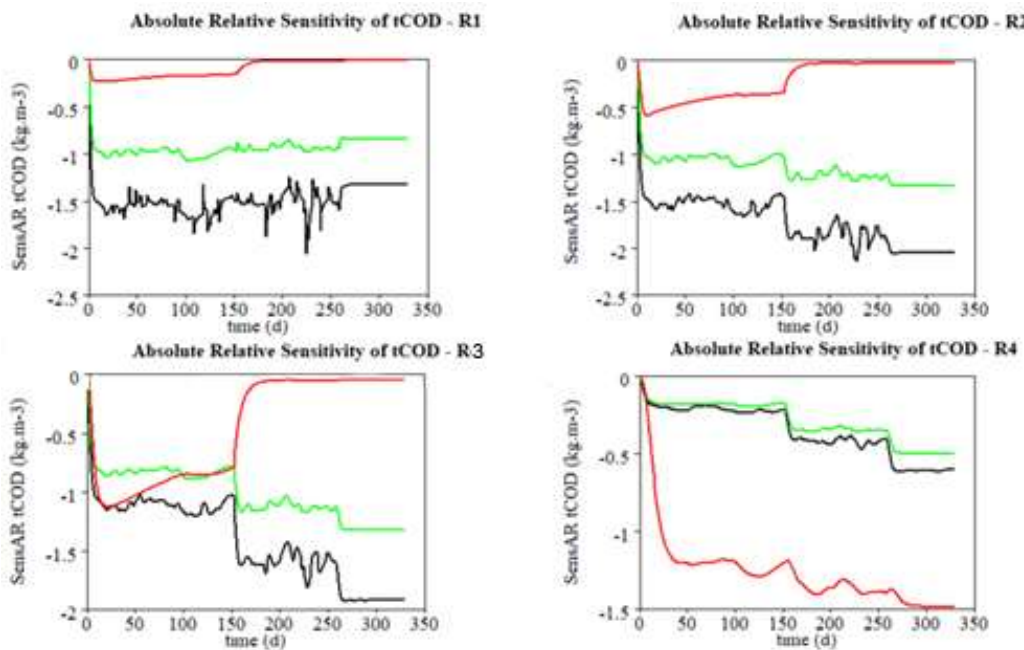


Figure 5 - SensAR function for tCOD (reactor 1 - 4 of the cascade system) with respect to the hydrolysis rate parameters k_{hyd} :
(black for carbohydrates, green for proteins and red for lipids)

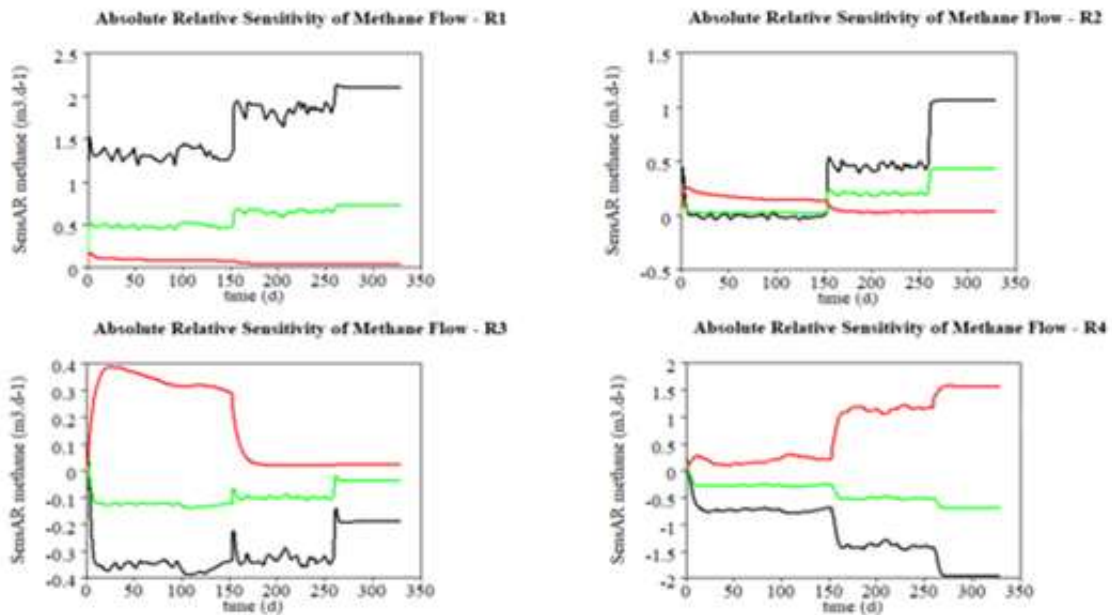


Figure 6 - SensAR function for methane (reactor 1 - 4 of the cascade system) with respect to the hydrolysis rate parameters k_{hyd} : (black for carbohydrates, green for proteins and red for lipids)

Discussion

It is questionable if a calibration of the three hydrolysis rate coefficients would yield a representative set of parameters that truly reflects the characteristics of the hydrolysis process. A solution to this problem could be to simplify the hydrolysis process in the ADM1 model by using only one hydrolysis rate coefficient for the sludge. This simplification is reasonable in the given context since little is known about the degradation kinetics of the individual sludge fractions. However, in other studies the description in ADM1 might have its justification for instance when a set of experimentally verified hydrolysis rate coefficients for the different sludge fractions exists.

5.2 Proposed Changes to ADM1 based on Parameter Identifiability Analysis

The results of the parameter identifiability (see Section 5.1) revealed that the complexity of the hydrolysis functions as they are implemented in ADM1 (described in Section 3.1) can be reduced for the modelling study at hand. Due to an identifiability problem of the hydrolysis rate parameters for the individual sludge fractions, the number of parameters is reduced from three to one. Furthermore, the disintegration step

of ADM1 is omitted in the empirical model as it was found to have little impact on the overall performance of ADM1. It is instead proposed to split the sludge with the loading to the reactor into a degradable fraction (X_d) and particulate inserts (X_i). The loading replaces the disintegration step ($j = 1$). Process 2, 3 and 4 of the standard ADM1 are combined in one hydrolysis step, i.e. process 2 (see Table 14). Only the degradable fraction is considered to be degradable in the hydrolysis rate expressions. The structure of the simplified ADM1 that was applied in combination with the empirical model as presented in Tables 13 and 14.

Table 13 – Applied changes to the standard ADM1 (Batstone, 2002) for this study; Biochemical rate coefficients ($v_{i,j}$) and kinetic rate equations (ρ_j) for particulate components ($i = 13 - 16$ and 24 , $j = 1 - 2$), for a full overview of ADM1 see Appendix D

Component →		i	13, 14, 15, 16	...	24	Rate (ρ_j , kg COD·m ⁻³ ·d ⁻¹)
j	Process ↓		$X_c, X_{ch}, X_{pr}, X_{li} \rightarrow$ X_d	...	X_i	
1	Loading		$f_{degradable}$		$1 - f_{degradable}$	$Q_{in} \cdot X_{WAS}$
2	Hydrolysis of WAS		-1			$k_{hyd,ch} \cdot X_d$
			Degradable particulates (kgCOD·m ⁻³)		Particulate inerts (kgCOD·m ⁻³)	

Table 14 - Applied changes to the standard ADM1 (Batstone, 2002) for this study; Biochemical rate coefficients ($v_{i,j}$) and kinetic rate equations (ρ_j) for particulate components ($i = 1 - 3$, $j = 1 - 2$), for a full overview of ADM1 see Appendix D

Component →		i	1	2	3	Rate (ρ_j , kg COD·m ⁻³ ·d ⁻¹)
j	Process ↓		S_{su}	S_{aa}	S_{fa}	
1	Loading					
2	Hydrolysis of Carbohydrates		$(f_{su,Xd}) + (1 - f_{fa,Xd})$	$f_{pr,Xd}$	$f_{fa,Xd}$	$k_{hyd,ch} \cdot X_{ch}$
			Monosaccharides (kgCOD·m ⁻³)	Amino acids (kgCOD·m ⁻³)	Long chain fatty acids (kgCOD·m ⁻³)	

5.3 Results of Statistical and Cascade System Analysis

5.3.1 Linear Regression for VS/TS

A linear regression was performed for the ratio of VS to TS (see Figure 7). The data implies a linear relationship between the VS concentration and the TS concentration with good agreement ($R^2 = 0.99$). However, at lower solids concentrations which are observed at the end of the cascade system the data points in Figure 7 indicate a stabilisation of the ratio of VS/TS. The ratio of VS/TS (0.74) was used to calculate the degradable fraction of WAS (see Table 10 in Section 4.5).

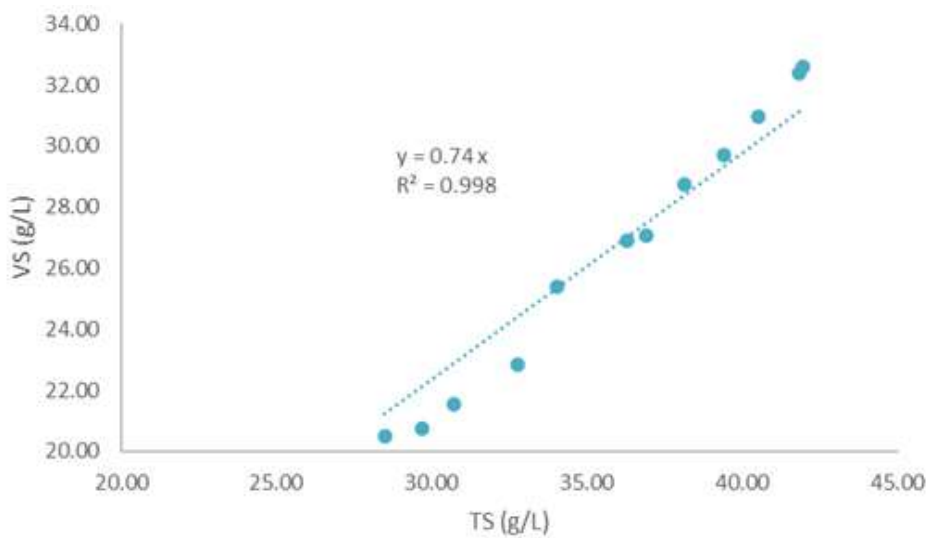


Figure 7- Linear regression for VS and TS, the dots represent average values of each reactor at different applied SRTs.

5.3.2 Linear Regression for gCOD/gVS

For the sludge input of the models the COD content of VS is required. Therefore, a linear regression was performed for the tCOD concentration and the VS concentration (see Figure 8). The data implies a linear relationship with good agreement ($R^2 = 0.99$). The linear coefficient of 1.55 was used as COD content for 1 g of VS. This COD content is somewhat higher than the generally assumed 1.42 g for biomass cells. The factor 1.55 was still used for the sludge input of degradable material and inert material for both hydrolysis models.

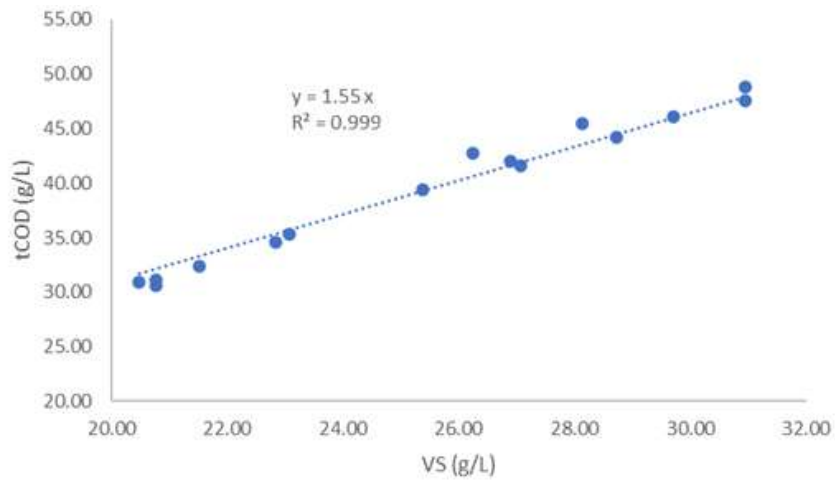


Figure 8 - Linear regression for tCOD and VS, the dots represent average values of each reactor at different applied SRTs.

5.3.3 Linear Regression for Specific Hydrolysis Rates against Enzymatic Activity

Guo et al. (2021) mentioned a higher increase in enzymatic activity compared to the calculated specific hydrolysis rates. The linear regression for specific hydrolysis rates against the total EA (see Figure 9) implies a linear correlation between the two variables but still supports Guo et al.'s (2021) observation since the slope of the regression line is far below 1. For the regression that is presented in this section the total enzymatic activity ($U \cdot g \text{ sludge}^{-1}$) was used.

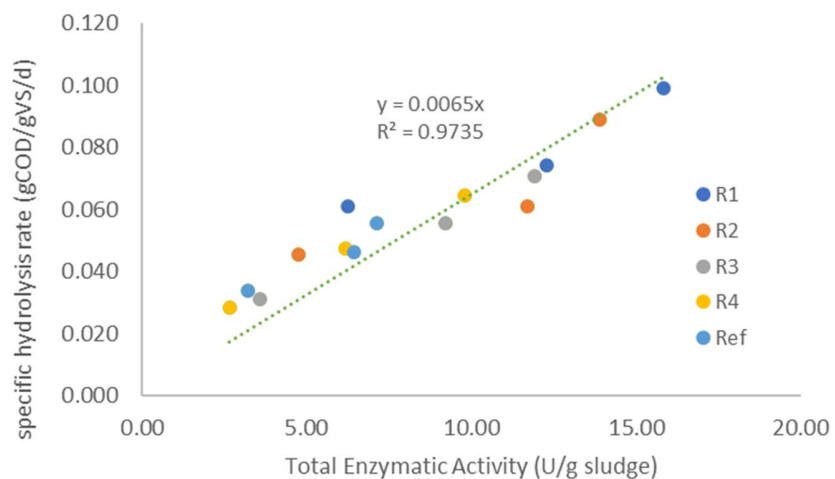


Figure 9 - Linear regression of specific hydrolysis rates and total enzymatic activity. The dots represent average values of each reactor at different applied SRTs.

5.3.4 Linear Regression for HRsp OLR and Load

The statistical analysis revealed that there is no clear linear correlation between the determined specific hydrolysis rates and the COD concentrations in each reactor for all applied SRT. This observation agrees with Guo et al., (2021). Figure 1 in Section 1.2 visualises this trend. However, in this study a strong linear correlation was found for the calculated specific hydrolysis rates with respect to the applied local Organic Loading Rate (OLR, ($\text{g VS} \cdot \text{L}^{-1} \cdot \text{d}^{-1}$)) for each reactor (see Figure 10). The specific hydrolysis rates are strongly linearly correlated with the OLR when looking at reactor one to three of the cascade system. The same accounts for the fourth reactor and the reference which show very similar behaviour (see Figure 10). An even stronger correlation of HRsp was found in relation to the load to each reactor (massflow of COD or solids per day, ($\text{g COD} \cdot \text{d}^{-1}$ or $\text{g VS} \cdot \text{d}^{-1}$)). This implies that the hydrolysis rate is mainly determined by the load (see Figure 11). However, Figure 10 indicates that hydraulically the cascade system might be seen as two distinct units. Reactors one to three can be seen as one unit and the fourth reactor as another. Logically, the fourth reactor is strongly influenced by the first three reactors in the system.

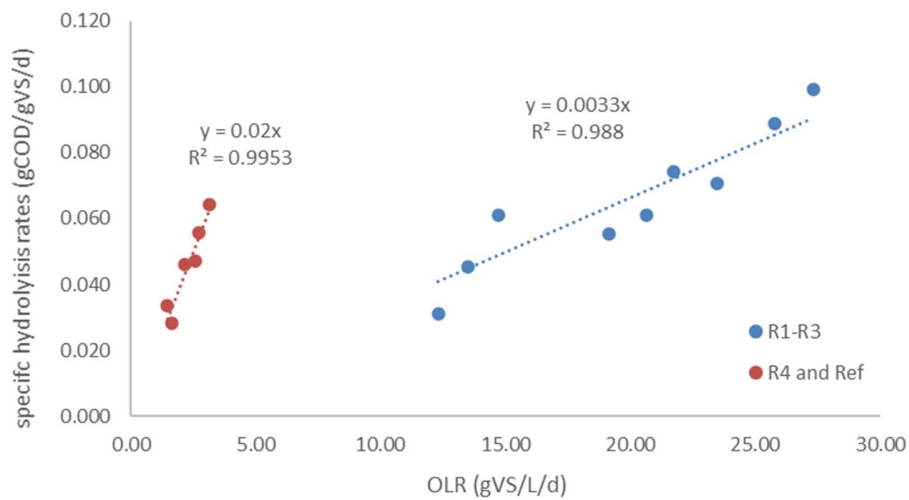


Figure 10 - Linear correlations between OLR and the HRsp for reactors 1 - 3 (R1-R3; blue) of the cascade and reactor 4 (R4, red) of the cascade and the Reference (Ref, red). The dots represent average values of each reactor at different applied SRTs.

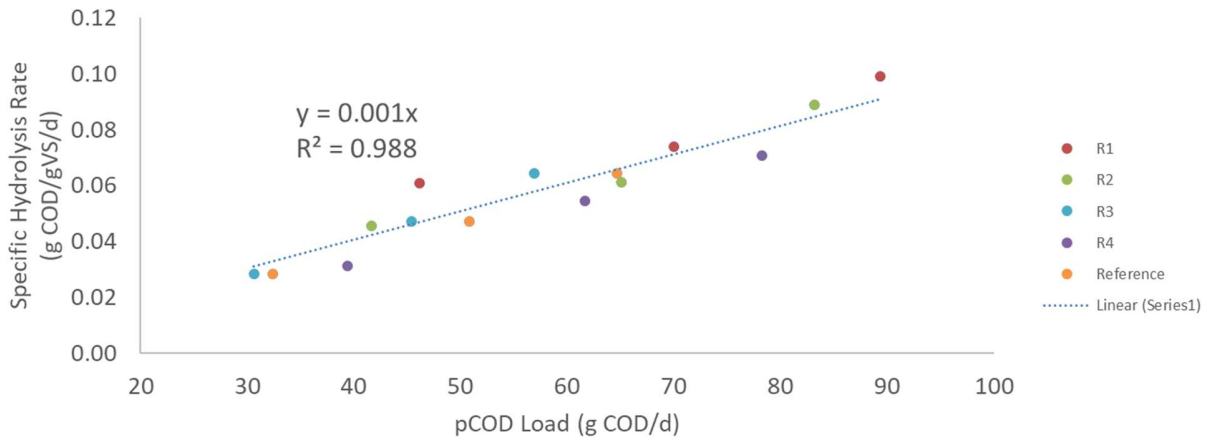


Figure 11 - Linear correlations between specific hydrolysis rates and the load for the cascade the Reference. The dots represent average values of each reactor at different applied SRTs.

Discussion

Based on Figure 10 it is possible that for the specific case of digestion of WAS in a cascade system a hydrolysis model with multiple hydrolysis rate coefficients for each reactor or one for reactors one to three and one for reactor four might perform better than the first-order hydrolysis model as currently implemented in ADM1 which assumes a hydrolysis rate constant for the entire system. The fact that the reactors during Guo et al.'s (2021) study were operated at constant influent tCOD and VS concentrations in combination with an increase at lowered SRTs inevitably leads to the assumption that the first-order hydrolysis rate constant is double-defined and must in fact be a coefficient. This statement assumes that an increase in specific hydrolysis rates would lead to a lower effluent COD or solids concentration. However, in the case of the reference we observe an increase of effluent concentrations even though that specific hydrolysis rates increased. Therefore, making the hydrolysis rate dependent on the load and the time available for hydrolysis seems reasonable.

5.4 Results of Cascade Systems Analysis

A series of CSTRs is approximating the behaviour of a plug-flow reactor but with the advantage of better controllability of the overall process. As pointed out in the literature review (see Section 2.5) a CSTR with low loading but a long retention time resembles the end of a batch experiment, whereas a CSTR with high loading and a short retention time resembles the beginning of a batch experiment. Since the cascade systems consists of a series of CSTRs it offers a good opportunity to look at the degradation of WAS with time. During the system's analysis this approach was used to describe the system mathematically. Each

reactor which each tested SRT was treated as an intermediate step of a batch experiment. The system analysis at hand revealed that the cascade might be describable by a batch with its different stages during digestion. Theoretically, a true plug-flow system without recycling stream is like a batch. In the case of the cascade system however there is a recycling stream from the third to the first reactor in series. The above-mentioned approach might therefore have its limitations in the given context of this study.

When looking at the specific hydrolysis rates that were calculated by Guo et al. (2021) (see Figure (12)) one can see that they change along the reactor and with the individual experimental phases (see Figure 12). This indicates that there are at least two unique factors influencing the specific hydrolysis rate.

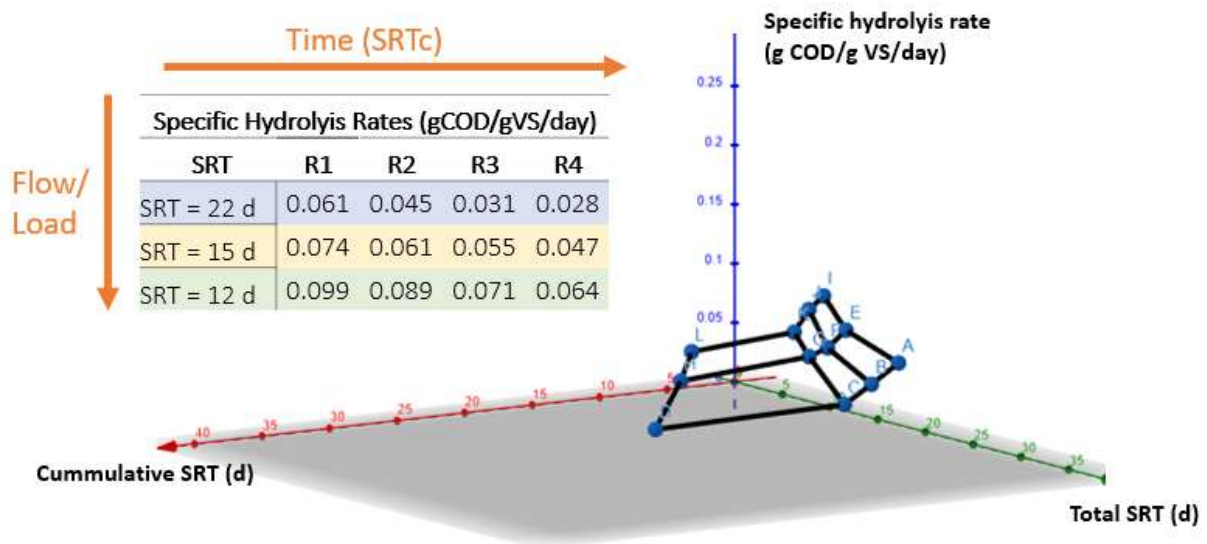
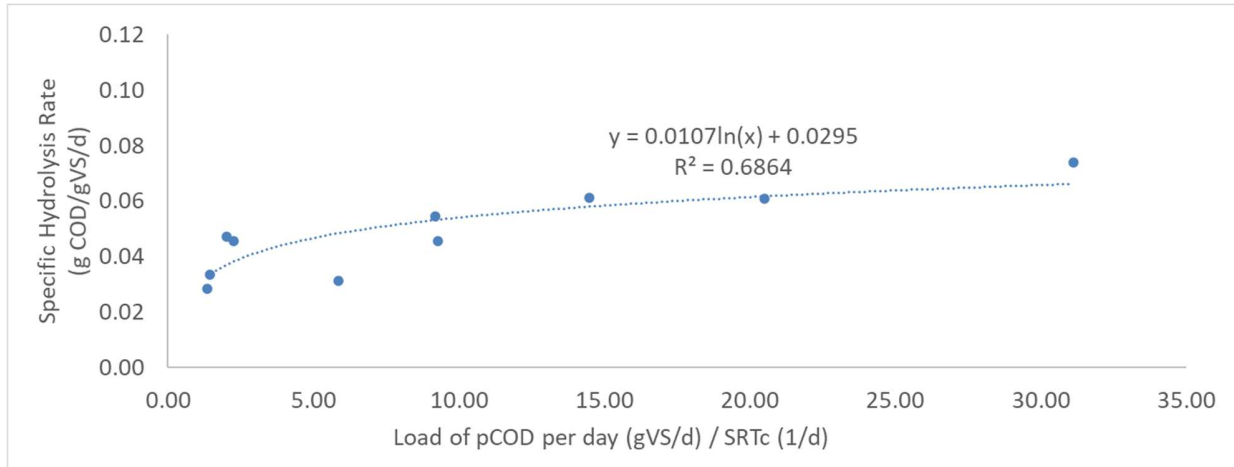


Figure 12 - Cascade system analysis with respect to specific hydrolysis rates, the individual dots in the graphic represent the HRsp plotted against total SRT (or flow) and against the SRTc (residence time in the system).

A plug flow reactor or a series of CSTRs differ from a single CSTR since they cause a change of concentration and loading along the reactor or with residence time in the system. Therefore, the term cumulative SRT (SRTc) is introduced to describe the solids retention time up to a certain point in the cascade system. The only real operational parameter that changes during the individual experimental phases of Guo et al.'s study (2021) is the inflow to the system or the load, meaning the mass flow of solids to the reactor per day. The load in Guo et al.'s (2021) study was inevitably changed by the inflow ($L \cdot d^{-1}$) to the systems. With the increase of the flow ($L \cdot d^{-1}$) also the total SRT of the system lowered and in consequence influenced the local residence times of each reactor in the system (described by SRTc).

Since the parameters load (massflow of solids to the system) and SRTc along the system are the only two factors that change it was hypothesised that the pattern that can be observed in the determined specific hydrolysis rates is dependent on the load and SRTc. Therefore, by mathematically combining these two factors it was tried to derive a relationship which can reproduce said specific hydrolysis rates. When dividing the load of particulate COD by the SRTc a similar pattern was achieved as can be seen in the change of specific hydrolysis rates with respect to a decrease in SRT. A logarithmic regression of the calculated specific hydrolysis rates with respect to the ratio of the $Load_{VS}$ to the SRTc yielded a function (see equation x) that can estimate the specific hydrolysis rates in the cascade system with good agreement ($R^2 = 0.69$).

Table 15 - Logarithmic regression for specific hydrolysis rates with respect to load and SRTc.



$$k_{hyd} \left(\frac{gCOD}{gVS \cdot d} \right) = 0.0107 \cdot \ln \left(\frac{Load_{COD} \left(\frac{gCOD}{d} \right)}{SRTc \left(\frac{1}{d} \right)} \right) + 0.0295 \quad Eq. 4.2$$

$$\alpha = 0.0107 \left(\frac{d}{gVS} \right) \quad Eq. 4.3$$

Since a pre-calibration of the empirical model (see Section 4.5.2) with the specific hydrolysis rates as dynamic time series yielded good results for the hydrolysis of WAS in the cascade system. The empirically derived logarithmic function (see Eq. 4.2) was implemented in the empirical model to replace the dynamic time-series so that the model can also be applied without hard data. This derived function can be seen as

a modification of the general first-order hydrolysis model by considering the ratio of substrate to biomass (S/X) by applying the load and a cumulative SRT. In Eq. 4.2, the load represents the substrate whereas the biomass is represented by the dilution rate (SRT^{-1}) or in the case of the cascade system ($SRTc^{-1}$).

Discussion

The mathematical description for the reproduction of specific hydrolysis rates that was derived in this section takes the ratio of sludge mass flow to $SRTc$ into account. The factor α in front of the natural logarithm, and therefore the shape of the curve, might be sludge dependent. The same accounts for the constant that is added to the logarithm. As can be seen in Eq. 4.2 there is a discrepancy of the units with the calculated specific hydrolysis rate. One solution could be to give the factor α in front of the \ln an adequate unit ($d \cdot g VS^{-1}$) (see Eq. 4.3). The unit of the factor α seems reasonable since it is sludge dependent how long it takes to degrade 1 g VS of a certain type of sludge. Potentially, it is possible that the factor α is recycling dependent, especially if the recirculation from reactor three to reactor one of the cascade functions as a pre-treatment for the post-digester (fourth reactor). In the empirical model the specific hydrolysis rates were multiplied with the pCOD (see Eq 4.1 in Section 4.4.2) which leads to somewhat unusual units. Therefore, this mathematical description of the system probably entails some other unknown factor which is needed to correct the units of the hydrolysis rate to the common unit of $gCOD \cdot d^{-1}$. For instance, this factor could be the contribution of VS to the total COD ($gVS \cdot g COD^{-1}$) which would correct the units adequately.

Arguably, the correlation between specific hydrolysis rates and the load (Figure 11) is much stronger than for the empirically derived function (Eq.4.2 in this Section). However, the logarithmic function (Eq. 4.2) has the benefit of limiting the hydrolysis rate for increasing loads since the logarithmic curve approaches a limit (see Figure 15). Intuitively, this description seems reasonable since above a certain ratio of load to residence time the biomass in the reactor would not have sufficient time to degrade the sludge any faster. However, Eq. 4.2 has its limitations. Since it is calibrated to Guo et al.'s (2021) cascade system it is unsure if it would work for a different reactor system or a different type of sludge. Future studies could test if this description is applicable to other systems or if it is unique for the researched cascade system. The second limitation for Eq. 4.2 is that it is only applicable if there is no washout of hydrolysing bacteria, meaning that the system SRT must already be correctly adjusted to maintain biomass at steady-state.

5.5 Modelled Results of ADM1

5.5.1 Results of ADM1 for Cascade System

This section qualitatively analysis the results of the modelled variables. Based on visual inspection the ADM1 managed to describe the experimental data of the cascade reactor for the first 150 days with respect to the measured variables tCOD ($\text{kg}\cdot\text{m}^{-3}$), methane flow ($\text{m}^3\cdot\text{d}^{-1}$) and acetate concentrations ($\text{kg}\cdot\text{m}^{-3}$) reasonably well (see Figure 13). The model underestimated the methane flow from day 260 onwards. This can be linked to the constant increase in particulate COD in the fourth reactor. The measured pH was consistently underestimated for all reactors of the cascade system. The strong decrease in pH of reactor 1 of the cascade could be explained by the sharp increase that can be seen in acetate concentrations (see Figure 13).

The graphs of the other modelled variables sCOD, ammonia, propionate and alkalinity are presented in Appendix C. Measured ammonia (mg/L) concentrations are consistently underestimated by the model. The same accounts for the alkalinity. Propionate is simulated similarly well as the acetate concentrations. The sCOD concentrations are in a reasonable range but the trends in the experimental data were not reproduced by the model.

Discussion

From visual inspection one can see that the standard ADM1 hydrolysis model was applicable for the first SRT of 22 days (until day 152). However, it seems that the model with one hydrolysis rate coefficient was not able to adapt to a lowered SRT with respect to solids concentration and methane flow in the fourth reactor (see modelled particulate COD in Figure 13). The representation of the methane flow and the tCOD concentrations deteriorated with shortening of SRT from 22 to 15 days in phase 3 (days 153 -259) and from 15 to 12 days in Phase 4 (days 260 - 330), respectively. The consistent underestimation of the ammonia concentration especially in reactor four might be linked to this observed trend. The modelled methane flow shows an increase even though effluent solids concentration increased. This seems logical, provided that no washout of biomass occurs, since when more solids are fed to the reactor per day there is more material that can be hydrolysed. However, the effluent solids concentration will still decrease at steady state since there is less time available for the biomass for solids hydrolysis.

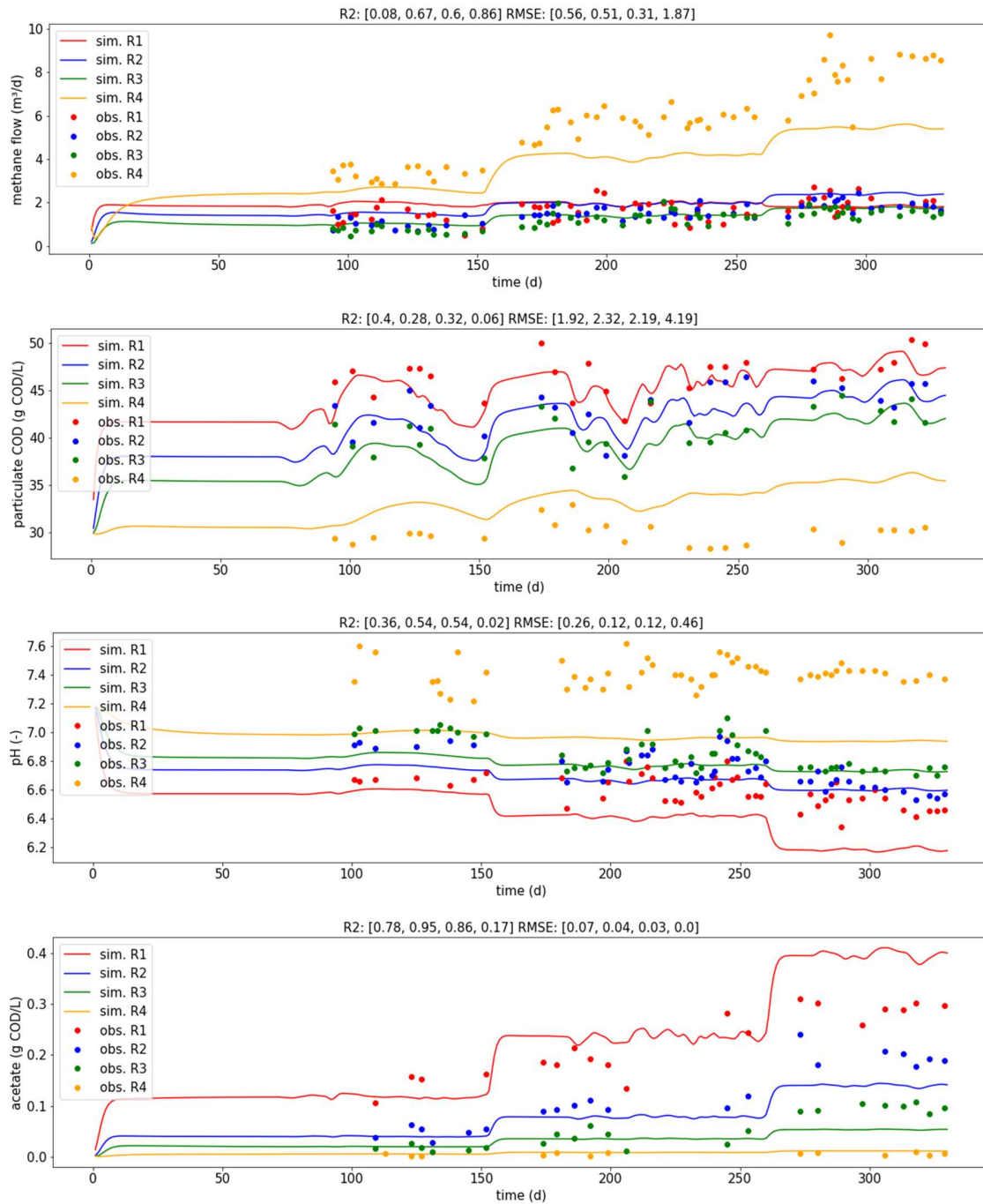


Figure 13 - Modelled results of the standard ADM1 hydrolysis model for the cascade system for the variables methane flow, tCOD, pH and acetate and plotted with the experimental data of Guo et al. (2021), The R² values and RMSE values in the title refer to reactor

5.5.2 Results of ADM1 for Reference System

This section qualitatively analysis the results of ADM1 for the reference reactor. Visually it is observable that ADM1 managed to describe the experimental data of the reference over all experimental phases with respect to the measured variables tCOD ($\text{kg}\cdot\text{m}^{-3}$), methane flow ($\text{m}^3\cdot\text{d}^{-1}$) reasonably well (see Figure 14). The modelled range of methane flow and COD concentrations fits to the experimental data. Also, the stepwise increase in methane flow is observable. The trends of increasing COD concentrations is reproduced by the model. The measured pH is in the range of what can be considered reasonable, especially towards the end of the simulation. Contradictory is that we observe a decrease in pH for the reference based on experimental data. The model shows a rather constant pH, likely linked to the low modelled acetate concentrations. This might be due to the calibration of the uptake rates for VFAs since the same can be observed with propionate. It seems that the calibration of these values fits for the cascade system but not for the reference which makes sense since the reference reactor suffered from process deterioration and VFA accumulation for the lowered SRTs of 15 and 12 days. This is not observed in the cascade which is possibly linked to some sort of microbial adaption as indicated by Guo et al. (2021).

The other modelled variables sCOD, ammonia, propionate and alkalinity are presented in Appendix C. Measured ammonia (mg/L) concentrations are consistently underestimated by the model. The same accounts for the alkalinity. Propionate is simulated similarly well as the acetate concentrations. The sCOD concentrations are in a reasonable range but the trends in the experimental data were not reproduced by the model.

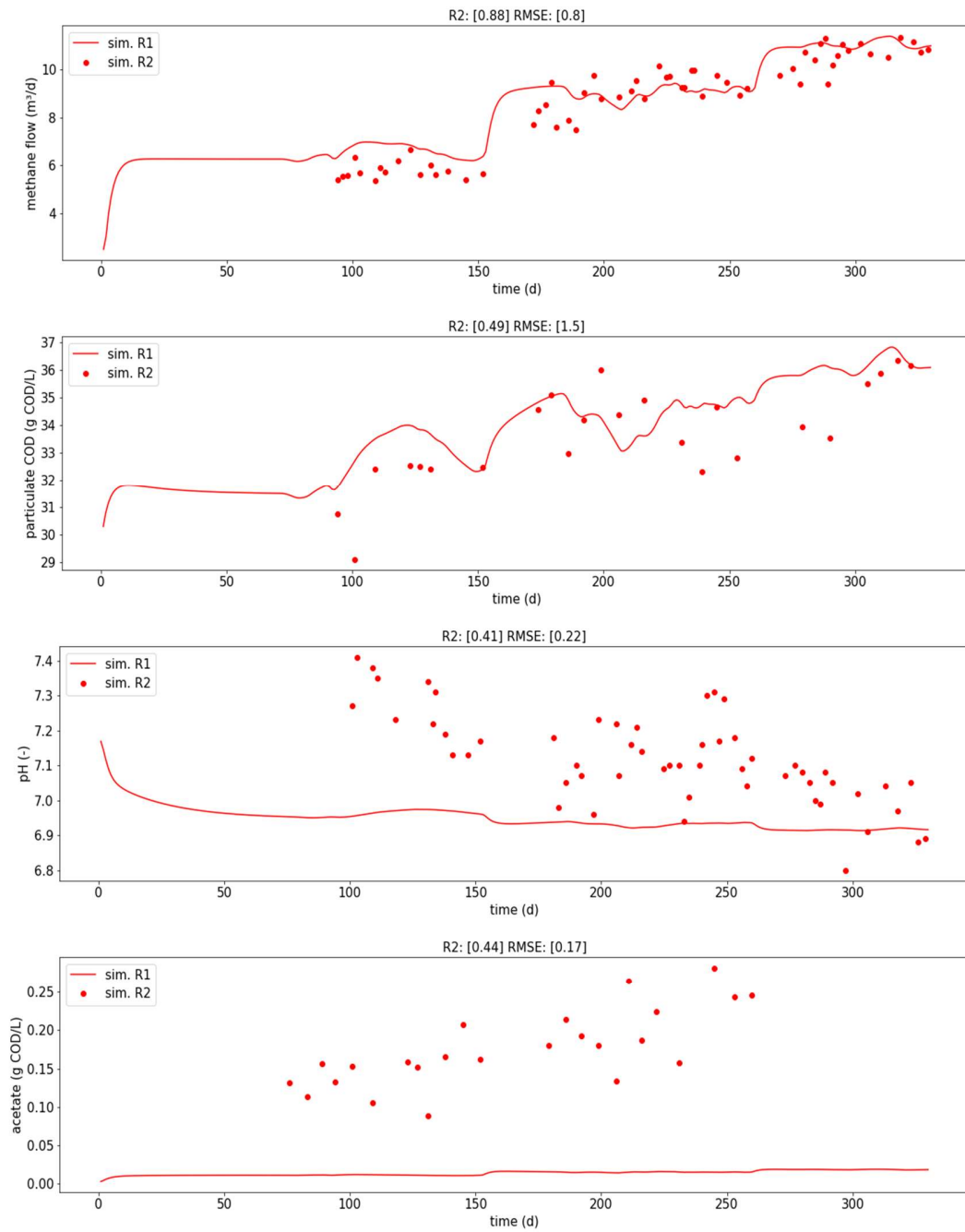


Figure 14 - Modelled results of ADM1 for the reference system for the variables methane flow, tCOD, pH and acetate and plotted with the experimental data of Guo et al. (2021), The R^2 values and RMSE values in the title refer to reactor one to four (from left to right).

5.6 Results of Empirical Hydrolysis Model

5.6.1 Results of Empirical Model for Cascade System

Just based on visual inspection it seems that the empirical hydrolysis model in combination with the simplified ADM1 managed to describe the cascade system better than the general first-order model (see Figure 15) for most variables and tested SRTs. This is especially obvious for the particulate COD in reactor four of the cascade (see figure x). The empirical model somewhat overestimated the methane flow during the first 150 days of the model for all reactors. For the other experimental phases (days 152 – 259 and 260 – 330) the methane flow is represented better. The range of ammonia concentrations was estimated significantly better than by the standard ADM1 (see Appendix C). In experimental phase 4 (days 260 – 330) the empirical model slightly overestimated the acetate concentrations in reactor 1 which possibly lead to a sharp modelled decrease in pH. Based on visual inspection the empirical hydrolysis model seems to perform well. The modelled variables sCOD, ammonia, propionate and alkalinity are presented in Appendix C.

Discussion

The visual inspection shows that the empirical model which applied a changing hydrolysis rate coefficient based on load and SRTc was applicable with good agreement for all applied SRTs (22, 15 and 12 days). With respect to the results of the ADM1 for the cascade system it seems that one hydrolysis rate coefficient was not able to fully describe the experimental data at the low SRTs with respect to solids concentration and methane flow in the fourth reactor (see Figure 15). Interestingly, the deterioration in predictive capability of ADM1 occurred for the fourth reactor. Therefore, it is possible to assume that the model was well calibrated with respect to the first three reactors. However, it is possible that the first three reactors of the cascade function as a sort of pre-treatment to the fourth reactor where most of sludge solids are converted. It might be that the first three reactors of the cascade enhance the hydrolysis rate in the fourth reactor. Assuming this is true, it would be difficult to capture this trend with only one hydrolysis rate coefficient since a calibration for the entire system would always entail a trade-off between the reactors. This shows the benefit of an equation that is based on the design of the reactor due to which the hydrolysis rate can adapt to the position along the cascade.

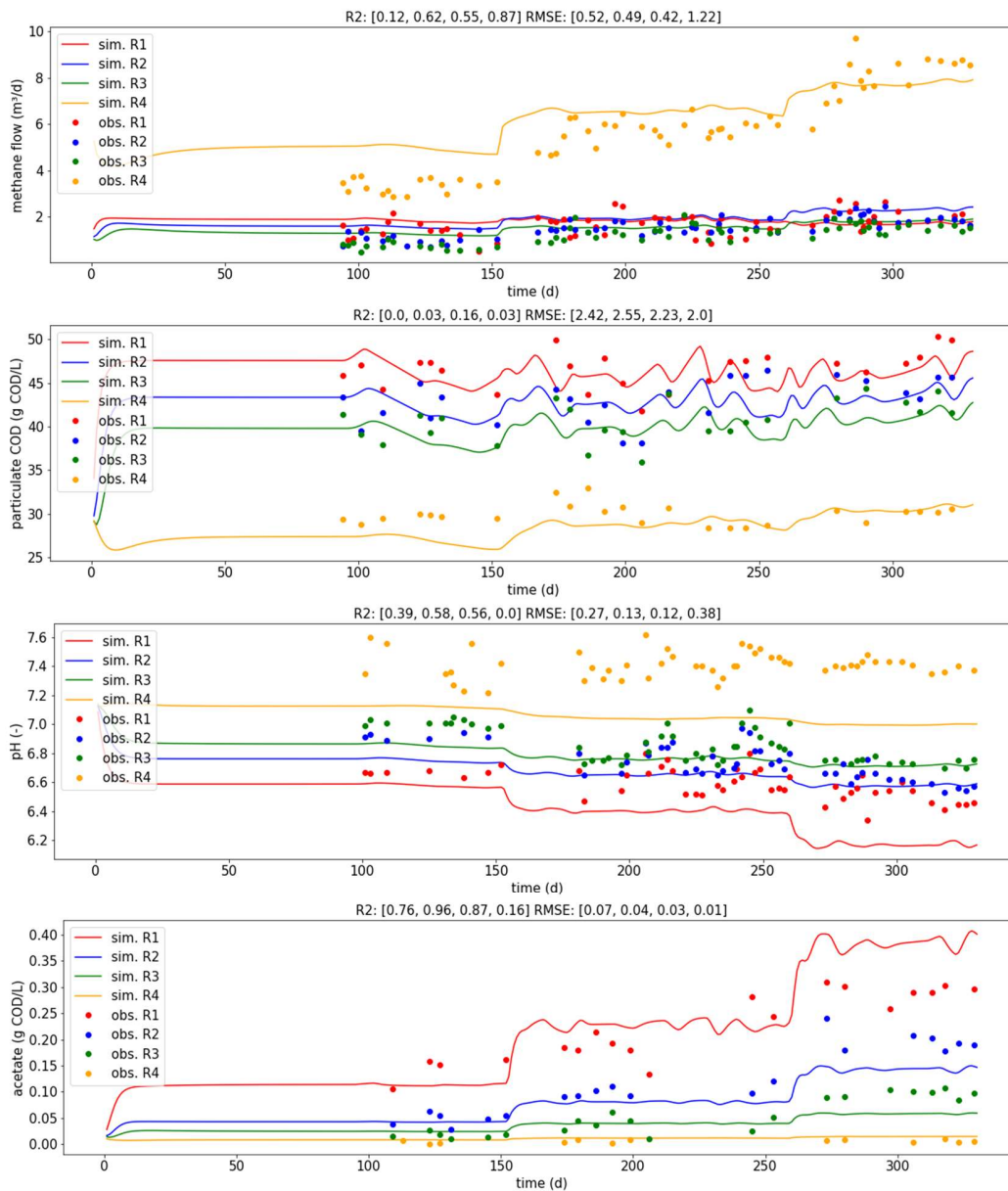


Figure 15 - Modelled results of the empirical hydrolysis model for the cascade system for the variables methane flow, tCOD, pH and acetate and plotted with the experimental data of Guo et al. (2021), The R^2 values and RMSE values in the title refer to reactor one to four (from left to right).

5.6.2 Results of Empirical Model for Reference System

Similar as for ADM1 the empirical model can reproduce the increase of particulate COD in the reference reactor (see Figure 16) for the shorter SRTs (15 and 12 days). Same as for the cascade system the empirical model overestimated the methane flow for the first 150 days of the simulation (Figure 16). The variables pH and acetate are represented in a similarly as by ADM1. The empirical model performs better in terms of prediction of ammonia concentration and alkalinity (see Appendix C). Modelled propionate concentrations and sCOD are shown in the Appendix C as well.

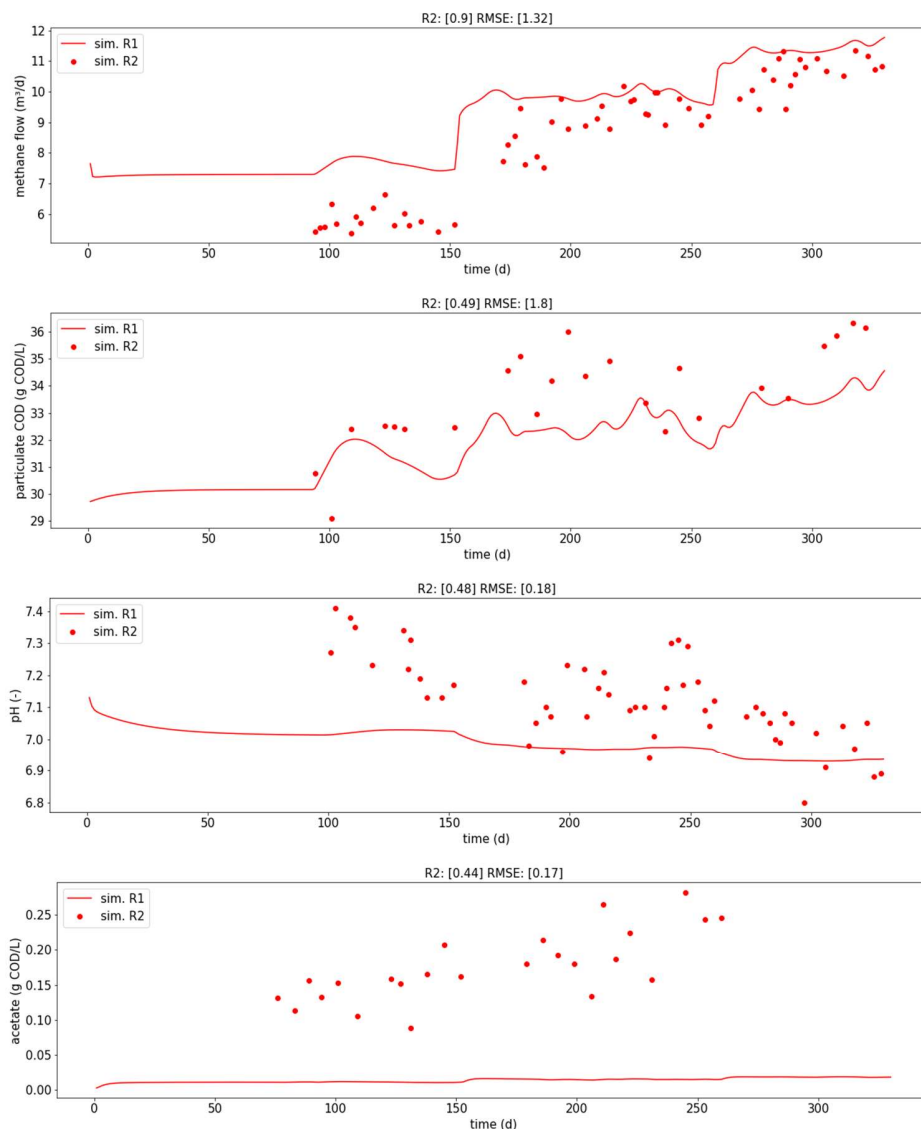


Figure 16 - Modelled results of the empirical model for the reference system for the variables methane flow, tCOD, pH and acetate and plotted with the experimental data of Guo et al. (2021), The R^2 values and RMSE values in the title refer to reactor one to four (from left to right).

5.9 Results of Quantitative Model Analysis (R^2 and RMSE)

Both models were quantitatively analysed in terms of R^2 and RMSE. The calculated R^2 and RMSE-values respectively are presented in Tables 16 and 17.

Table 16 - R^2 and RMSE values for the cascade system. Green cells mean that the respective model performed better than the other tested model.

Calculated R^2 -values for the Cascade System

Variable	Standard ADM1				Empirical hydrolysis model			
	R1	R2	R3	R4	R1	R2	R3	R4
pCOD	0.4	0.28	0.32	0.06	0	0.03	0.16	0.03
methane	0.08	0.67	0.6	0.86	0.12	0.62	0.55	0.87
pH	0.36	0.54	0.54	0.02	0.39	0.58	0.56	0
acetate	0.78	0.95	0.86	0.17	0.76	0.96	0.87	0.16
propionate	0.62	0.92	0.82	0.06	0.6	0.93	0.82	0.09
sCOD	0.66	0.05	0.1	0.43	0.65	0.02	0.11	0.47
ammonia	0.03	0.14	0.1	0.04	0.05	0.19	0.14	0.06
bicarbonate	0.02	0	0.17	0.46	0.01	0.02	0.23	0.5

Calculated RMSE-values for the Cascade System

Variable	Standard ADM1				Empirical hydrolysis model			
	R1	R2	R3	R4	R1	R2	R3	R4
pCOD	1.92	2.32	2.19	4.19	2.42	2.55	2.23	2
methane	0.56	0.51	0.31	1.87	0.52	0.49	0.42	1.22
pH	0.26	0.12	0.12	0.46	0.27	0.13	0.12	0.38
acetate	0.07	0.04	0.03	0	0.07	0.04	0.03	0.01
propionate	0.05	0.01	0.01	0	0.04	0.01	0.01	0
sCOD	0.53	0.8	1.14	0.33	0.41	0.67	1.04	0.29
ammonia	0.09	0.11	0.12	0.29	0.1	0.12	0.12	0.14
bicarbonate	369	296	271	801	331	320	377	215

From visual inspection both models seem to perform reasonably well. However, the quantitative analysis shows relatively low R^2 values for both models for almost all variables and reactors. This is likely due to

the many processes that are implemented in ADM1. This detailed description in ADM1 of the AD process might lead to peaks where no peaks are observable in the experimental data. The agreement of the modelled output with the range of the experimental data is of sufficient for most applications in practice. Therefore, a low R^2 value does not necessarily mean that the predictive capacity of the models is low. The level of detail that ADM1 produces is not required for most practices and the modelled output is within the range of the experimental data. It makes therefore sense to also look at the RMSE which is in reasonable agreement with the experimental data and good agreement with the standard deviations of the experimental data (see Appendix B).

Table 17 - R^2 and RMSE values for the reference system. Green cells mean that the respective model performed better than the other tested model.

Calculated R^2 -values for the Reference System			Calculated RMSE-values for the Reference System		
Variable	Model		Variable	Model	
	ADM1	Empirical		FO	Empirical
pCOD	0.49	0.49	pCOD	1.5	1.8
methane	0.88	0.9	methane	0.8	1.32
pH	0.41	0.48	pH	0.22	0.18
acetate	0.44	0.85	acetate	0.17	0.03
propionate	0	0.44	propionate	0.1	0.1
sCOD	0.22	0.24	sCOD	0.36	0.32
ammonia	0.03	0.02	ammonia	0.42	0.5
bicarbonate	0.74	0.81	bicarbonate	621	289

Discussion

Based on the quantitative analysis R^2 values are low for both models. However, the RMSE is in reasonable agreement with the experimental data for most variables. Therefore, the overall predictive capability can be considered as acceptable for both models. Based on the visual inspection the empirical model with dynamic hydrolysis rate coefficient is representing the cascade system better, especially with respect to the model performance in the fourth reactor. This is a strong point for the empirical model since the correct representation of particulate COD is one of the main points of interest when modelling the hydrolysis of sludge solids. The first-order hydrolysis model's predictive performance deteriorated with

lowered SRT, whereas the empirical model with dynamic hydrolysis rate coefficient was able to adapt and maintain to the lowered SRT (especially in phase 4, days 260 -330) and reproduce the stable particulate COD concentrations observed in the cascade system. The fact that the calculated specific hydrolysis rates of Guo et al. (2021) worked well to calibrate the empirical model and that the derived logarithmic function (see Eq. 4.2) based on load and SRT_c can be applied is an indication that the representation of the hydrolysis process in the cascade system with a varying hydrolysis rate coefficient based on load and residence time along the system is valid. This can at least be assumed for the cascade system and might be true for other plug-flow systems as well. In case of the reference system, it seems more practical to use the standard first-order model since it is easy to apply.

The implemented simplification of ADM1 (see Section 5.2) that was applied for the empirical model did not have any clear negative impact on the predictive performance of the model. However, this might be different for other systems or other sludge types. Therefore, the proposed simplification to ADM1 in this study seems to be reasonable since the parameter identifiability problem makes it difficult to meaningfully calibrate the hydrolysis rate coefficients for ADM1. It is possible that the partitioning in three individual sludge fractions makes sense when they hydrolysis rate coefficients are validated experimentally. However, this is rarely done in research and not common practice in anaerobic digester control and operation.

6 | GENERAL DISCUSSION

The modelling study at hand tested an empirical model based on experimental data (provided by Guo et al. (2021)) in combination with a simplified ADM1. The developed model was compared to the standard ADM1 which uses the general first-order hydrolysis model as suggested by Eastman and Ferguson (1981). Both models were applied for Guo et al.'s (2021) multi-stage cascade system and compared in terms of data fit.

The sensitivity analysis for parameter identifiability was used to see whether the hydrolysis rate coefficients that are currently applied in the standard ADM1 are identifiable by means of computational or manual parameter estimation. The sensitivity analysis showed that there is a parameter identifiability problem for the hydrolysis rate coefficients as they are currently implemented in ADM1. Therefore, a simplification of the model as discussed in Section 5.2 seems to be justified, at least for the modelled case of AD of WAS in the Guo et al.'s (2021) cascade system. The description of the hydrolysis process by means of three individual hydrolysis rate coefficients might be adequate for other sludge types and other reactor systems. However, if additionally, the hydrolysis rate coefficient for the individual sludge fractions would change with reactor design, as was indicated in this study, the mathematical description of the hydrolysis process would get overly complex and probably impossible to calibrate. Therefore, a simplification of ADM1 in terms of hydrolysis rates is proposed.

The general first-order hydrolysis description showed to be applicable as long as the systems HRT did not change. However, once the system SRT was lowered from 22, to 15 and then to 12 days respectively the predictive capacity of the first-order model decreased. Measured methane flows and COD concentrations were not accurately represented by the general first-order model. The empirical model with a hydrolysis rate coefficient based on load and retention time managed to describe the experimental data with good agreement except for ammonia concentrations and pH. This however, also applied for the general first-order model and might therefore be due to an improper calibration with respect to nitrogen contents of the WAS feed.

The fact that a single hydrolysis rate coefficient was not able to completely model Guo et al.'s (2021) cascade system for the digestion of WAS shows that the general first-order hydrolysis model might indeed need some sort of modification to be universally applicable as was previously proposed by other authors (see Section 2.3). One hydrolysis rate coefficient might be enough for sludges or substrates that are readily

biodegradable. However, it might be a more accurate description to use a hydrolysis rate coefficient for each reactor in a cascade system, especially for those sludges that experience significant structural changes in the sludge matrix (such as WAS) with degradation time. Multiple hydrolysis rate coefficients could potentially represent this gradual change in sludge structure and composition along the system.

The statistical analysis of Guo et al.'s (2021) system showed that the specific hydrolysis rates were dependent on the loading rate as well as the load and the SRT_c in the respective CSTRs of the cascade. The calibration of the empirical model by means of the calculated specific hydrolysis rates (Guo et al. 2021) strongly supports these results. Furthermore, the calibration by means of specific hydrolysis rates supports the calculation method of hydrolysis rate coefficients that was used by Guo et al. (2021) which is a method derived for batch experiments. It seems, that, as stated by Koch and Drewes (2014), methods that were developed for batch experiments are to some extent transferable to modelling CSTRs and cascading systems. In this context, the developed method of describing Guo et al.'s (2021) cascade system in terms of load and cumulative SRT (SRT_c) seems reasonable.

By means of regression models an empirical function was derived to calculate the specific hydrolysis rates or hydrolysis rate coefficients. The function was applied in the empirical model to estimate the hydrolysis rate coefficient dependent on load per day (mass flow) and retention time along the system. The reasoning behind this model is that not only the substrate concentration but the mass flow must play a significant role in the description of difficultly degradable sludge types as it takes time to break down the structure of WAS which might be represented by the here newly introduced factor α in the model. The factor $1/\text{SRT}_c$ included in the empirical logarithmic function might be comparable to the results of Nelson and Holder (2009) who showed that the effluent concentration of each CSTR in a series of CSTRs was dependent on the factor $1/\tau$ (τ = total residence time). A microbiological explanation for this description could be that the applied factor $1/\text{SRT}_c$ or $1/\tau$ (representing in fact the dilution rate of the cascade system or individual CSTRs) must be equal to the growth rate of the biomass otherwise washout of bacteria would occur.

It seems logical that the dilution rate in combination with the loading are two parameters that strongly influence the hydrolysis process of sludge solids. Whether the empirically derived logarithmic function to describe the hydrolysis of WAS in a cascade system can be transferred to other systems and sludge types remains to be seen. This could be the focus of future laboratory or modelling studies.

7 | CONCLUSIONS AND RECOMMENDATIONS

7.1 Conclusions

The study at hand revealed that the specific hydrolysis rates calculated by Guo et al. (2021) are strongly dependent on the applied loading rate and load. The specific hydrolysis rates also seem to be time dependent which was described by introducing the term cumulative SRT for cascade systems. These observations lead to development of an empirical model that can be seen as a modification to the first-order model that is implemented in ADM1.

The empirical model was shown to be applicable for the given context and managed to describe the hydrolysis of WAS in the cascade system to a reasonable extent. The performance of the empirical model in combination with the simplified ADM1 did not perform worse than the standard ADM1. With respect to the fourth reactor the empirical model managed to predict the experimental data significantly better than the standard ADM1. The empirical model also showed better performance for the variables ammonia and alkalinity where the ADM1 performed relatively low.

The results of this study indicate that the hydrolysis rate coefficients not only depend on sludge type and substrate concentration but also on the applied load of sludge solids per day and the local residence time in the system, the implementation of multiple hydrolysis rate coefficients could be a good approach to model cascade or multi-stage type systems.

The description of the hydrolysis process as currently implemented in ADM1, namely the partition of the sludge in individual fractions, seems to be too complex in the context of this study. Therefore, a simplification to one hydrolysis rate coefficient for the entire sludge, but dependent on sludge type and reactor design, is proposed.

The cascade system of Guo et al. (2021), as other cascade systems too, shows a concentration profile along the reactor. The description of the cascade system in terms of different stages of a batch reactor experiment was hypothesised and seems reasonable with view on the results of the study at hand. Therefore, the term cumulative SRT was used to describe the residence time up to certain point in the cascade system. The use of the SRT at each stage of the system seems reasonable in context of the modelled output.

The factor $1/SRT_c$ was applied in the empirical logarithmic function (see equation 4.3) to calculate the specific hydrolysis rates for the cascade system. The developed function showed to function reasonably well in the modelled context for most engineering applications. However, it is unclear at this stage if the derived empirical function can be applied to other systems and sludge types as well. Therefore, a follow up study to explore the potential of this description of the hydrolysis process is highly recommended.

7.2 Recommendations

With respect to the results of this study it is recommended to further investigate what setups for cascade reactors are most efficient for the hydrolysis of sludges such as WAS since the design of the overall system, i.e. the applied SRTs, loads as well as recycling ratios are crucial for the hydrolysis of solids. Furthermore, the position of the recycling stream seems to play an essential role in the hydrolysis of sludge solids and overall reactor performance.

It is further recommended to test if the application of multiple hydrolysis rate coefficients is also applicable for other systems and sludges. It is certainly interesting to further explore this direction for the modelling of cascade reactors.

The ADM1 seems to be overly complex with respect to the variables that are commonly measured in engineering practice, therefore it is proposed to reduce the number of hydrolysis rate equations. Even more so since there seems to be parameter identifiability issue for the hydrolysis rate coefficients as currently implemented in ADM1. The complexity could be reduced by implementing only one hydrolysis rate expression for the overall substrate instead of one individual expression for each sludge fractions. The partitioning into carbohydrates, proteins and lipids can still be accounted for by means of stoichiometric factors.

The empirical model implemented the degradable fraction of WAS as part of the feed by splitting it up in a degradable and a non-degradable fraction. The modelled results imply that this is a reasonable simplification for the given context where biomass and substrate were not clearly distinguishable.

A | References

- Alqahtani, R.T., Nelson, M.I. and Worthy, A.L. (2012) A fundamental analysis of continuous flow bioreactor models with recycle around each reactor governed by Contois kinetics. III. Two and three reactor cascades. *Chemical Engineering Journal* 183, 422-432.
- Alqahtani, R.T., Nelson, M.I. and Worthy, A.L. (2013) A fundamental analysis of continuous flow bioreactor models governed by Contois kinetics. IV. Recycle around the whole reactor cascade. *Chemical Engineering Journal* 218, 99-107.
- Angelidaki, I., Ellegaard, L. and Ahring, B.K. (1999) A Comprehensive Model of ANaerobic Bioconversion of Complex Substrate to Biogas.
- Appels, L., Baeyens, J., Degrève, J. and Dewil, R. (2008) Principles and potential of the anaerobic digestion of waste-activated sludge. *Progress in Energy and Combustion Science* 34(6), 755-781.
- Batstone, D.J. (1999) High Rate Anaerobic Treatment of Complex Wastewater, University of Queensland, Queensland.
- Batstone, D.J., Keller, J., Angelidaki, I., Kalyuzhnyi, S., Pavlostathis, S.G., Rozzi, A., Sanders, W.T.M., Siegrist, H. and Vavilin, V.A. (2002) The IWA Anaerobic Digestion Model 1 (ADM1). *Water Science and Technology* 45(10), 65 - 73.
- Batstone, D.J., Puyol, D., Flores-Alsina, X. and Rodríguez, J. (2015) Mathematical modelling of anaerobic digestion processes: applications and future needs. *Reviews in Environmental Science and Bio/Technology* 14(4), 595-613.
- Bolzonella, D., Pavan, P., Battistoni, P. and Cecchi, F. (2005) Mesophilic anaerobic digestion of waste activated sludge: influence of the solid retention time in the wastewater treatment process. *Process Biochemistry* 40(3-4), 1453-1460.
- Donoso-Bravo, A., Mailier, J., Martin, C., Rodriguez, J., Aceves-Lara, C.A. and Vande Wouwer, A. (2011) Model selection, identification and validation in anaerobic digestion: a review. *Water Res* 45(17), 5347-5364.
- Donoso-Bravo, A., Sadino-Riquelme, C., Gomez, D., Segura, C., Valdebenito, E. and Hansen, F. (2018) Modelling of an anaerobic plug-flow reactor. Process analysis and evaluation approaches with non-ideal mixing considerations. *Bioresour Technol* 260, 95-104.
- Eastman, J.A. and Ferguson, J.F. (1981) Solubilisation of Particulate Organic Carbon During the Acid Phase of Anaerobic Digestion. *Water Pollution Control Federation* 53(3), 352 - 366.
- Ersahin, M.E. (2018) Modeling the dynamic performance of full-scale anaerobic primary sludge digester using Anaerobic Digestion Model No. 1 (ADM1). *Bioprocess Biosyst Eng* 41(10), 1539-1545.
- Gosh, S. (1987) Improved Sludge Gasification by Two-Phase Anaerobic Digestion. *Journal of Environmental Engineering* 113(6).
- Gosh, S., Conrad, J.R. and Klass, D.L. (1975) Anaerobic acidogenesis of wastewater sludge. *Journal of Water Pollution Control Federation* 47(1), 30 - 45.

- Guo, H., Felz, S., Lin, Y., van Lier, J.B. and de Kreuk, M. (2020a) Structural extracellular polymeric substances determine the difference in digestibility between waste activated sludge and aerobic granules. *Water Res* 181, 115924.
- Guo, H., Oosterkamp, M.J., Tonin, F., Hendriks, A., Nair, R., van Lier, J.B. and de Kreuk, M. (2021) Reconsidering hydrolysis kinetics for anaerobic digestion of waste activated sludge applying cascade reactors with ultra-short residence times. *Water Res* 202, 117398.
- Guo, H., van Lier, J.B. and de Kreuk, M. (2020b) Digestibility of waste aerobic granular sludge from a full-scale municipal wastewater treatment system. *Water Res* 173, 115617.
- Koch, K. and Drewes, J.E. (2014) Alternative approach to estimate the hydrolysis rate constant of particulate material from batch data. *Applied Energy* 120, 11-15.
- Mairet, F., Bernard, O., Ras, M., Lardon, L. and Steyer, J.P. (2011) Modeling anaerobic digestion of microalgae using ADM1. *Bioresour Technol* 102(13), 6823-6829.
- Maspolim, Y., Zhou, Y., Guo, C., Xiao, K. and Ng, W.J. (2015) Comparison of single-stage and two-phase anaerobic sludge digestion systems - Performance and microbial community dynamics. *Chemosphere* 140, 54-62.
- Nelson, M.I. and Holder, A. (2009) A fundamental analysis of continuous flow bioreactor models governed by Contois kinetics. II. Reactor cascades. *Chemical Engineering Journal* 149(1-3), 406-416.
- Odnell, A., Recktenwald, M., Stensen, K., Jonsson, B.H. and Karlsson, M. (2016) Activity, life time and effect of hydrolytic enzymes for enhanced biogas production from sludge anaerobic digestion. *Water Res* 103, 462-471.
- Reichert, P. (1998) *Aquasim 2.0 - User Manual, Computer Program for the Identification and Simulation of Aquatic Systems*, Swiss Federal Institute for Environmental Science and Technology (EAWAG), Switzerland.
- Sanders, W.T.M. (2001) *Anaerobic hydrolysis during digestion of complex substrates*. Doctoral thesis, University of Wageningen.
- Vavilin, V.A., Fernandez, B., Palatsi, J. and Flotats, X. (2008) Hydrolysis kinetics in anaerobic degradation of particulate organic material: an overview. *Waste Manag* 28(6), 939-951.
- Vavilin, V.A., Rytov, S.V. and Lokshina, L.Y. (1996) *A Description of Hydrolysis Kinetics in Anaerobic Degradation of Particulate Organic Matter*.
- Zhen, G., Lu, X., Kato, H., Zhao, Y. and Li, Y.-Y. (2017) Overview of pretreatment strategies for enhancing sewage sludge disintegration and subsequent anaerobic digestion: Current advances, full-scale application and future perspectives. *Renewable and Sustainable Energy Reviews* 69, 559-577.

B | APPENDIX – Data Overview

This is an overview of the mean values including standard deviations for each reactor for experimental phase 2 (SRT = 22 days), phase 3 (SRT = 15 days) and phase 4 (SRT = 12 days) respectively. The data provided by Guo et al. (2021) presented here was cleaned from outliers. Data of instable reactor periods were excluded as well. The cleaning process led to some means not having a standard deviation (marked with (-)) because only one value remained. These are exceptions and those data was not used for the model.

Table 18 - Mean values of total enzymatic activity for each reactor and all tested SRTs.

Enzymatic Activity (U/g sludge)	Cascade					Reference
	Feed	R1	R2	R3	R4	Reference
SRT=22 days	2.97	6.25	4.76	3.58	2.65	3.23
Std. Dev.	0.43	0.50	0.41	0.33	0.31	0.39
SRT=15 days	3.46	12.28	11.71	9.20	6.16	6.43
Std. Dev.	0.67	1.05	0.74	0.46	0.24	0.34
SRT=12 days	3.55	15.84	13.89	11.91	9.80	7.13
Std. Dev.	0.70	0.88	0.82	0.65	0.48	0.66

Table 19 - Mean values of specific hydrolysis rates for each reactor and all tested SRTs.

Specific Hydrolysis Rates (gCOD/gVS/day)	Cascade				Reference
	R1	R2	R3	R4	
Ph 2 (SRT 22 = d)	0.061	0.045	0.031	0.028	0.034
Std. Dev.	0.007	0.012	0.004	0.003	0.003
Ph 3 (SRT 15 = d)	0.074	0.061	0.054	0.047	0.046
Std. Dev.	0.014	0.016	0.011	0.006	0.005
Ph 4 (SRT 12 = d)	0.099	0.089	0.071	0.064	0.056
Std. Dev.	0.014	0.011	0.012	0.009	0.009

Table 20 - Mean values of tCOD for each reactor and all tested SRTs.

Mean tCOD (g/L) at each tested SRT in each reactor						
	Feed	Reactor 1	Reactor 2	Reactor 3	Reactor 4	Reference
SRT 22 d	50.86	46.41	41.83	39.83	30.45	32.92
Std. dev.	2.35	1.85	1.78	1.28	0.51	0.62
SRT 15 d	50.84	47.44	44.16	41.93	30.75	34.38
Std. dev.	1.97	2.41	2.81	2.55	1.20	1.01
SRT 12 d	52.01	49.14	46.01	43.26	31.00	35.57
Std. dev.	1.02	1.62	1.36	1.57	0.21	1.26

Table 21 - Mean values of sCOD for each reactor and all tested SRTs.

Mean sCOD (g/L) at each tested SRT in each reactor						
	Feed	Reactor 1	Reactor 2	Reactor 3	Reactor 4	Reference
SRT 22 d	0.53	0.92	0.71	0.65	0.56	0.59
Std. dev.	0.30	0.34	0.26	0.25	0.21	0.23
SRT 15 d	0.64	1.06	0.81	0.66	0.62	0.64
Std. dev.	0.19	0.10	0.08	0.07	0.07	0.08
SRT 12 d	0.65	1.30	1.13	0.93	0.78	0.79
Std. dev.	0.07	0.06	0.04	0.02	0.06	0.08

Table 22 - Mean values of particulate COD for each reactor and all tested SRTs.

Mean particulate COD (g/L) at each tested SRT in each reactor						
	Feed	Reactor 1	Reactor 2	Reactor 3	Reactor 4	Reference
SRT 22 d	51.32	46.01	42.02	39.70	29.51	31.73
Std. dev.	1.78	1.48	1.98	1.54	0.40	1.32
SRT 15 d	49.50	46.09	42.78	40.11	30.08	34.11
Std. dev.	2.30	2.42	2.94	2.42	1.64	1.12
SRT 12 d	51.48	48.16	44.95	42.99	30.11	35.21
Std. dev.	1.32	1.64	1.14	1.18	0.58	1.19

Table 23 - Mean values of methane flow for each reactor and all tested SRTs.

Mean methane flow (L/d) at each tested SRT in each reactor						
	Cascade	Reactor 1	Reactor 2	Reactor 3	Reactor 4	Reference
SRT 22 d	6.54	1.35	1.01	0.72	3.33	5.78
Std. dev.	0.40	0.41	0.23	0.15	0.32	0.36
SRT 15 d	10.29	1.64	1.53	1.33	5.71	9.05
Std. dev.	0.87	0.44	0.23	0.32	0.53	0.76
SRT 12 d	13.30	1.99	1.92	1.54	7.91	10.59
Std. dev.	0.92	0.38	0.27	0.23	1.09	0.59

Table 24 - Mean values of pH for each reactor and all tested SRTs.

Mean pH (-) at each tested SRT in each reactor						
	Feed	Reactor 1	Reactor 2	Reactor 3	Reactor 4	Reference
SRT 22 d	6.46	6.67	6.91	7.01	7.39	7.26
Std. dev.	0.10	0.03	0.02	0.02	0.14	0.10
SRT 15 d	6.34	6.63	6.77	6.85	7.42	7.13
Std. dev.	0.15	0.10	0.09	0.10	0.09	0.10
SRT 12 d	6.41	6.50	6.63	6.74	7.40	7.00
Std. dev.	0.06	0.08	0.07	0.02	0.03	0.09

Table 25 - Mean values of total VFA concentrations for each reactor and all tested SRTs.

Mean total VFA concentration (mg/L) at each tested SRT in each reactor						
	Feed	Reactor 1	Reactor 2	Reactor 3	Reactor 4	Reference
SRT 22 d	118	282	79	32	6	9
Std. dev.	8	91	25	21	3	4
SRT 15 d	151	365	163	58	6	6
Std. dev.	138	49	15	24	3	4
SRT 12 d	115	518	324	144	6	84
Std. dev.	18	19	43	30	3	13

Table 26 - Mean values of acetate for each reactor and all tested SRTs.

Mean acetate concentration (mg/L) at each tested SRT in each reactor						
	Feed	Reactor 1	Reactor 2	Reactor 3	Reactor 4	Reference
SRT 22 d	49	144	48	17	3	2
Std. dev.	6	26	13	6	3	1
SRT 15 d	60	201	95	37	6	4
Std. dev.	32	45	20	16	3	0
SRT 12 d	19	292	198	97	7	61
Std. dev.	10	16	21	8	3	6

Table 27 - Mean values of propionate for each reactor and all tested SRTs.

Mean propionate concentration (mg/L) at each tested SRT in each reactor						
	Feed	Reactor 1	Reactor 2	Reactor 3	Reactor 4	Reference
SRT 22 d	26	97	21	4	3	5
Std. dev.	-	28	8	2	-	0
SRT 15 d	20	105	56	18	6	-
Std. dev.	18	20	5	9	-	
SRT 12 d	18	170	101	45	5	20
Std. dev.	10	24	14	8	2	5

Table 28 - Mean values of ammonia for each reactor and all tested SRTs.

Mean ammonia (NH₄⁺) concentration (mg/L) at each tested SRT in each reactor						
	Feed	Reactor 1	Reactor 2	Reactor 3	Reactor 4	Reference
SRT 22 d	60	372	506	576	1099	968
Std. dev.	19	53	19	17	35	19
SRT 15 d	100	391	524	623	1101	1028
Std. dev.	41	52	53	74	62	81
SRT 12 d	68	410	578	672	1150	1076
Std. dev.	16	49	39	40	70	30

Table 29 - Mean values of phosphate for each reactor and all tested SRTs.

Mean phosphate (PO₄³⁺) concentration (mg/L) at each tested SRT in each reactor						
	Feed	Reactor 1	Reactor 2	Reactor 3	Reactor 4	Reference
SRT 22 d	360	647	682	663	600	584
Std. dev.	43	14	29	1	90	-
SRT 15 d	410	656	641	656	626	608
Std. dev.	113	43	54	60	70	72
SRT 12 d	412	676	683	738	739	677
Std. dev.	97	19	9	40	26	23

Table 30 - Mean values of alkalinity for each reactor and all tested SRTs.

Mean alkalinity (CaCO₃) (mg/L) at each tested SRT in each reactor						
	Feed	Reactor 1	Reactor 2	Reactor 3	Reactor 4	Reference
SRT 22 d	677	1435	1831	2161	3957	3638
Std. dev.	98	316	305	181	17	95
SRT 15 d	691	1577	1809	1991	3656	3254
Std. dev.	86	361	305	115	159	62
SRT 12 d	888	1502	1767	2029	3868	3306
Std. dev.	-	-	-	-	-	-

Table 31 - Mean values of volatile solids for each reactor and all tested SRTs.

mean volatile solids concentration (g/L)						
	Feed	Reactor 1	Reactor 2	Reactor 3	Reactor 4	Reference
SRT 22 d	32.4	29.7	27.1	25.4	20.8	21.5
Std. dev.	2.3	1.6	1.3	1.8	1.1	1.1
SRT 15 d	32.5	30.9	28.6	26.9	20.5	22.8
Std. dev.	1.8	1.7	1.7	1.8	0.9	0.6
SRT 12 d	32.7	30.8	28.0	26.2	20.9	23.1
Std. dev.	0.9	1.3	1.3	1.2	0.7	0.8

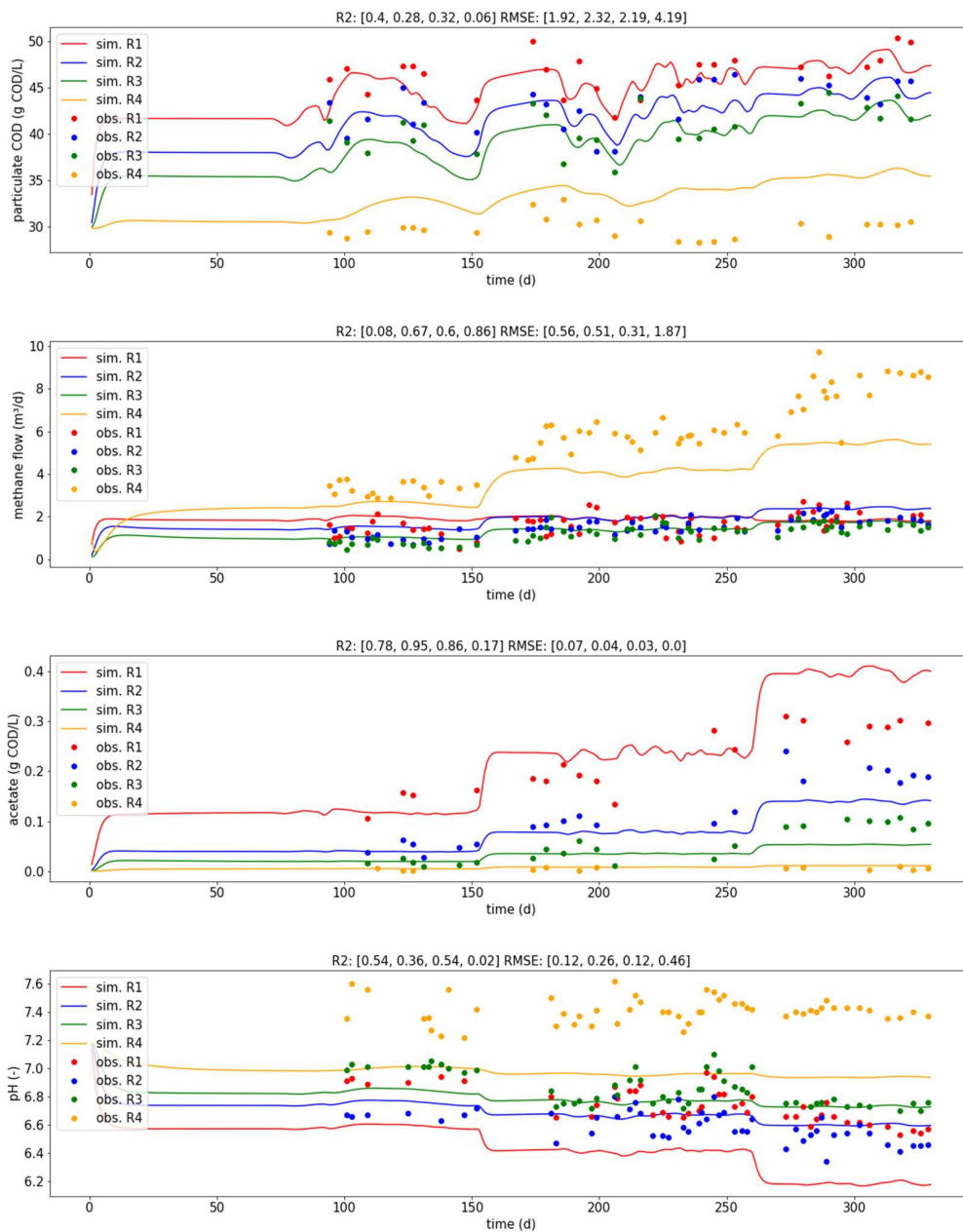
Table 32 - Mean values of total solids for each reactor and all tested SRTs.

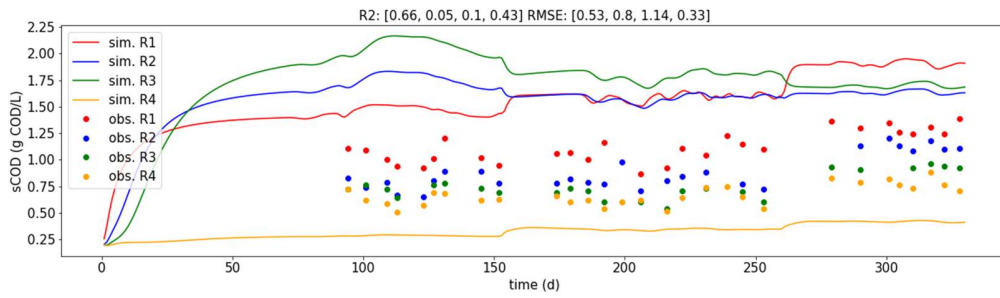
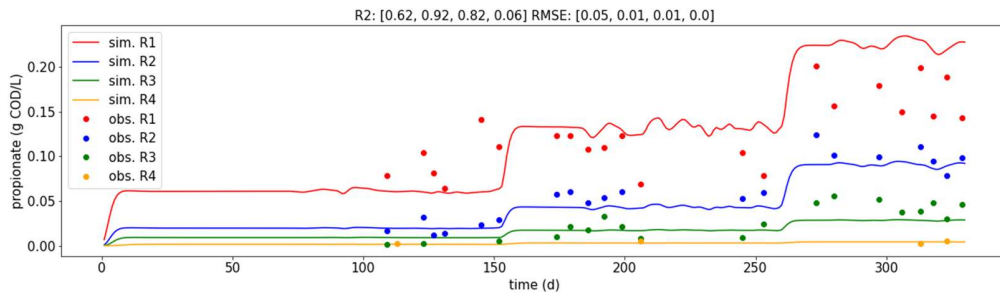
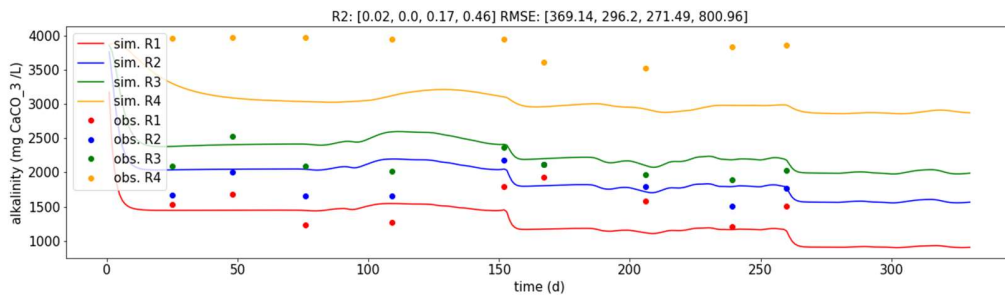
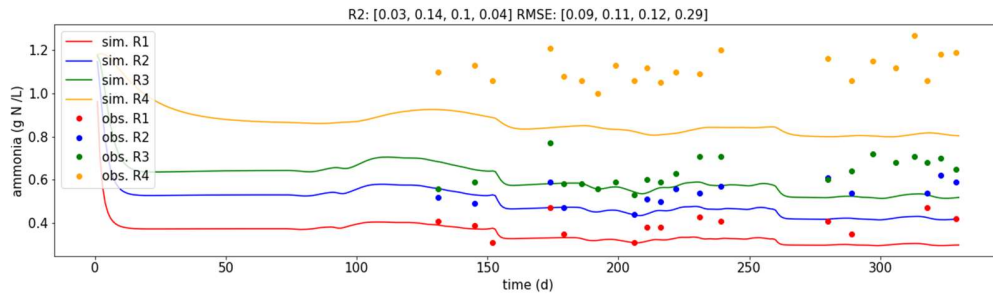
mean total solids concentration (g/L)						
	Feed	Reactor 1	Reactor 2	Reactor 3	Reactor 4	Reference
SRT 22 d	41.8	39.4	36.9	34.0	29.7	30.7
Std. dev.	1.9	1.9	2.3	3.1	1.6	1.4
SRT 15 d	41.9	40.4	38.0	36.2	28.5	32.8
Std. dev.	2.1	1.7	1.9	2.6	1.3	1.1
SRT 12 d	-	-	-	-	-	-
Std. dev.	-	-	-	-	-	-

C | Appendix – Additional Figures

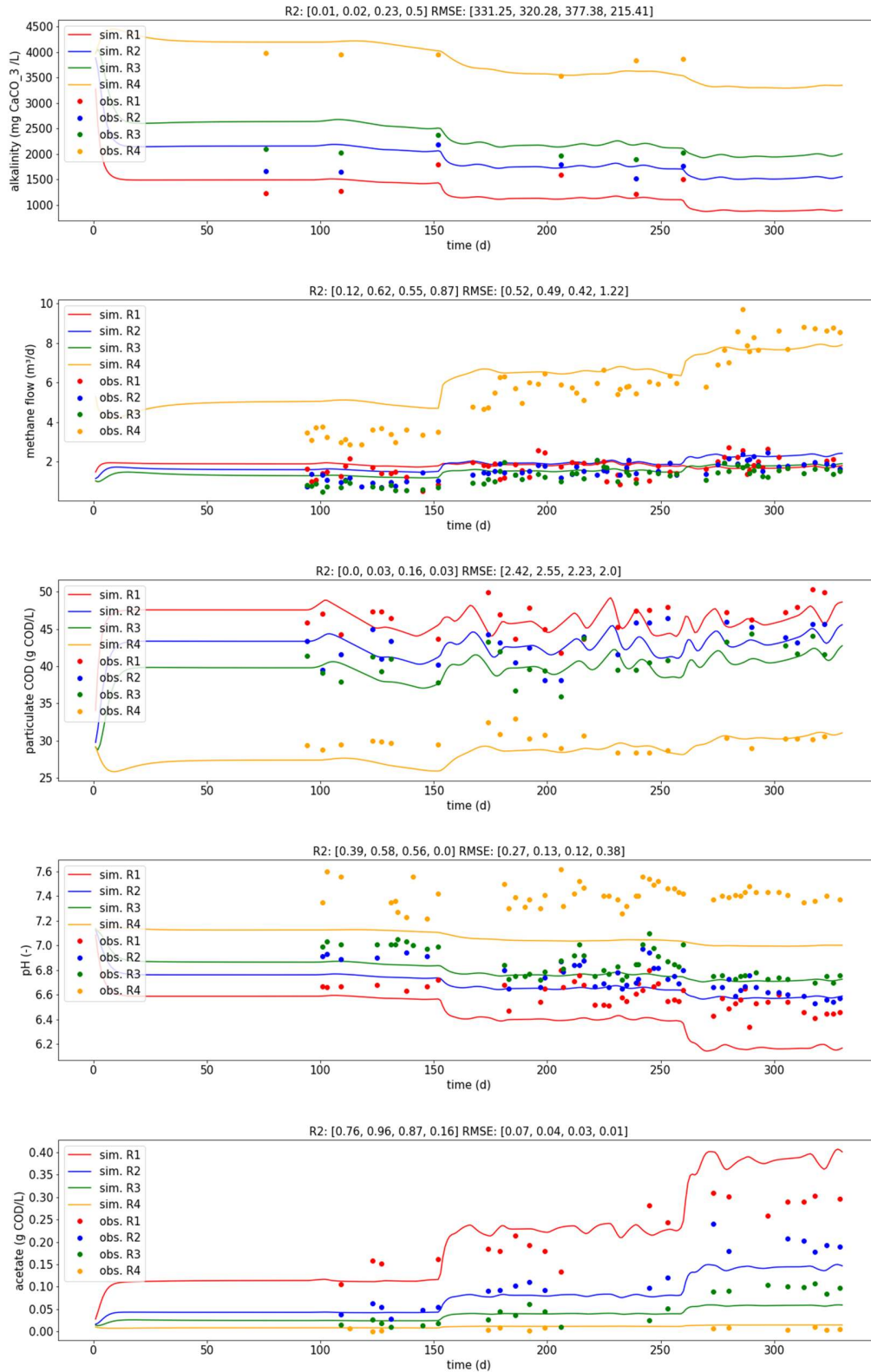
Modelled Outputs

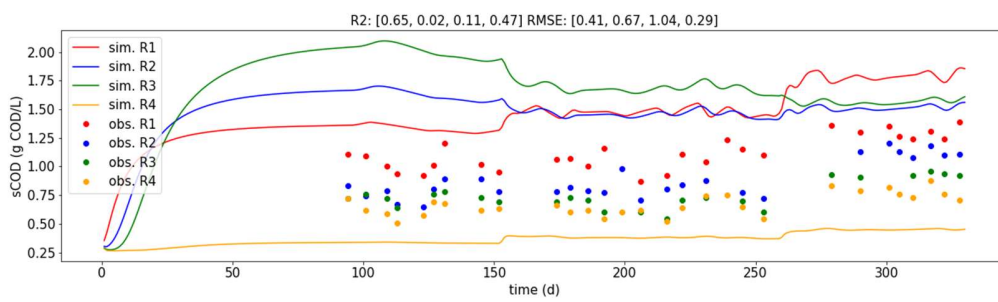
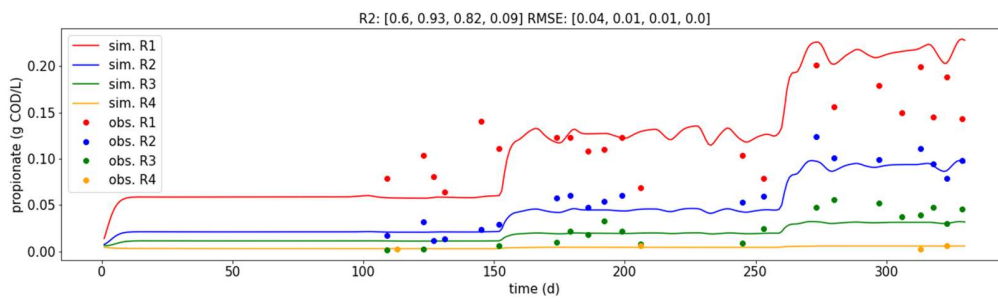
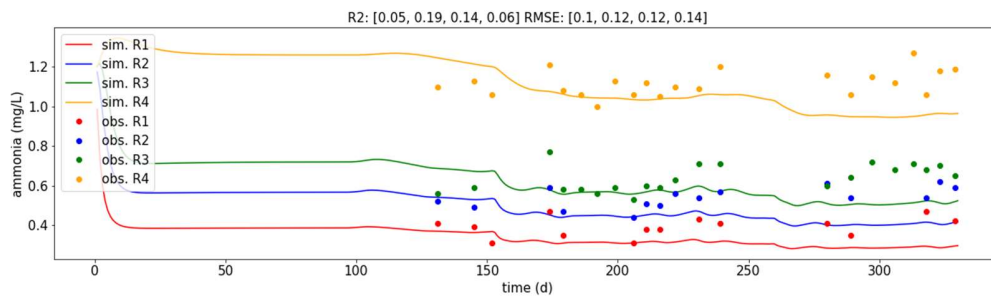
ADM1 – Results for Cascade System



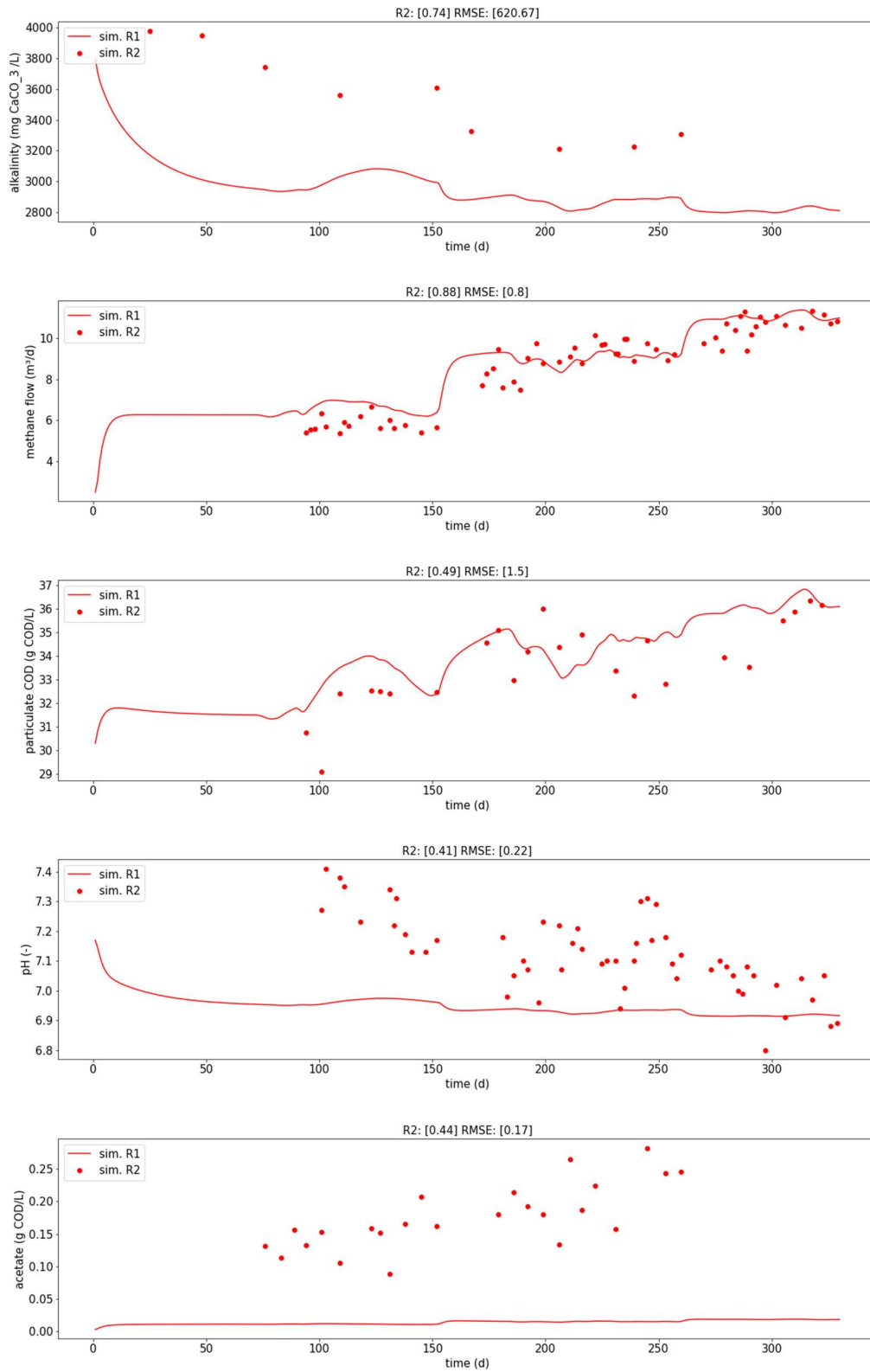


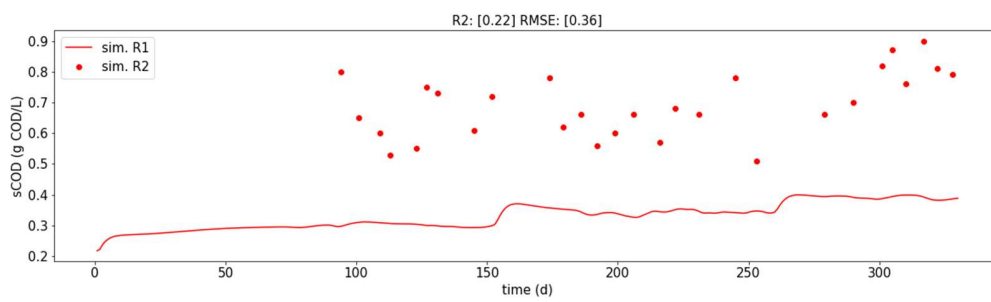
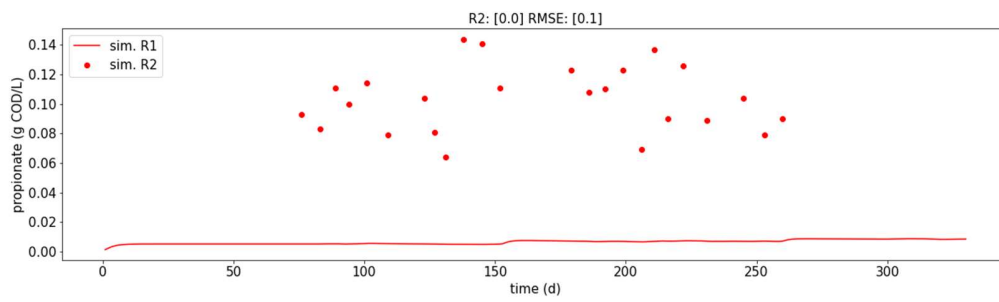
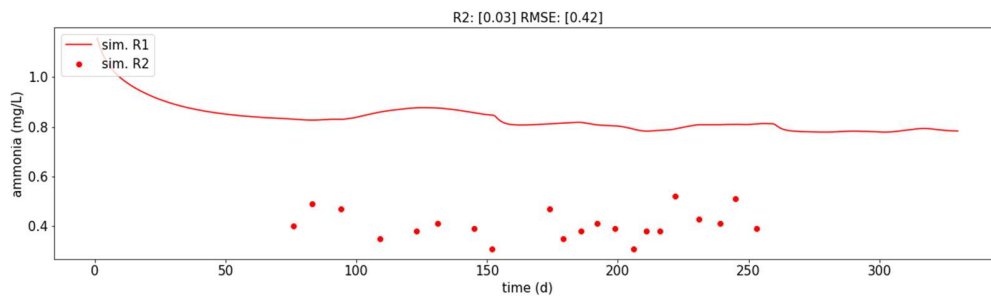
Modified First-Order Model (Empirical) – Results for Cascade System



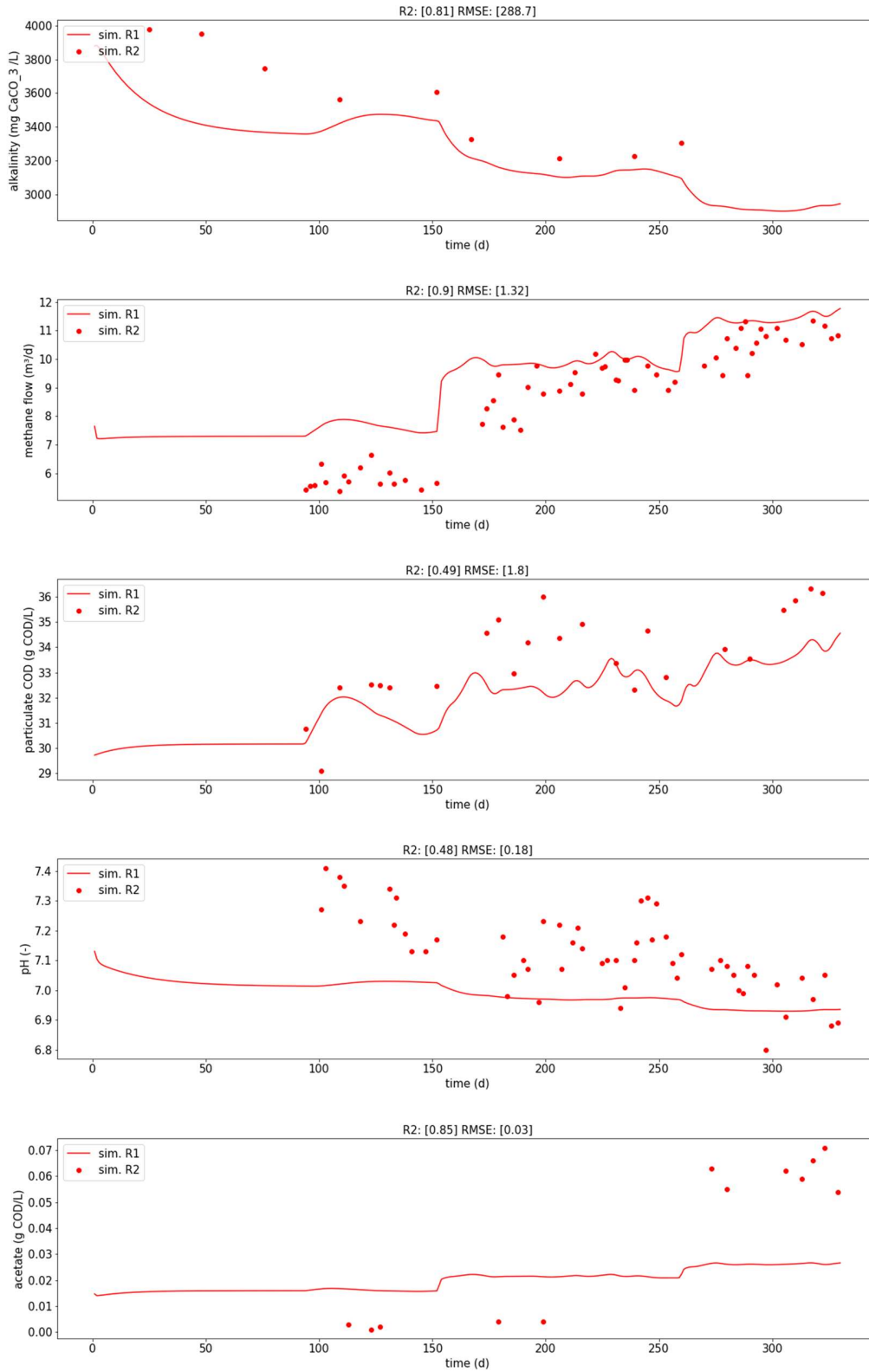


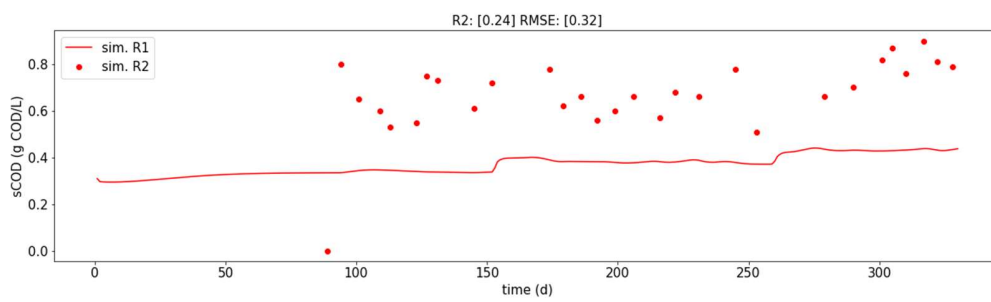
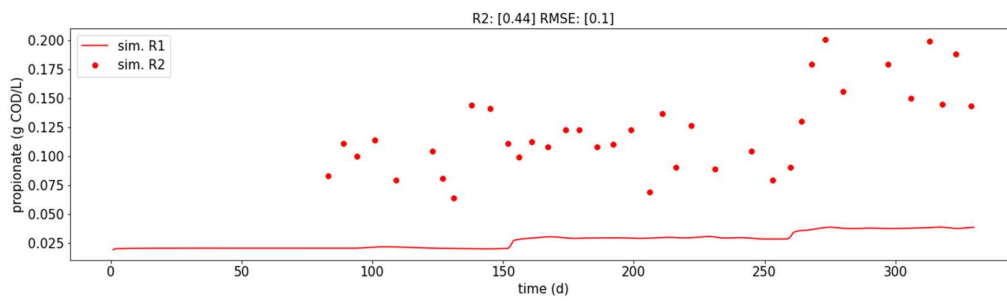
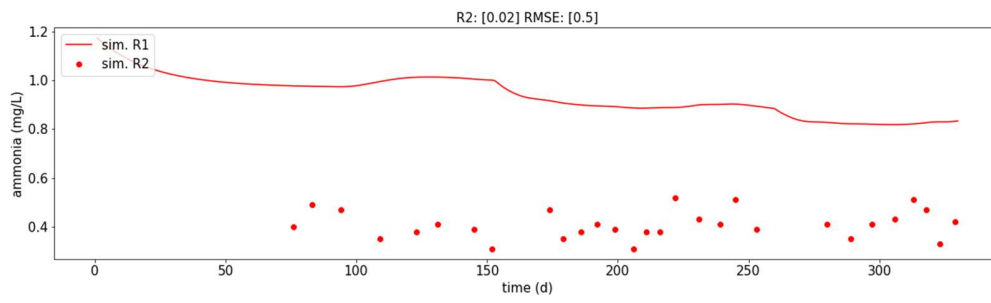
ADM1 – Results for Reference System





Modified First-Order Model (Empirical) – Results for Reference System





D | Appendix – ADM1 Overview

The presented Tables in this section are retrieved from Batstone et al. (2002).

Table A1 Nomenclature and units used

Symbol	Description	Units
C_i	carbon content of component i	kmoleC·kgCOD ⁻¹
i	component index (see appendix)	
I	inhibition function (various, see Table A2)	
j	process index (see appendix)	
$k_{A/B,i}$	acid-base rate constant for component i	M ⁻¹ ·d ⁻¹
k_{dec}	first order decay rate for biomass death	d ⁻¹
$k_{l,a}$	gas-liquid transfer coefficient	d ⁻¹
k_m	specific Monod maximum uptake rate	kgCOD·m ⁻³ ·S·kgCOD·m ⁻³ ·X·d ⁻¹
K_a	acid-base equilibrium constant	M (kmole·m ⁻³)
$K_{H,i}$	Henry's law coefficient	M·bar ⁻¹
K_i	inhibition constant	nominally kgCOD·m ⁻³
K_S	Monod half saturation constant	kgCOD·m ⁻³
N_i	nitrogen content of component i	kmoleN·kg COD ⁻¹
p_{gas}	pressure of gas	bar
pH	$-\log_{10}[S_{H,i}]$	
pK _a	$-\log_{10}[K_a]$	
q	flow	m ³
S_i	soluble component i (dynamic or algebraic variable)	nominally kgCOD·m ⁻³
S_i	inhibitory component	nominally kgCOD·m ⁻³
t	time	d
T	temperature	K
V	volume	m ³
X_i	particulate component i	kgCOD·m ⁻³
$Y_{substrate}$	yield of biomass on substrate	kgCOD·X·kgCOD·S ⁻¹
$v_{i,j}$	rate coefficients for component i on process j	nominally kgCOD·m ⁻³
$f_{product,substrate}$	yield (catabolism only) of product on substrate	kgCOD·kgCOD ⁻¹
ρ_j	rate for process j	kgCOD·m ⁻³

Table A2 Inhibition expressions

Description	Equation	Used for	ref
Non-competitive inhibition	$I = \frac{1}{1 + S_i / K_i}$	hydrogen inhibition free ammonia inhibition	1
Substrate limitation	$I = \frac{S_i}{S_i + K_i}$	total ammonia limitation	
Empirical	$I = \frac{1 + 2 \times 10^{0.5(pH_{UL} - pH_{LL})}}{1 + 10^{(pH - pH_{UL})} + 10^{(pH_{LL} - pH)}}$	pH inhibition when both high and low pH inhibition occur	2
	$I = \exp\left(-3 \left(\frac{pH - pH_{UL}}{pH_{UL} - pH_{LL}}\right)^2\right)$	pH inhibition when only low pH inhibition occurs	3
	$I = 1$		

Note: For the first pH function, pH_{UL} and pH_{LL} are upper and lower limits where the group of organisms is 50% inhibited, respectively. For example, acetate utilising methanogens with a pH_{UL} of 7.5 and a pH_{LL} of 6.5 have an optimum at pH 7. For the second function, pH_{UL} and pH_{LL} are points at which the organisms are not inhibited, and at which inhibition is full respectively. Acetate utilising methanogens with a pH_{UL} of 7 and a pH_{LL} of 6 will be completely inhibited below pH 6 and not inhibited above pH 7.

References: 1. Pavlostathis and Giraldo-Gomez (1991), 2. Angelidaki et al. (1993), 3. Ramsay (1997)

E | Appendix - Python Script for Quantitative Model Analysis

The script was written in jupyter Notebooks. The code is shown as images for overview. At the end of this Appendix the code is given as text so that it can be copied and run for other users, as well. The code is given separately. When copying this code make sure to change the directory paths.

Imports

```
In [1]: 1 import numpy as np
        2 import pandas as pd
        3 import scipy.stats
        4 import matplotlib.pyplot as plt
        5
        6 import os
        7
        8 # plt.style.use('ggplot')
```

R2 function

```
In [2]: 1 def rsquared(x, y):
        2     """ Return R^2 where x and y are array-like."""
        3
        4     slope, intercept, r_value, p_value, std_err = scipy.stats.linregress(x, y)
        5     return r_value**2
        6
        7 def rmse(x, y):
        8     return np.sqrt(float(((x - y)**2).mean()))
```

Path to csv files and results

fill in correct path

```
In [3]: 1 csv_dir = 'C:/Users/Sebastian/Desktop/Working docs for thesis writing/pytonskript für analyse/ExportierteDaten/'
        2 results_dir = 'C:/Users/Sebastian/Desktop/Working docs for thesis writing/pytonskript für analyse/Results/'
```

```
In [4]: 1 os.getcwd()
```

```
Out[4]: 'C:\\Users\\Sebastian\\Desktop\\Working docs for thesis writing\\pytonskript für analyse'
```

Find all filenames in folder

```
In [5]: 1 file_names = []
        2
        3 for file in os.listdir(csv_dir):
        4     if file.endswith('.csv'):
        5         file_names.append(file)
        6
        7 file_names
```

```
Out[5]: ['FirstOrder_k_calc_COD.csv', 'FirstOrder_k_calc_gasflow.csv']
```

Analysis for all files at once

```
1 df_dict = {}
2
3 for count, fp in enumerate(file_names):
4
5     ## get column names from file
6     file = pd.read_csv(fp, skiprows=8, header=None, delimiter=';')
7     name_model = file.loc[0, 0].split('_')[-2] + '_' + file.loc[0, 0].split('_')[-1]
8
9     columns = {}
10    columns_exp = []
11    columns_model = []
12    time_exp = False
13    time_model = False
14
15    for i, col in enumerate(file.loc[4].values):
16        if col.startswith('exp'):
17            columns[i] = 'exp_R' + col[-1]
18            columns_exp.append('exp_R' + col[-1])
19        if not time_exp:
20            columns[i-1] = 'time_exp'
21            time_exp = True
22            columns_exp.append('time_exp')
23
24
25    elif col != 't' and col != 'Variable:':
26        reactor = file.loc[7].values[i].split('_')[-1]
27        columns[i] = col + '_R' + reactor
28        columns_model.append(col + '_R' + reactor)
29        if not time_model:
30            columns[i-1] = 'time_model'
31            time_model = True
32            columns_model.append('time_model')
33
34    ## load file
35    file = pd.read_csv(fp, skiprows=20, header=None, delimiter=';', usecols=list(columns.keys()))
36    file = file.rename(mapper=columns, axis=1)
37
38    # shift day indices so that later the mean is taken from 0.1 ..1, 1.1..2 and so on
39    file['time_model'] = file['time_model'] + 0.9
40    file = file.round({'time_model': 1})
41
42
43    ## model dataframe
44    # chose columns
45    model_df = file[columns_model]
46
47    # drop first row with indice 0.9
48    model_df = model_df.drop(model_df[model_df.time_model == 0.9].index)
49
50
51    # use time column as index, convert to str
52    model_df.set_index('time_model', inplace=True)
53    model_df.index = model_df.index.astype(dtype=str)
54
55    # create multiindex: level 0 is day, level 1 are 10 values per day
56    model_df.index = pd.MultiIndex.from_tuples(model_df.index.str.split('.').tolist())\
57        .set_names(names=['time_model', 'count'], level=[0, 1])
58
59    # convert index back from str to int
60    idx = model_df.index
61    model_df.index = model_df.index.set_levels([idx.levels[0].astype(int), idx.levels[-1].astype(int)])
62
63
64    ## get mean value per day
65    model_mean_df = model_df.groupby(level=0).mean()
66
67
68    ## experiments dataframe
69    # chose columns
70    exp_df = file[columns_exp]
71
72    # remove rows without values (Nan)
73    exp_df = exp_df.dropna(axis=0, how='all')
74
```

```

79
80  ## determine r2 and rmse
81  # make sure both dataframes have same column names
82  exp_df = exp_df.rename(columns={col: col.split('_')[-1] for col in exp_df.columns})
83  model_mean_df = model_mean_df.rename(columns={col: col.split('_')[-1] for col in model_mean_df.columns})
84
85  # sort columns by name (R1 .. R4)
86  exp_df = exp_df.reindex(sorted(exp_df.columns), axis=1)
87  model_mean_df = model_mean_df.reindex(sorted(model_mean_df.columns), axis=1)
88
89
90  # chose only 1 rows (days) that are in both model and exp data
91  model_mean_df_2 = model_mean_df[model_mean_df.index.isin(exp_df.index)]
92
93  # calculate r2 and rmse for all 4 reactors
94  r2_values = []
95  rmse_values = []
96  for col in exp_df.columns:
97      x = model_mean_df_2[col]
98      y = exp_df[col]
99      r2 = rsquared(x, y)
100     r2_values.append(r2)
101
102     RMSE = rmse(x, y)
103     rmse_values.append(RMSE)
104
105  r2_values = [round(num, 2) for num in r2_values]
106  rmse_values = [round(num, 2) for num in rmse_values]
107

```

```

107
108  ## plot
109  fig, ax = plt.subplots(1, 1, figsize=(20, 5))
110  colors = ['r', 'b', 'g', 'orange']
111  model_mean_df.plot(ax=ax, color=colors)
112  exp_df.plot(ax=ax, ls='--', marker='.', color=colors)
113  # plt.title(f'{name_model} - R1: {r2_values[0]:.2f}, R2: {r2_values[1]:.2f}, R3: {r2_values[2]:.2f}, R4: {r2_values[3]:.2f}')
114  plt.title(name_model + '\n R2: ' + str(r2_values) + '\n RMSE: ' + str(rmse_values))
115  plt.legend(loc='upper left')
116
117  ## save dataframes to .csv, r2 values to .txt and plot to .png
118  # combined dataframe with ALL MEAN model and exp data
119  joined_df_1 = model_mean_df.join(exp_df, how='left', rsuffix='_exp')
120  joined_df_1.index.rename('time', inplace=True)
121
122  # combined dataframe with OVERLAPPING MEAN model and exp data
123  joined_df_2 = model_mean_df.join(exp_df, how='right', rsuffix='_exp')
124  joined_df_2.index.rename('time', inplace=True)
125
126  joined_df_1.to_csv(results_dir + name_model + '_all_means.csv')
127  joined_df_2.to_csv(results_dir + name_model + '_overlap_means.csv')
128
129  # R2 values to txt file
130  with open(results_dir + name_model + "_r2_values.txt", "w") as output:
131      output.write(str(r2_values))
132

```

```

132
133  # RMSE values to txt file
134  with open(results_dir + name_model + "_rmse_values.txt", "w") as output:
135      output.write(str(rmse_values))
136
137
138  # plot to .png
139  plt.savefig(results_dir + name_model + '_plot.png')

```



Reconsidering hydrolysis kinetics for anaerobic digestion of waste activated sludge applying cascade reactors with ultra-short residence times

Hongxiao Guo^{a,*}, Margreet J. Oosterkamp^a, Fabio Tonin^b, Alexander Hendriks^c, Revathy Nair^a, Jules B. van Lier^a, Merle de Kreuk^a

^a Section Sanitary Engineering, Department of Water Management, Faculty of Civil Engineering and Geosciences, Delft University of Technology, Stevinweg 1, 2628 CN Delft, The Netherlands

^b Group Biocatalysis, Department of Biotechnology, Faculty of Applied Science, Delft University of Technology, Van der Maasweg 9, 2629 HZ Delft, The Netherlands

^c Royal HaskoningDHV, Laan 1914 No. 35, 3818 EX Amersfoort, The Netherlands

ARTICLE INFO

Keywords:

Waste activated sludge
Cascading anaerobic digesters
First-order kinetics
Hydrolytic enzyme activity
Microbial community structure

ABSTRACT

Hydrolysis is considered to be the rate-limiting step in anaerobic digestion of waste activated sludge (WAS). In this study, an innovative 4 stages cascade anaerobic digestion system was researched to (1) comprehensively clarify whether cascading configuration enhances WAS hydrolysis, and to (2) better understand the governing hydrolysis kinetics in this system. The cascade system consisted of three 2.2 L ultra-short solids retention times (SRT) continuous stirred tank reactors (CSTRs) and one 15.4 L CSTR. The cascade system was compared with a reference conventional CSTR digester (22 L) in terms of process performance, hydrolytic enzyme activities and microbial community dynamics under mesophilic conditions (35 °C). The results showed that the cascade system achieved a high and stable total chemical oxygen demand (tCOD) reduction efficiency of 40–42%, even at 12 days total SRT that corresponded to only 1.2 days SRT each in the first three reactors of the cascade. The reference-CSTR converted only 31% tCOD into biogas and suffered process deterioration at the applied low SRTs. Calculated specific hydrolysis rates in the first reactors of the cascade system were significantly higher compared to the reference-CSTR, especially at the lowest applied SRTs. The activities of several hydrolytic enzymes produced in the different stages revealed that protease, cellulase, amino peptidases, and most of the tested glycosyl-hydrolases had significantly higher activities in the first three small digesters of the cascade system, compared to the reference-CSTR. This increase in hydrolytic enzyme production by far exceeded the increase in specific hydrolysis rate, indicating that hydrolysis was limited by solids-surface availability for enzymatic attack. Correspondingly, high relative abundances of hydrolytic-fermentative bacteria and hydrogenotrophic methanogens as well as the presence of syntrophic bacteria were found in the first three digesters of the cascade system. However, in the fourth reactor, acetoclastic methanogens dominated, similarly as in the reference-CSTR. Overall, the results concluded that using multiple CSTRs that are operated at low SRTs in a cascade mode of operation significantly improved the enzymatic hydrolysis rate and extend in anaerobic WAS digestion. Moreover, the governing hydrolysis kinetics in the cascading reactors were far more complex than the generally assumed simplified first-order kinetics.

Introduction

Waste activated sludge (WAS) is an inevitable by-product generated in biological wastewater treatment plants (WWTPs). Due to quantitative and qualitative extension of wastewater treatment, the annual WAS production has increased in the European Union during the last two decades, from 10 million tons in 2008 to 11.5 million tons in 2015, and is expected to approach 13 million tons by 2020 (Rorat et al., 2019).

Anaerobic digestion (AD) is a proven key technology for both stabilization of WAS and recovery of the biochemical energy stored in the sludge in the form of biogas. WAS usually contains complex particulate organics, such as proteins, polysaccharides, lignocellulosic matters, and fats (Gonzalez et al., 2018). Hydrolysis of WAS into soluble substrates is the first step in AD and is generally regarded as the rate-limiting step in this process (Appels et al., 2008). Therefore, conventional digesters using continuous stirred tank reactors (CSTRs) have to be operated

* Corresponding author.

E-mail address: h.guo-2@tudelft.nl (H. Guo).

<https://doi.org/10.1016/j.watres.2021.117398>

Received 24 February 2021; Received in revised form 6 June 2021; Accepted 27 June 2021

Available online 1 July 2021

0043-1354/© 2021 The Author(s). Published by Elsevier Ltd. This is an open access article under the CC BY license (<http://creativecommons.org/licenses/by/4.0/>).

under prolonged sludge retention times (SRTs) exceeding 20 days for an acceptable WAS conversion.

To accelerate the conversion rate of WAS and decrease these long SRTs, process optimisation has been applied as well as the development of hydrolysis enhancement technologies, including thermal, chemical and enzymatic methods (Zhen et al., 2017). Enzymatic hydrolysis enhancement seemingly offers unique advantages compared to chemical or physical processes, as it neither causes generation of toxic substances, nor needs operations under extreme conditions, thus receiving an increased attention in the recent years (Gonzalez et al., 2018). Most of these studies focused on the direct addition of highly active hydrolytic enzymes into the digester (Yang et al. 2010) or on pre-fermentation by specific hydrolytic bacteria prior to AD (Agabo-Garcia et al., 2019). These proof-of-concept methods showed remarkable improvement in WAS hydrolysis and bio-degradation; however, full scale applications require a continuous purchase of enzymes and/or the need for preservation of specific biomass while working with poorly defined substrates.

Hydrolysis of organic matter during AD is performed by extracellular and/or membrane-bound hydrolytic enzymes (Kim et al., 2012). Enhancement of WAS hydrolysis also can be achieved by accelerating the reaction rates and/or increasing the activity of these hydrolytic enzymes instead of adding external hydrolytic enzymes or applying pre-fermentation. A commonly applied strategy is to perform WAS digestion under thermophilic (55 °C) conditions, which roughly results in a doubling of the enzymatic reaction rates compared to the commonly applied mesophilic (35 °C) conditions (Ge et al., 2011a). Nevertheless, decreased process performance was often observed under thermophilic conditions due to the accumulation of organic intermediates to a toxic level, or to a drop in pH (Kim et al., 2003), negatively impacting the actual enzymatic reaction rates. In addition, other constraints of thermophilic WAS digestion include higher energy requirement, poor effluent quality and a poorer digestate's dewaterability (De la Rubia et al. 2013). Thus, there is a great interest to search for alternative technologies.

The enzymatic hydrolysis of WAS is commonly described by empirical first-order kinetics (Vavilin et al., 2008), meaning that the observed solids conversion rate is dependant on the solid substrate concentration and the first-order hydrolysis rate constant (Eq. (1)).

$$\frac{dS}{dt} = -k_H S \quad (1)$$

Where S = substrate concentration, t = time, and k_H = first-order hydrolysis rate constant.

Theoretically, in a CSTR, the concentration S in the reactor equals the effluent S concentration, indicating that in-reactor conversion rates decrease with decreasing S (Eq. (1)), agreeing with an increased conversion ratio (η) (Fig. 1a). Based on Eq. 2, the required volume of a CSTR at a given inlet feeding rate (F_0) is fully determined by the required η and is graphically presented by the large rectangular area shown in Fig. 1b (Levenspiel 2006). On the contrary, by cascading CSTRs, small reactor volumes in series are applied that result in high intermediate S concentrations. Consequently, the first CSTRs can be operated at high reaction rates, whereas the last CSTR of the cascade system will have a similar reaction rate as the single stage CSTR. Thus, the series of small CSTRs will eventually reach to a similar η but to a significant smaller

working volume, compared to the single stage CSTR (Fig. 1c). The overall required volume of the cascade system is reciprocally correlated to the number of CSTRs.

$$V = F_0 \frac{1}{-r} \eta \quad (2)$$

Where V = volume of the CSTR (m^3), F_0 = substrate feeding rate (kg COD/day), $-r$ = substrate conversion rate (kg COD/ m^3 /day), and η = substrate conversion ratio (0–100%).

Cascade CSTR configurations are commonly applied to accelerate catalytic substrate conversions that are characterised by Eq. (1) (Miyawaki et al., 2016). In case reaction rates are substrate dependant, such as for soluble substrates in Michaelis-Menten and/or Monod kinetics, the impact of reactor cascading will even be higher. However, for solid substrates such as WAS, concentration dependant reaction rates are rarely documented (Miron et al., 2000) and generally first-order reaction rate constants are considered (Blumensaat and Keller 2005).

Up to now, application of the cascade CSTR configurations for WAS has been mainly reported in the scope of co-digestion in food waste (Liu et al., 2013) or agricultural waste (Zhou et al., 2019), in which WAS contributed to improved buffer capacities and more balanced nutrient profiles. In the past decade, several researchers found higher WAS conversion efficiencies by using two-stage (two CSTRs in series) mesophilic AD systems, either with or without addition of primary sludge, for which no clear mechanistic explanation was given (Athanasoulia et al., 2012; Maspolim et al., 2015b). Ge et al. (2011b) and Wu et al. (2015) observed an improved hydrolysis rate in temperature-phased (thermophilic CSTR–mesophilic CSTR) WAS anaerobic digestion processes. Nonetheless, the authors attributed the enhanced hydrolysis merely to the thermophilic conditions applied. Despite the fact that staging has resulted in improved WAS digestion, it remains unclear whether accelerated enzyme activities, increased surface area of the solid substrates, and/or other factors were determinative. However, the published wide range of assessed hydrolysis rate constants for WAS (Batstone et al., 2002), gives room for further research and process optimisation.

In order to (1) comprehensively clarify whether a cascade configuration enhances WAS hydrolysis, and to (2) better understand the governing hydrolysis kinetics in this system, a novel cascade AD system for WAS treatment was researched in this study, which consisted of four CSTRs in series, i.e., three small-volume CSTRs and a large-volume CSTR. Considering that digestate recycle improves process stability in staged anaerobic digestion (Qin et al., 2019), the cascade system was equipped with a modest digestate recirculation, applying a much lower ratio than reported in literature (Wu et al., 2015). As such, the whole system can be interpreted as a semi plug-flow device with only a negligible hydraulic impact of the recycle flow. Reactor performance in the different steps of the system were investigated. Detailed research on prevailing specific hydrolysis rates, activities of key hydrolytic enzymes and the bacterial/archaeal community structure was performed to explain the results of the reactor performance and unveil the impact of cascading on hydrolysis kinetics. All results from the cascade system were compared to those obtained from a reference conventional CSTR system operated under the same conditions with regard to feeding regime, total organic loading and temperature.

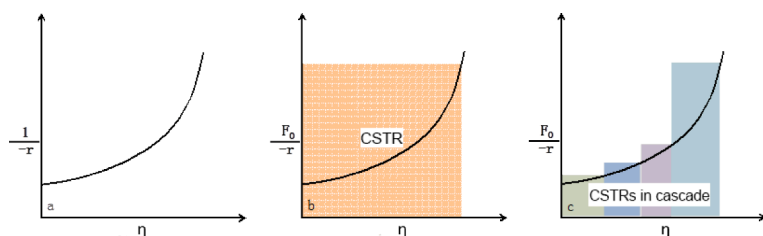


Fig. 1. Theoretical reactor volume reduction by applying a cascade CSTR configuration versus a single stage CSTR (Levenspiel 2006). (a) Relationship between the substrate conversion ratio (η) and the reciprocal first order conversion reaction rate ($-r$), (b) required reactor volume of a single stage CSTR for a required conversion ratio η , indicated by the total surface area of the rectangle, and (c) required reactor volume for the cascade CSTR configuration for the same η , by summing the 4 subsequent surface areas.

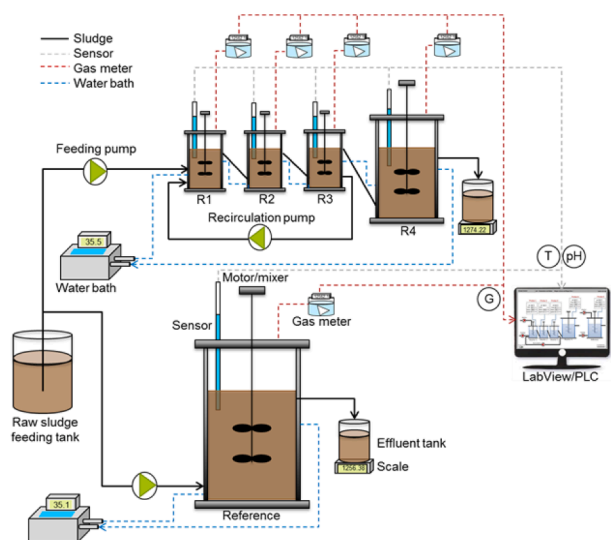


Fig. 2. Schematic illustration of the experimental set-ups.

Materials and methods

Source and characteristics of inoculum and substrate

All reactors were seeded with anaerobic sludge collected from a full-scale mesophilic anaerobic digester (SRT of 20 days) at the municipal WWTP Harnaspolder, The Netherlands, treating primary sludge and centrifuge-thickened WAS from an enhanced biological phosphorus removal (EBPR) process. More information regarding the configuration and the operational parameters of the EBPR process can be found elsewhere (Guo et al., 2020b). The inoculum characteristics were: pH 8.1 ± 0.4 , total solids (TS) 3.3 ± 0.1 wt%, and volatile solids (VS) 2.3 ± 0.0 wt%. The WAS from the same WWTP was collected weekly as feed sludge, and was characterized by a total chemical oxygen demand (tCOD) concentration between 40 and 70 g/L. The tCOD concentration of the feed sludge was adjusted to approximately 53 g/L by centrifugation or dilution with the fresh centrifuged supernatant obtained from the same WWTP, and stored at 4 °C before use.

Experimental set-up and operation

The experiments were carried out using two digestion systems operated in parallel: 1) a cascade AD system consisting of three CSTRs

$$\text{Specific hydrolysis rate (g COD / g VS / day or l / day)} = \frac{\left(\frac{\text{mass_sCOD} + \text{mass_COD}_{\text{CH}_4}}{\text{day}} \right)_{\text{eff.}} - \left(\frac{\text{mass_sCOD}}{\text{day}} \right)_{\text{inf.}}}{\text{mass of VS within reactor}} \quad (3)$$

with 2.2 L each (R1, R2, R3) and a 15.4 L CSTR (R4); 2) a conventional CSTR as the reference with a working volume of 22 L (Fig. 2). The experimental set-ups were both equipped with feed pumps (Watson-Marlow 120 U/DV-220Du, USA), temperature & pH sensors (Endress & Hauser, The Netherlands), and biogas flow meters (Ritter Milligas Counter MGC-1-PMMA, Germany). The digestate was discharged from all reactors in both systems via overflow. In addition, for the cascade system a sludge recirculation system from R3 to R1 with a flow ratio of 10% (recirculation/feed) was implemented using a recirculation pump (Watson-Marlow 120 U/DV-220Du, USA). The temperature of all water-jacket equipped CSTRs was 35 ± 1 °C, controlled by thermostatic water baths (Tamson Instruments, The Netherlands). Both systems were

Table 1

Operational conditions of the cascade AD system and the reference-CSTR.

Experimental time (day)	SRT (days) Cascade System	Reference-CSTR	Total organic loading rate (g COD/L/d)	Phase
0–71	R1-R3: 2.2 each R4: 15.4	Reference: 22	2.41	I
72–152	R1-R3: 2.2 each R4: 15.4	Reference: 22	2.41	II
153–259	R1-R3: 1.5 each R4: 10.5	Reference: 15	3.54	III
260–330	R1-R3: 1.2 each R4: 8.4	Reference: 12	4.41	IV

monitored via a computer running LabView software (National Instruments, USA).

The total SRT of both systems was decreased from 22 to 12 days in four phases. The operational conditions during all these phases are shown in Table 1.

Analysis and calculation methods

The tCOD and soluble COD (sCOD) were measured using spectrophotometry-based test kits (Hach Lange LCK, Germany). TS and VS were analysed according to standard protocols (APHA, 2005). The pH was determined with a multi-functional metre (WTW Multi 720, Germany). VFAs were measured by a gas chromatograph (GC) equipped with a flame ionisation detector (FID) (Agilent 7890A, USA) and a column (Agilent 19091F-112). Helium was used as carrier gas (1.8 mL/min); injection port and oven temperatures were 240 °C and 80 °C, respectively. Methane content of the biogas was analysed using a GC (Varian CP 4900, USA) with thermal conductivity detector (TCD) and columns, i.e. Mol-Sieve-5A-PLOT and argon as carrier gas (1.47 mL/min, 80 °C) and Poraplot-U and helium as carrier gas (1.47 mL/min, 65 °C).

The specific hydrolysis rate, referring to the hydrolysis rate constant k_H (Yasui et al., 2008), was calculated by Eq. (3) based on Wu et al. (2015). As the AD system was equipped with a digestate recirculation of 10% from R3 to R1, the recycled sCOD and the recycle flow were also considered in the calculation of the specific hydrolysis rates for these three reactors.

Where mass_sCOD = sCOD weight (g); mass_COD_{CH₄} = CH₄wt calculated as COD (g); eff. = effluent + methane; inf. = influent. It should be noted that inf. for R1 is composed of both the feeding and the recirculated digestate; inf. for R2 is the effluent from R1; inf. for R3 is the effluent from R2; inf. for R4 is composed of the effluent from R3, without the recycle flow.

Hydrolytic enzyme activity

Sampling and enzyme extraction

Triplicate sludge samples, including feed and digestates, were collected for enzyme extraction at the end of Phase-II (day 145 and 151),

Phase-III (day 252 and 258) and Phase-IV (323 and 329) of the individual reactors of both digestion systems. The hydrolytic enzymes were separated into free and sludge-attached fractions. The free enzymes are defined as the enzymes that are present in the WAS's supernatant, whereas the sludge-attached enzymes are either membrane-bound or in other ways attached to the sludge particles. The extraction method of the hydrolytic enzymes was implemented according to Zhang et al. (2007) with a slight modification for sludge samples. Briefly, 1 mL sludge sample was centrifuged in a 1.5-mL tube (Eppendorf, Germany) at 14,000 rpm for 1 min. The supernatant was transferred to a clean tube and was used for the measurement of free enzyme activities. The pellet was washed twice, using potassium dihydrogen phosphate buffer (pH 7.0, 0.1 mol/L) and was subsequently resuspended in sodium acetate buffer at pH 6.0 to the original volume to release sludge-attached enzymes. After centrifugation the suspension at 3000 g for 10 min, the supernatant was used for the determination of sludge-attached enzyme activities.

Quantification of enzyme activity

This work mainly focused on two hydrolytic enzymes: protease and cellulase. The activities of protease and cellulase were individually analysed by Pierce fluorescent protease assay kit (Thermo Fisher, USA) and MarkerGene fluorescent cellulase assay kit (MarkerGene, USA), using a 96-well microplate spectrophotometer (BioTek Synergy-HTX, USA). Meanwhile, API ZYM® strip (BioMerieux, France) was used to determine the activities of specific amino peptidases (leucine arylamidase, valine arylamidase and cystine arylamidase) and glycosylhydrolases (α -galactosidase, β -galactosidase, β -glucuronidase, α -glucosidase, β -glucosidase, n-acetyl glucosamidase, α -mannosidase and α -fucosidase). This commercial semi-quantitative micro-cell method works via colour development, with a numerical level of 1–5 (from low, 5 nmol, to high, >20 nmol) assigned to each sample, based on the colour chart provided by the manufacturer. The measurements of enzyme activity for both methods were performed at 35 °C.

Microbial community analysis

During the experiment, duplicate biomass samples were analysed to evaluate the microbial community dynamics, including one inoculum sample, two feed samples and 15 digestate samples from the digestion systems. The feed samples were taken individually on day 79 (summer season) and day 235 (winter season), and the digestates were sampled from R1, R2, R3, R4 and reference-CSTR at the end of each phase, i.e. days 151, 258, and 329. The FastDNA® SPIN-Kit-for-Soil (MP Bio-medicals, USA) was used to extract DNA according to the manufacturer's instructions. The obtained DNA's quality was checked by Qubit3.0 DNA detection (Qubit® dsDNA-HS-Assay-Kit, Life Technologies, USA). High throughput sequencing was performed using the HiSeq Illumina platform and a universal primer 515F/806R (5'-GTGCCAGCMGCCGCGGTAA-3'/5'-GGACTACHVGGGTWTCTAAT-3') for bacterial and archaeal 16S rRNA genes (Novogene, UK). Raw reads were deposited in the European Nucleotide Archive under accession number PRJEB40450. Sequences were analysed by the QIIME pipelines (Version 1.7.0) to pair forward and reverse sequences, and removal of chimeras' sequences was performed by UCHIME algorithm.

Sequences with $\geq 97\%$ similarity were clustered into one operational taxonomic unit (OTUs) by UCLUST algorithm. Singletons were removed, and OTUs with an occurrence less than three times in at least one sample were excluded. Taxonomic assignment was performed in Mothur software against the SILVA Database.

Statistical analysis

Student's *t*-test was used for variance analysis by SPSS Statistics 25 (IBM, USA), with the threshold for significance set at a P-value < 0.05. Shannon index and principal coordinate analysis (PCoA) based on the ordination of Bray-Curtis similarities were used to evaluate Alpha diversity and Beta diversity, respectively, by "vegan" microbial community ecology package in R software (version 4.0.2). Prediction of functional pathways from 16S rRNA gene sequences were conducted by

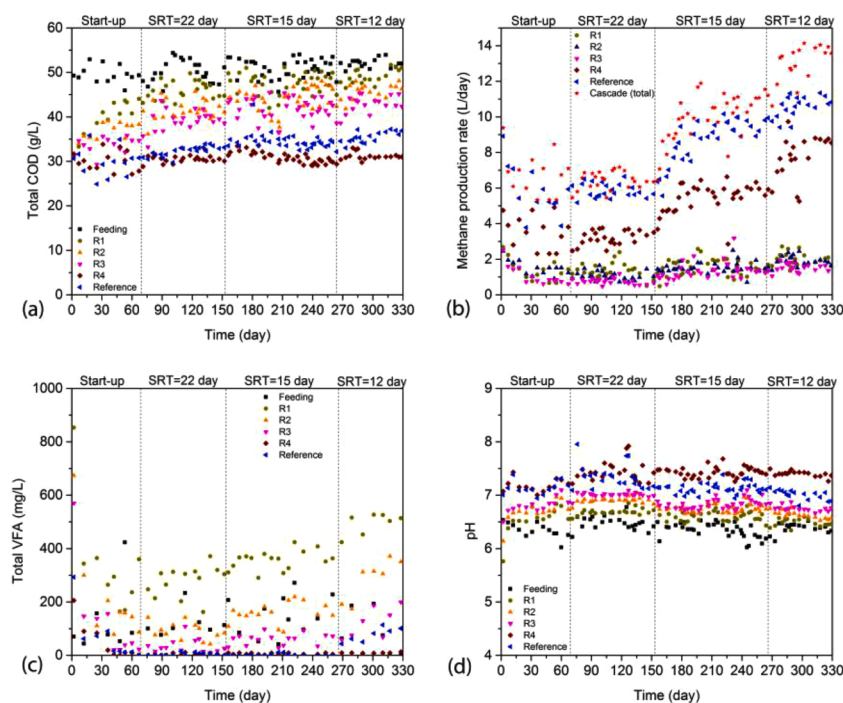


Fig. 3. Operational performance of the cascade AD system and the reference digester, respectively. (a) tCOD concentration, (b) methane production rate, (c) total VFA concentration and (d) pH.

“Tax4Fun2” software package that provides functional annotations based on the Kyoto encyclopedia of Genes and Genomes (KEGG) pathway database.

Results and discussion

Performance comparison between the cascade AD system and the reference-CSTR

During the start-up phase, the effluent tCOD concentrations and methane production rate fluctuated in all reactors (Fig. 3a). Both parameters gradually stabilised from day 71 onward, after which the cascade and reference system were both operated under stable conditions for 81 days (Phase-II). During both Phase-I and Phase-II, the cascade system and the reference-CSTR were operated with an SRT of 22 days. The tCOD removal efficiency of the entire cascade system was $43 \pm 6\%$, versus $40 \pm 5\%$ of the reference-CSTR during this period. Both removal efficiencies were within typical ranges of mesophilic WAS digestion, reported by previous studies (Maspolim et al., 2015b). On average, the methane production rate was around 8% higher in the cascade system than in the reference-CSTR (Fig. 3b).

After the total SRT was lowered to 15 days (Phase-III), effluent tCOD concentrations of both R4 and the reference-CSTR increased due to the sudden increase in total organic loading rate (OLR) from 2.4 to 3.5 g COD/L/d. This reduction in tCOD removal efficiency was also observed at the start of Phase-IV, when the total SRT was further decreased to 12 days and the total OLR correspondingly increased to 4.4 g COD/L/d. Strikingly, only the cascade system recovered to a tCOD removal efficiency between 40% and 42% at the applied increased OLR, whereas the tCOD removal efficiency in the reference-CSTR reduced to around 38% in Phase-III and 31% in Phase-IV. The difference in treatment performance was reflected by the increasing difference in methane production (Fig. 3b). The cascade system showed an average 13% higher methane production rate in Phase-III and even an average 29% higher rate in Phase-IV than the reference-CSTR. The obtained results clearly demonstrated the advantage of applying a cascade configuration, particularly at reduced SRTs. In fact, at 12 days SRT, the overall capacity referring to the tCOD removal efficiency of the cascade digester was 30–35% higher, compared to the reference-CSTR with the same total volume.

Zooming into the separate reactors of the cascade system reveals that the reactors R1, R2 and R3, with an SRT of 2.2 days each (Phase-II), contributed to 20–24% of the total methane volume that was produced in the cascade system (Fig. 3b). These results agree with a reported study on two staged AD systems under similar SRT conditions, which showed that the methane production in the first CSTR was on average 25% of the total (Maspolim et al., 2015b). When the SRT in the cascade reactors R1, R2 and R3 was decreased to 1.5 and 1.2 days each in Phase-III and Phase-IV, respectively, the methane production stayed between 12 and 16% of the overall total methane production. The biogas in these three reactors contained 46–53% methane, while the methane content of the biogas of R4 and of the reference-CSTR was 56–62%. Negligible hydrogen partial pressure was found in all the anaerobic reactors ($< 0.01\%$). These observations showed that, despite their short SRT and most probably due to the 10% recirculation flow, active methanogens were present in R1, R2 and R3.

VFA concentrations and pH are commonly used as indicators for process perturbation and/or reactor control (Franke-Whittle et al., 2014). The total VFA concentration in the feed and all reactors is presented in Fig. 3c. As expected, the VFA concentration was always the highest in R1 and was gradually reduced along the system. Acetate and propionate accounted for 60–80% of the total VFAs, showing their predominance in all reactors (Fig. S1 in supplementary materials). With increased OLR, or decreased SRT, an elevation in VFA concentration in R1, R2 and R3 was observed, from 310, 100 and 60 mg/L at SRT 22 days to 590, 380 and 175 mg/L at SRT 12 days, respectively. Very low total VFAs (< 5 mg/L) were found in reactor R4 in all phases, demonstrating

that all VFAs were eventually converted to methane in the last step of the cascade system. In the reference-CSTR there was no VFA accumulation observed, even at the shortest SRT (12 days) when total VFA concentration slightly increased to around 110 mg/L. Clearly, the VFA concentrations remained far below the inhibition threshold for methanogenic activity (Wang et al., 2009), and thus cannot explain the difference in WAS degradation between the cascade system and the reference-CSTR at short SRTs. However, the pH in both R1 and R2 of the cascade system was between 6.3 and 6.5, somewhat lower than the pH in the rest of the reactors. The lower pH coincided with the somewhat higher VFA concentrations in R1 and R2 and can be attributed to increased acidifying activity and reduced methanogenic activity in the first reactors of the cascade (Maspolim et al., 2015b). In reactors R3 and R4, as well as in the reference system, the pH remained neutral (Fig. 3d). Nonetheless, the relatively stable pH in R1 and R2 could be ascribed to alkalinity supplementation by digestate recirculation from R3 to R1, introducing sufficient buffer capacity as presented in Fig. S2 in Supplementary material.

To be able to explain the different tCOD removal efficiencies between the cascade and the reference system, the specific hydrolysis rates were calculated using Eq. (3), the tCOD and sCOD variations (Fig. 1 and Fig. S3 in Supplementary materials), and the methane production (Fig. 3b) in each reactor. Computed specific hydrolysis rates, resembling the first-order hydrolysis rate constant k_H (Eq. (1)), are shown in Fig. 4. Under all tested operational conditions, the specific hydrolysis rate was highest in R1 of the cascade system, and steadily decreased throughout the subsequent reactors of the cascade. During Phase-II, the specific hydrolysis rate calculated for the reference-CSTR was slightly higher than that in R3 of the cascade system. Reducing the SRT from 22 to 12 days led to approximately a doubling of the specific hydrolysis rate in the reactors of the cascade system, while it increased only 1.5 times in the reference-CSTR. It should be noted that the bar-presented specific hydrolysis rates are in fact underestimates of the actual values, since these were calculated using Eq. (3), which includes both the substrate and biomass VS in each reactor. However, particularly in reactors R1–3, the contribution of the substrate VS to the total VS is relatively large. We, therefore, recalculated the apparent k_H values using the VS content in R4, which resembles the non-digestible VS fraction in the entire cascade system. The corrected k_H values are presented above each bar of R1–3 in Fig. 4, showing an even higher increase in specific hydrolysis rates in the first stages of the cascade reactor.

Strikingly, under all loading conditions, the assessed specific

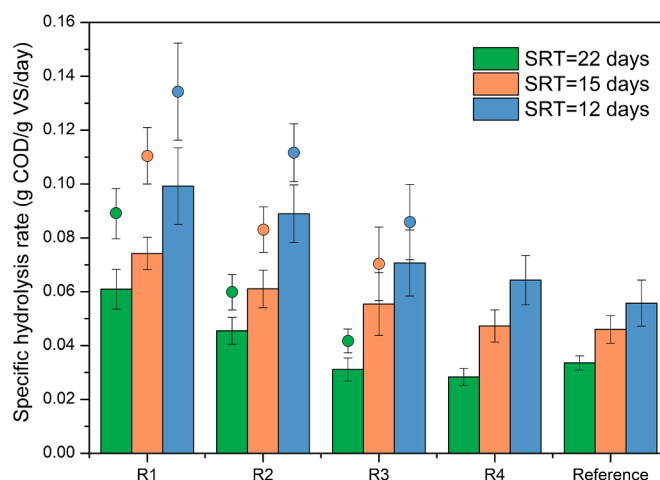


Fig. 4. Specific hydrolysis rate calculated based on the COD balance and the VS concentration of each reactor (bars). The circles displayed above the bars of R1, R2 and R3 represent the calculated specific hydrolysis rate using the stabilized VS concentration of R4 at each SRT, which resembles the non-digestible VS fraction in the cascade system.

hydrolysis rates in R4 of the cascade system and the reference-CSTR were very similar. Nonetheless, at the highest OLR, the overall specific hydrolysis rate in the reference-CSTR was significantly lower (p -value < 0.05) than the separate specific hydrolysis rates in all reactors of the cascade system. Apparently, the specific hydrolysis rate was process-condition dependant and results in Fig. 4 showed that in all reactors the specific hydrolysis rate increased with increasing OLRs. Similar observation were previously done by Miron et al. (2000). Our present results clearly indicate that the potential volume reduction, which can be attained by implementing cascade configurations, is indeed much more than based on solely the theoretical considerations as explained in Fig. 1 (Levenspiel 2006), where the same first-order reaction rate is applied for all individual reactors in the cascade system and the single stage CSTR. Moreover, at the applied low SRTs, or imposed extreme OLRs, the specific hydrolysis rates increased significantly more (p -value < 0.05) in the first reactors of the cascade system compared to that in the reference-CSTR (Fig 4). Most likely, the maximum organic loading potentials of the cascade system were not reached yet, as process performance remained stable even at an SRT of 12 days (Fig. 3).

Results further indicate that for increasing the sludge treatment capacity at a common WWTP, the present AD installation can be upgraded in a relatively easy manner to a very compact cascade reactor system via retrofitting existing parallel-fed large-scale conventional CSTR-based sludge digesters. For instance, one CSTR digester could be divided into a sequence of several compartments and subsequently be connected with another digester in series.

Hydrolytic enzyme activity

To explain the large differences in observed specific hydrolysis rates between the different reactors, the hydrolytic enzyme activities were assessed (Parawira et al., 2005). Cellulosic fibres and proteins are identified as the two predominated organic components in WAS (Guo et al., 2020b). Therefore, the activity of cellulase and protease were chosen as representative enzyme activities for a first characterisation of WAS hydrolysis in both systems, applying a widely reported enzymes extraction protocol for anaerobic samples (Zhang et al., 2007). Meanwhile, automatic measurements in a 96-well microplate reader rather than manual measurements were conducted for the analysis of enzyme activities in this study (Bonilla et al., 2018), with the duplicate extraction of enzymes from the same reactor at three inconsecutive days. Results in Fig. 5 showed that both free and sludge-associated enzymes are present in the digester, regardless of the configuration type, i.e. cascade or single CSTR. The results showed that protease activities were two orders of magnitude higher than cellulase activities, which could be possibly due to the significant higher proportion of protein than

cellulose in WAS (Guo et al., 2020b). Highest protease and cellulase enzyme activities were present in the sludge-associated fraction of both reactor configurations. Enzyme activities are proportionally related to the enzyme's amount (Kim et al., 2012), suggesting that the hydrolytic enzymes were mainly adsorbed on, or attached to the sludge matrix, in line with a previous publication by Maspolim et al. (2015a).

In both free and sludge-associated fractions, the activity of hydrolytic enzymes distinctly increased from the feed to R1, especially at short SRTs, indicating that hydrolysis in R1 was indeed accelerated owing to increased presence of hydrolytic enzymes. Significant higher enzyme activities (p -value < 0.05) were observed in the three small reactors in comparison with the reference-CSTR: the protease activities in R1 were double the activities in the reference-CSTR; even the protease activities in R4 were slightly higher than those in the reference-CSTR. Meanwhile, the cellulase activities in R1, R2 and R3 were statistically higher than those in R4, while the digestate of R4 showed a similar cellulase activity as the reference-CSTR (Fig. 5d). The observed higher hydrolytic enzyme activities in the cascade AD system, compared to those of the reference-CSTR, could be attributed to the imposed high OLRs (corresponding to short SRTs) in reactors R1, R2 and R3. Following first order reaction kinetics (Eq. (1)), the application of increased OLRs results in accelerated hydrolytic enzyme activities (Menzel et al., 2020; Xiao et al., 2017). Results showed that enzyme activities, especially the sludge-associated ones, in all reactors increased over three times when the total SRT was reduced from 22 to 12 days (Fig. 5). Notably, the increase in the enzyme activities in both systems exceeded the increase in the calculated specific hydrolysis rates in each reactor (Fig. 4). This mismatch strongly indicates that the actual solids hydrolysis in the cascade system was limited by the available free surface for enzymatic attack, rather than by the presence of sufficient hydrolytic conversion capacity.

A more detailed semi-quantitative analysis of amino peptidases and glycosyl-hydrolases in both free and sludge-associated fractions using API ZYM® strips, were carried out at the same moments as described above (Fig. 6). Similar to protease and cellulase activities, the activities of all hydrolases tested with this method increased at short SRTs, and showed a downward trend in activity from R1 to R4 of the cascade digester. Surprisingly, however, the β -glucuronidase, α -mannosidase and α -fucosidase activities increased stepwise along the cascade system, which indicates that the hydrolysis of target substrates of these enzymes occurs later in the process. The presence and the role of the target substrates, namely, glucuronic acid, mannose and fucose in the sludge matrix have been researched in several studies, showing that they act as main building blocks in the structural extracellular polymeric substances (SEPS) that form the gel-like structures of the sludge (Guo et al., 2020a). Regarding the degradation of SEPS in both digestion systems (Fig. S4 in Supplementary materials), results showed that SEPS were mostly

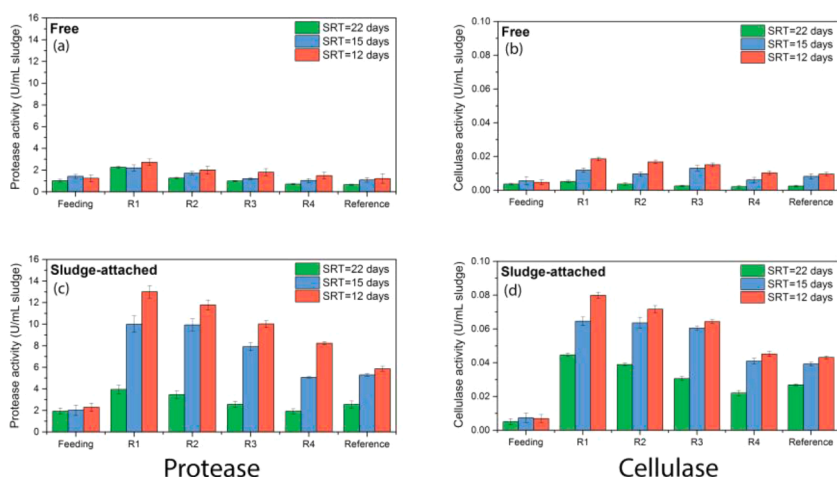


Fig. 5. Enzyme activity in U per mL of sludge from the feeding and each reactor. The TS concentration of the feeding was: 4.1–4.2 wt%, and of each individual reactor: 3.9–4.1, 3.7–4.0, 3.0–3.7, 2.8–3.0 and 3.1–3.3 wt% for R1, R2, R3, R4 and the reference-CSTR, respectively. (a) Free protease. (b) Free cellulase. (c) Sludge-associated protease. (d) Sludge-associated cellulase. Samples for each measurement were taken during stabilised performance at each operational period. Error bars refer to the standard deviation ($n = 6$).

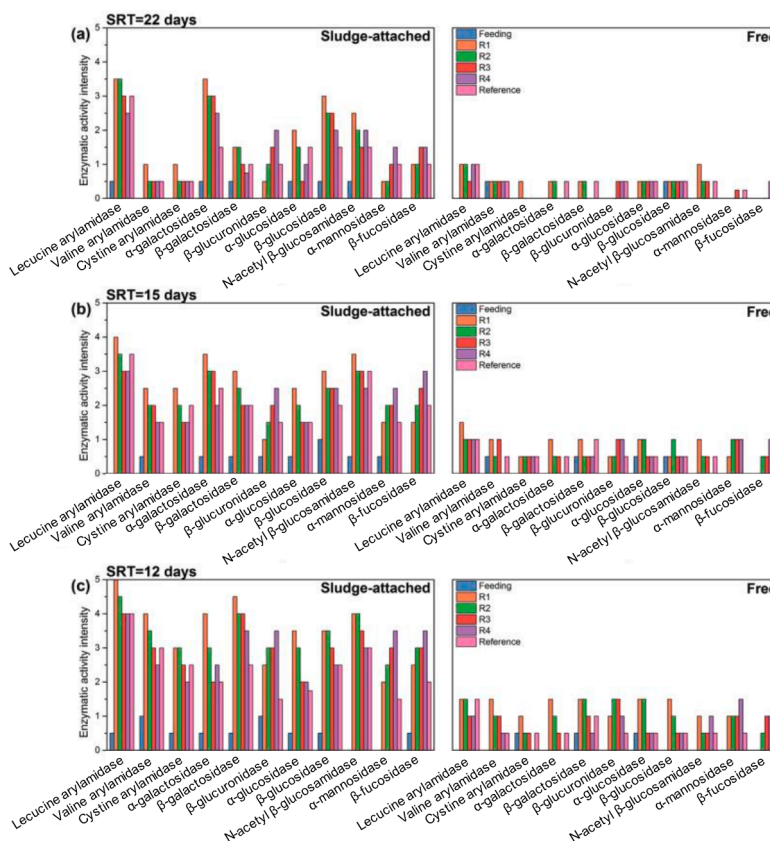


Fig. 6. Average ($n = 3$) enzyme intensity of specific amino peptidases and glycosyl-hydrolases in both cascade system and reference-CSTR, which were analysed using API ZYM® strips for sludge-attached and free enzymes collected at the end of (a) SRT = 22 days, (b) SRT = 15 days and (c) SRT = 12 days.

converted in R4, irrespective of changes in SRT, which was in line with the distributions of the β -glucuronidase, α -mannosidase and α -fucosidase activities. In addition, observations from the cascade system reveal that in the first reactors the more easily biodegradable (poly-)saccharides and (poly-)proteins were degraded, while in the remaining of the cascade system, the more refractory organic residuals in WAS, such as SEPS related saccharides, were degraded. As a consequence, the cascade system revealed a more stepwise and improved reduction of different

types of organics, which e.g. resulted in 14% more SEPS reduction at the total SRT of 22 days compared to the reference-CSTR. At the shortest tested SRT of 12 days, SEPS reduction was even 64% higher (Fig. S4 in Supplementary materials).

Pyrosequencing analysis of the microbial communities

Diversity indices

The results of Alpha diversity based on Shannon diversity were listed in Table S in Supplementary material. Substrate sample 1 & 2, and the inoculum had the highest and lowest values, respectively, meaning that the WAS substrate contained the most diverse bacterial communities, whereas the anaerobically grown inoculum had the least biodiversity. Shannon diversity decreased in both AD systems when operated at the total SRT of 22 days and slightly increased as the SRT was reduced. This indicates that the initial microbiome members that were present in the feed partially disappeared in the cascade AD process and thus, a narrowed AD community was eventually formed.

A microbial dynamic transition alongside with the cascade system from R1 to R4 could be clearly demonstrated by the Beta diversity described via PCoA based on the matrix distance between the samples (Fig. 7). In all operational conditions, R1, R2 and R3 were clustering closely to each other, while R4 was obviously separated from R1–3 and near the inoculum, revealing a different microbial composition presented in R4 compared to other reactors in the cascade system. The microbial structure of the reference-CSTR and the R1–3 was similar to that of WAS under the reduced SRTs, suggesting less cell decay of the fed WAS at this short SRT, which is possibly linked to the deterioration in tCOD reduction efficiency (Fig. 3a).

It should be noted that the applied cascade AD system was equipped with a digestate recirculation system operating at a recirculation ratio of 10%. It has been reported that recycling the digestate from a

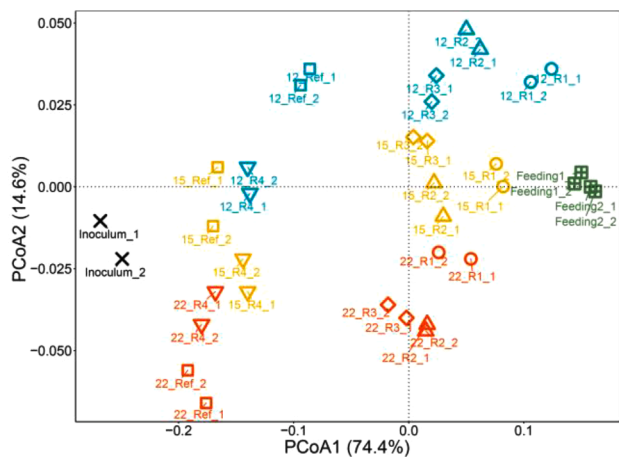


Fig. 7. PCoA analysis for the microbial community of feed sludge, inoculum and digestates from all reactors operated at the different SRTs. The samples analysed for PCoA were plotted in duplicates grouped by the same symbol and colour. Symbols in black and green represented the inoculum and the feed, respectively. Symbols in blue, yellow and red refer to the reactors operated at SRT of 12 days, 15 days and 22 days, respectively.

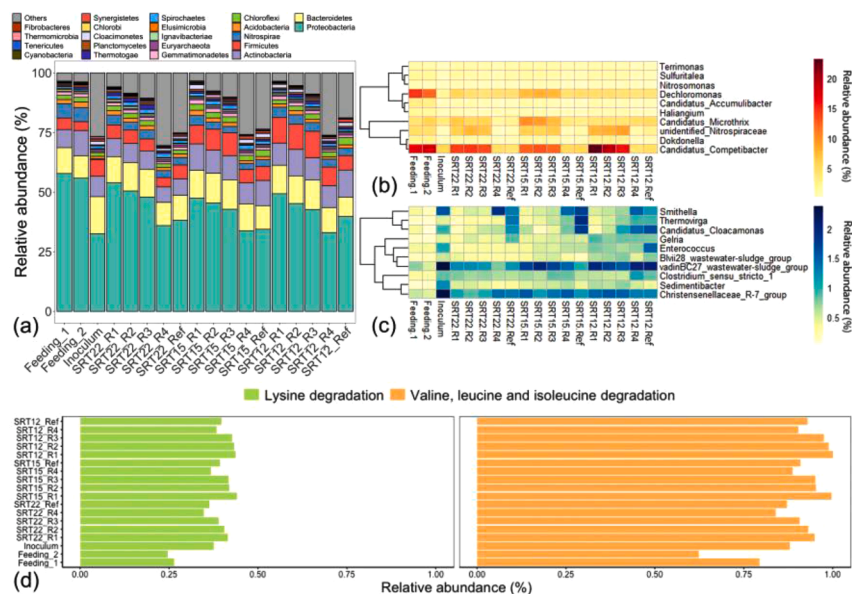


Fig. 8. (a) Species taxonomy of bacteria at the phylum level: the species, whose sums of percentage in all the samples are less than 1%, are classified as “the others”, (b) relative abundance of taxa related to feeding dominated bacteria of interest (top 10 species that presented in feeding), (c) anaerobic hydrolytic bacteria (top 10 species that appeared in all anaerobic reactors) at the genus level and (d) prediction of functional pathways related to amino acids degradation (average value, $n = 2$).

methanogenic reactor to an acidogenic reactor at a recycling ratio of 100% resulted in a changed and improved diversity of bacteria and archaea in the acidogenic reactor (Wu et al., 2016). Thus far, the effect of only 10% recycling is unknown. Nonetheless, in our present study, considerable methane production was observed in R1, R2 and R3 (Fig. 3b), which might be ascribed to the supplement of methanogens via digestate recirculation. However, based on the PCoA results, showing the clear microbial shift within the cascade system from R1 to R4 (Fig. 7), it seems that this impact of 10% recycling was limited.

Bacterial communities

The bacterial species taxonomy at phylum level is shown in Fig. 8a. Proteobacteria (55–60%), followed by Bacteroidetes (8–10%) and Actinobacteria (7–9%) were the most dominant phyla in the raw WAS, which is in line with previous studies (Westerholm et al., 2016). The changes in microbial composition between samples were most pronounced for Proteobacteria, because the total reduction in the relative abundance of this phylum was distinctly higher than for the other phyla in both cascade system and reference-CSTR. The relative abundance of the genus *Candidatus_Compitibacter* belonging to the phylum Proteobacteria was reduced by approximately 30% in R1, R2 and R3 together, while it was declined by 60% in the post digester (R4) of the cascade AD system. A similar observation was also found for other genera from this phylum, such as *Candidatus_Accumulibacter* related to phosphorus removal and *Dechloromonas* sp. for denitrification (Luo et al., 2020), even though the fractions in WAS were relatively low in this study (Fig. 8b). The results imply that the aforementioned dominant phyla largely disappeared due to cell decay in the AD process. Considering that 9–24% of WAS consists of microorganisms (Gonzalez et al., 2018), the released amount of intracellular organics due to endogenous decay of cells cannot be ignored in the cascade system and would become part of the tCOD that was available as substrate for the investigated hydrolytic enzymes (Fig. 5 and 6). Firmicutes were not predominant in the WAS, but clearly, the relative abundance of this phylum increased in R1, R2 and R3 to approximately 6.7% compared to 4.5% in the feed sludge at the total SRT of 22 days. Furthermore, the relative abundance of Firmicutes increased to 8.8% and 11.3% as the SRT reduced to 15 and 12 days, respectively. Firmicutes have been identified to hydrolyse and ferment large numbers of organic compounds under a variety of conditions in AD systems (Karthikeyan et al., 2016; Liu et al., 2019). The

increase in relative abundance of this type of species implies that the role of hydrolysis and acidogenesis processes in R1, R2 and R3 of the cascade system became increasingly more important as the SRTs decreased, in line as was reported by Zhang et al. (2019).

To relate the identified microbes to hydrolysis and acidogenesis of WAS in the cascade AD system under different operational conditions, the top 10 genera that governed the hydrolysis/acidogenesis of the organic compounds in both systems were selected and ranked by the relative abundance, while the changes in relative abundance were shown in Fig. 8c. Bacteria affiliated to genera *VadinBC27_wastewater-sludge_group*, *Clostridium_sensu_stricto_1*, *Enterococcus*, *Gelria*, *Bivl28_wastewater-sludge_group* and *Sedimentibacter* had significantly higher (p -value < 0.05) relative abundance in R1, R2 and R3 than in the reference-CSTR at the SRT of 22 days. This might have been due to the greater abundance of non-hydrolysed substrates that were present in R1, R2, and R3, since these genera have been frequently reported as the prevalent fermenters that were capable of hydrolysing protein or carbohydrate in AD (Kirkegaard et al., 2017; Liu et al., 2016; Wang et al., 2020). Possibly, the mentioned genera can be recognised as the main contributors to the enhanced hydrolysis rate in the cascade digester system. Moreover, lowering the total SRT of these reactors further increased the relative abundance of the aforementioned bacteria, which implies their higher metabolic activities in the degradation of WAS at higher loading rates. On the other hand, an upward trend in relative abundance of *Smithella*, *Candidatus_Cloacamonas* and *Thermovirga* was detected in the cascade system, especially in R1, R2 and R3, at the short SRTs. These recently characterized microorganisms might oxidize propionate and ferment sugars and amino acids to produce hydrogen and carbon dioxide, indicating that these species may possibly constitute acidifying and syntrophic associations (Stolze et al., 2015; Zamanzadeh et al., 2013). It should be noted that a small proportion of *VadinBC27_wastewater-sludge_group* and *Bivl28_wastewater-sludge_group* was also found in WAS. These strains directly might have contributed to the hydrolysis and degradation of WAS when they entered the cascade system. Moreover, because of their continuous seeding, they might have persisted as functional biomass in R1–3, where short SRTs were applied (Kim and Speece 2002). However, the exact role of the WAS-related cultures in the cascade system needs further studies.

Besides the investigation on the relative abundance of the functional bacteria, the microbial functional pathways including amino acid and

carbohydrates metabolisms in different experimental phases were also researched and the results were summarized in the Excel file, Supplementary materials. It was found that lysine degradation (Ko00310) as well as valine, leucine and isoleucine degradation (Ko00280) were the dominant pathways related to biomass conversion. The relative abundance of these metabolic pathways in the different reactors indeed increased when the reactor SRT dropped from 22 to 12 days. Moreover, they showed a similar trend as the activities of valine and leucine arylamidase that catalyse the hydrolysis of valine and leucine from peptide chains (Fig. 8d and Fig. 6). These findings suggest that applying a cascade system results in an enhanced microbial metabolism of hydrolytic/acidogenic bacteria that caused the observed acceleration in hydrolytic enzyme activity and subsequent enhanced sludge reduction compared to the reference-CSTR. Obtained results also illustrated the microbial complexity of WAS hydrolysis, which is difficult to capture in first-order hydrolysis kinetics, particularly under high loading conditions.

Methanogenic archaeal communities

As for the archaeal domain displayed in Fig. 9, *Methanobrevibacter* and *Methanosaeta* were equally dominant in the feed (around 28% each in relative abundance). In Phase-II, when the cascade system was operated at an SRT of 22 days, *Methanobrevibacter*, a hydrogenotrophic methanogen, was the most abundant methanogen in R1, but gradually became the minor species in favour of *Methanosaeta* that utilize acetate as the sole substrate from R2 to R4 (Maspolim et al., 2015c). This means a clear microbial shift from hydrogenotrophic methanogens towards acetoclastic methanogens alongside the cascade system. Also, at the low SRTs of 15 and 12 days in Phase-III and Phase-IV, the composition of methanogens in R1–4 followed a similar trend as in Phase-II, whereas the proportion of hydrogenotrophic methanogens was at a higher level. The predominance and importance of hydrogenotrophic methanogens in the acidogenic first stage reactors of phased AD systems have been described in literature. The very high OLR in the first stages of the cascade system resulted in a very high acidogenesis rate, with a concomitant high hydrogen and carbon dioxide production rate (Huang et al., 2015; Liu et al., 2019; Shimada et al., 2011; Zhang et al., 2019). The increased hydrogen/carbon dioxide flux in reactors R1–3 resulted in an increased yield of hydrogenotrophic methanogens, leading to an increase and eventual dominance of hydrogenotrophic methanogenic subpopulations. Considering the maximum growth rate (μ_{max}) of hydrogenotrophic methanogens in the range between 2.00–2.85 d^{-1} , which is around 3–9 folds that of *Methanosaeta* species (0.33–0.71 d^{-1}) (Batstone et al., 2002; Van Lier et al. 2020), and the very short SRTs of reactors R1–3, the microbial abundancy of hydrogenotrophic methanogens could outcompete the acetoclastic *Methanosaeta* species. In contrast, the applied SRT in R4 and the prevailing acetate flux resulted in a pre-dominance of *Methanosaeta* in the final reactor of the cascade. Notably, the acetate concentrations in R1, R2 and R3 were all significantly higher (p-value < 0.05) than the threshold (< 600 $\mu g/L$) for *Methanosaeta* survival (Klocke et al., 2008). Therefore, unlike the reference-CSTR and R4, methane production from hydrogen and carbon dioxide, rather than from acetate, was most likely the dominating methanogenic pathway in R1, R2 and R3.

It is noteworthy that sequences affiliated with *Methanospirillum* had promoted relative abundance in all digesters from the Phase-II to Phase-IV, which implies the importance of this methanogen in AD under high loading conditions. Recently, *Methanospirillum* has been found to play an important role in syntrophic propionate oxidation in phased anaerobic digestion (Maspolim et al., 2015c). As an increase in relative abundance was also observed for propionate oxidisers such as *Smithella*, the applied cascade system apparently provides proper conditions for attaining efficient syntrophic propionate conversion (de Bok et al. 2001).

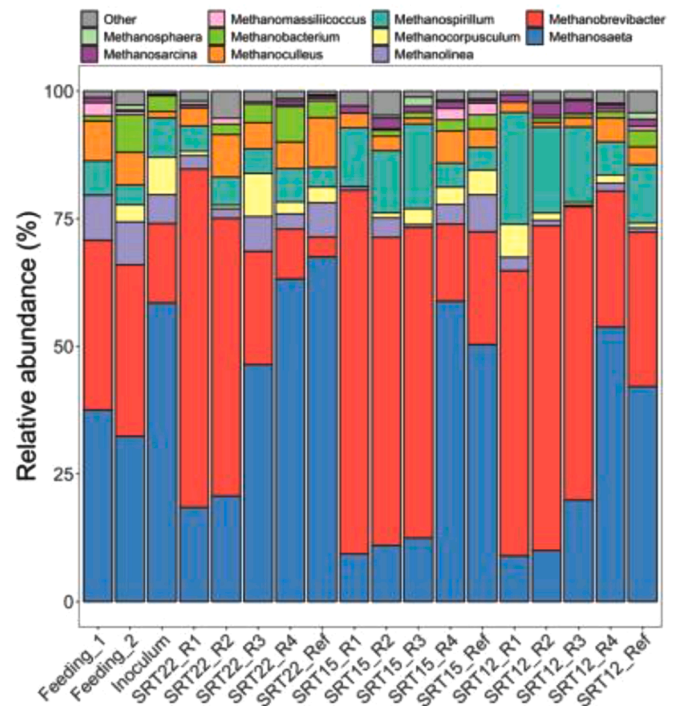


Fig. 9. Species taxonomy of methanogenic communities at the genus level. The species, whose sums of percentage in all the samples are less than 0.5%, are classified as “the others”.

Conclusions

The conclusions drawn from the current work can be summarized as follows:

1. AD in the cascade system led to 8% more tCOD reduction than the single stage CSTR digester, both operated at a total SRT of 22 days. Stepwise reduction of the total SRT from 22 to 12 days did not affect the tCOD removal efficiency for the cascade system, but showed a 29% decrease in the tCOD removal in the reference-CSTR. Maintaining stability at high organic loading rates in a cascade system denotes an enhanced sludge treatment capacity of 30–35%, compared to a conventional sludge digester of the same volume.
2. Normalised specific hydrolysis rates, resembling the first-order hydrolysis rate constant, differed per reactor and increased with decreasing SRTs. The highest increase by a factor of 2 was found in the individual reactors of the cascade system. Normalised hydrolysis increased by a factor 1.52 in the reference-CSTR.
3. Clear higher enzyme activities were found in the cascade system compared to the reference-CSTR, especially under short SRTs, which explains the overall accelerated specific hydrolysis rate in the cascade AD system. The overall hydrolytic enzyme activities increased with a factor up to 3 or even more, while this was a factor less than 2 for the specific hydrolysis rate, indicating that hydrolysis was limited by the solids-surface availability.
4. Several enzymes that target hydrolysis of SEPS-related organic compounds displayed reversed distribution and higher activity in the cascade system than in the reference-CSTR, indicating an additional degradation capacity of refractory compounds in the cascade system.
5. The increased relative abundance of key hydrolytic bacteria found in the first 3 reactors of the cascade system and the structural shift from hydrogenotrophic methanogens to acetoclastic methanogens alongside the cascade under low SRTs, demonstrated that cascading CSTRs possibly imposed selective pressures on the microbial

population, which contributed in achieving the enhanced enzymatic hydrolysis and sludge reduction.

Declaration of Competing Interest

The authors declare that they have no known competing financial interests or personal relationships that could have appeared to influence the work reported in this paper.

Acknowledgements

This research was funded by the Dutch Foundation for Applied Water Research (STOWA) and Royal HaskoningDHV B.V. (Amersfoort, The Netherlands) under project No. 432. 647. The study was also co-sponsored by L'Instrument Financier pour l'Environnement (LIFE) programme, Europe Union and Top Sector Energy subsidy, the Dutch Ministry of Economic Affairs. The authors would like to thank China Scholarship Council for the doctoral scholarship granted to the first author. Also, Nadia van Pelt (Delft University of Technology, The Netherlands) is specially acknowledged for her suggestion on English language usage.

Supplementary materials

Supplementary material associated with this article can be found, in the online version, at doi:[10.1016/j.watres.2021.117398](https://doi.org/10.1016/j.watres.2021.117398).

References

- Agabo-Garcia, C., Perez, M., Rodriguez-Morgado, B., Parrado, J., Solera, R., 2019. Biomethane production improvement by enzymatic pre-treatments and enhancers of sewage sludge anaerobic digestion. *Fuel* 255, 115713.
- APHA, 2005. Standard Methods for the Examination of Water and Wastewater, Twenty-First Ed. American Public Health Association, Washington, DC. USA.
- Appels, L., Baeyens, J., Degreve, J., Dewil, R., 2008. Principles and potential of the anaerobic digestion of waste-activated sludge. *Prog. Energy Combust. Sci.* 34 (6), 755–781.
- Athanasoulia, E., Melidis, P., Aivasidis, A., 2012. Optimization of biogas production from waste activated sludge through serial digestion. *Renew. Energy* 47, 147–151.
- Batstone, D.J., Keller, J., Angelidaki, I., Kalyuzhnyi, S.V., Pavlostathis, S.G., Rozzi, A., Sanders, W.T.M., Siegrist, H., Vavilin, V.A., 2002. The IWA anaerobic digestion model no 1 (ADM1). *Water Sci. Technol.* 45 (10), 65–73.
- Blumensaat, F., Keller, J., 2005. Modelling of two-stage anaerobic digestion using the IWA Anaerobic digestion model no. 1 (ADM1). *Water Res.* 39 (1), 171–183.
- Bonilla, S., Choolaei, Z., Meyer, T., Edwards, E.A., Yakunin, A.F., Allen, D.G., 2018. Evaluating the effect of enzymatic pretreatment on the anaerobic digestibility of pulp and paper biosludge. *Biotechnol. Rep.* 17, 77–85.
- de Bok, F.A., Stams, A.J., Dijkema, C., Boone, D.R., 2001. Pathway of propionate oxidation by a syntrophic culture of *Smithella propionica* and *Methanospirillum hungatei*. *Appl. Environ. Microbiol.* 67 (4), 1800–1804.
- De la Rubia, M.A., Riaú, V., Raposo, F., Borja, R., 2013. Thermophilic anaerobic digestion of sewage sludge: focus on the influence of the start-up. A review. *Crit. Rev. Biotechnol.* 33 (4), 448–460.
- Franke-Whittle, L.H., Walter, A., Ebner, C., Insam, H., 2014. Investigation into the effect of high concentrations of volatile fatty acids in anaerobic digestion on methanogenic communities. *Waste Manag. (Oxf.)* 34 (11), 2080–2089.
- Ge, H., Jensen, P.D., Batstone, D.J., 2011a. Relative kinetics of anaerobic digestion under thermophilic and mesophilic conditions. *Water Sci. Technol.* 64 (4), 848–853.
- Ge, H.Q., Jensen, P.D., Batstone, D.J., 2011b. Temperature phased anaerobic digestion increases apparent hydrolysis rate for waste activated sludge. *Water Res.* 45 (4), 1597–1606.
- Gonzalez, A., Hendriks, A., van Lier, J.B., de Kreuk, M., 2018. Pre-treatments to enhance the biodegradability of waste activated sludge: elucidating the rate limiting step. *Biotechnol. Adv.* 36 (5), 1434–1469.
- Guo, H., Felz, S., Lin, Y., van Lier, J.B., de Kreuk, M., 2020a. Structural extracellular polymeric substances determine the difference in digestibility between waste activated sludge and aerobic granules. *Water Res.*, 115924.
- Guo, H., van Lier, J.B., de Kreuk, M.J.W.R., 2020b. Digestibility of waste aerobic granular sludge from a full-scale municipal wastewater treatment system. *Water Res.* 173, 115617.
- Huang, W.H., Wang, Z.Y., Zhou, Y., Ng, W.J., 2015. The role of hydrogenotrophic methanogens in an acidogenic reactor. *Chemosphere* 140, 40–46.
- Karthikeyan, O.P., Selvam, A., Wong, J.W.C., 2016. Hydrolysis-acidogenesis of food waste in solid-liquid-separating continuous stirred tank reactor (SLS-CSTR) for volatile organic acid production. *Bioresour. Technol.* 200, 366–373.
- Kim, H.W., Nam, J.Y., Kang, S.T., Kim, D.H., Jung, K.W., Shin, H.S., 2012. Hydrolytic activities of extracellular enzymes in thermophilic and mesophilic anaerobic sequencing-batch reactors treating organic fractions of municipal solid wastes. *Bioresour. Technol.* 110, 130–134.
- Kim, M., Gomec, C.Y., Ahn, Y., Speece, R., 2003. Hydrolysis and acidogenesis of particulate organic material in mesophilic and thermophilic anaerobic digestion. *J. Environ. Technol.* 24 (9), 1183–1190.
- Kim, M., Speece, R.E., 2002. Aerobic waste activated sludge (WAS) for start-up seed of mesophilic and thermophilic anaerobic digestion. *Water Res.* 36 (15), 3860–3866.
- Kirkegaard, R.H., McLroy, S.J., Kristensen, J.M., Nierychlo, M., Karst, S.M., Dueholm, M. S., Albertsen, M., Nielsen, P.H., 2017. The impact of immigration on microbial community composition in full-scale anaerobic digesters. *Sci. Rep.* 7 (1), 9343.
- Klocke, M., Nettmann, E., Bergmann, I., Mundt, K., Souidi, K., Mumme, J., Linke, B., 2008. Characterization of the methanogenic Archaea within two-phase biogas reactor systems operated with plant biomass. *Syst. Appl. Microbiol.* 31 (3), 190–205.
- Levenspiel, O., 2006. Chemical Reaction Engineering, 3rd Ed. Wiley India Pvt. Limited.
- Liu, H.B., Wang, Y.Y., Yin, B., Zhu, Y.F., Fu, B., Liu, H., 2016. Improving volatile fatty acid yield from sludge anaerobic fermentation through self-forming dynamic membrane separation. *Bioresour. Technol.* 218, 92–100.
- Liu, X.Y., Li, R.Y., Ji, M., Han, L., 2013. Hydrogen and methane production by co-digestion of waste activated sludge and food waste in the two-stage fermentation process: substrate conversion and energy yield. *Bioresour. Technol.* 146, 317–323.
- Liu, Y., Wachemo, A.C., Yuan, H.R., Li, X.J., 2019. Anaerobic digestion performance and microbial community structure of corn stover in three-stage continuously stirred tank reactors. *Bioresour. Technol.* 287, 121339.
- Luo, K., Xie, X., Yang, Q., Chen, F., Zhong, Y., Xie, P., Wang, G., 2020. Multi-hydrolytic enzyme accumulation and microbial community structure of anaerobic co-digestion of food waste and waste-activated sludge. *Environ. Technol.* 41 (4), 478–487.
- Maspolim, Y., Zhou, Y., Guo, C., Xiao, K., Ng, W.J., 2015a. The effect of pH on solubilization of organic matter and microbial community structures in sludge fermentation. *Bioresour. Technol.* 190, 289–298.
- Maspolim, Y., Zhou, Y., Guo, C.H., Xiao, K.K., Ng, W.J., 2015b. Comparison of single-stage and two-phase anaerobic sludge digestion systems - performance and microbial community dynamics. *Chemosphere* 140, 54–62.
- Maspolim, Y., Zhou, Y., Guo, C.H., Xiao, K.K., Ng, W.J., 2015c. Determination of the archaeal and bacterial communities in two-phase and single-stage anaerobic systems by 454 pyrosequencing. *J. Environ. Sci. China* 36, 121–129.
- Menzel, T., Neubauer, P., Junne, S., 2020. Role of microbial hydrolysis in anaerobic digestion. *Energies* 13 (21), 5555.
- Miron, Y., Zeeman, G., Van Lier, J.B., Lettinga, G., 2000. The role of sludge retention time in the hydrolysis and acidification of lipids, carbohydrates and proteins during digestion of primary sludge in CSTR systems. *Water Res.* 34 (5), 1705–1713.
- Miyawaki, A., Taira, S., Shiraiishi, F., 2016. Performance of continuous stirred-tank reactors connected in series as a photocatalytic reactor system. *Chem. Eng. J.* 286, 594–601.
- Parawira, W., Murto, M., Read, J.S., Mattiasson, B., 2005. Profile of hydrolases and biogas production during two-stage mesophilic anaerobic digestion of solid potato waste. *Process Biochem.* 40 (9), 2945–2952.
- Qin, Y., Wu, J., Xiao, B.Y., Cong, M., Hojo, T., Cheng, J., Li, Y.Y., 2019. Strategy of adjusting recirculation ratio for biohythane production via recirculated temperature-phased anaerobic digestion of food waste. *Energy* 179, 1235–1245.
- Rorat, A., Courtois, P., Vandenbulcke, F., Lemiere, S., 2019. Industrial and Municipal Sludge. Elsevier, pp. 155–180.
- Shimada, T., Morgenroth, E., Tandukar, M., Pavlostathis, S.G., Smith, A., Raskin, L., Kilian, R.E., 2011. Syntrophic acetate oxidation in two-phase (acid-methane) anaerobic digesters. *Water Sci. Technol.* 64 (9), 1812–1820.
- Stolze, Y., Zakrzewski, M., Maus, I., Eikmeyer, F., Jaenicke, S., Rottmann, N., Siebner, C., Puhler, A., Schluter, A., 2015. Comparative metagenomics of biogas-producing microbial communities from production-scale biogas plants operating under wet or dry fermentation conditions. *Biotechnol. Biofuels* 8 (1), 1–18.
- Van Lier, J.B., Mahmoud, N., Zeeman, G., 2020. Anaerobic Wastewater Treatment Biological Wastewater Treatment: Principles, Modelling and Design, Second Edition. IWA Publishing, London, UK, pp. 701–756. Chapter 16.
- Vavilin, V.A., Fernandez, B., Palatsi, J., Flotats, X., 2008. Hydrolysis kinetics in anaerobic degradation of particulate organic material: an overview. *Waste Manag. (Oxf.)* 28 (6), 939–951.
- Wang, H., Li, J., Zhao, Y., Xu, C., Zhang, K., Li, J., Yan, L., Gu, J.D., Wei, D., Wang, W., 2020. Establishing practical strategies to run high loading corn stover anaerobic digestion: methane production performance and microbial responses. *Bioresour. Technol.* 310, 123364.
- Wang, Y., Zhang, Y., Wang, J., Meng, L., 2009. Effects of volatile fatty acid concentrations on methane yield and methanogenic bacteria. *Biomass Bioenergy* 33 (5), 848–853.
- Westerholm, M., Crauwels, S., Van Geel, M., Dewil, R., Lievens, B., Appels, L., 2016. Microwave and ultrasound pre-treatments influence microbial community structure and digester performance in anaerobic digestion of waste activated sludge. *Appl. Microbiol. Biotechnol.* 100 (12), 5339–5352.
- Wu, L.J., Higashimori, A., Qin, Y., Hojo, T., Kubota, K., Li, Y.Y., 2016. Upgrading of mesophilic anaerobic digestion of waste activated sludge by thermophilic pre-fermentation and recycle: process performance and microbial community analysis. *Fuel* 169, 7–14.
- Wu, L.J., Qin, Y., Hojo, T., Li, Y.Y., 2015. Upgrading of anaerobic digestion of waste activated sludge by temperature-phased process with recycle. *Energy* 87, 381–389.
- Xiao, X., Shi, W., Huang, Z., Ruan, W., Miao, H., Ren, H., Zhao, M.J.I.B., 2017. Process stability and microbial response of anaerobic membrane bioreactor treating high-strength kitchen waste slurry under different organic loading rates. *Biodegradation* 121, 35–43.

- Yang, Q., Luo, K., Li, X., Wang, D., Zheng, W., Zeng, G., J., Liu, 2010. Enhanced efficiency of biological excess sludge hydrolysis under anaerobic digestion by additional enzymes. *Bioresour. Technol.* 101 (9), 2924–2930.
- Yasui, H., Goel, R., Li, Y., Noike, T., 2008. Modified ADM1 structure for modelling municipal primary sludge hydrolysis. *Water Res.* 42 (1–2), 249–259.
- Zamanzadeh, M., Parker, W.J., Verastegui, Y., Neufeld, J.D., 2013. Biokinetics and bacterial communities of propionate oxidizing bacteria in phased anaerobic sludge digestion systems. *Water Res.* 47 (4), 1558–1569.
- Zhang, B., He, P.J., Lu, F., Shao, L.M., Wang, P., 2007. Extracellular enzyme activities during regulated hydrolysis of high-solid organic wastes. *Water Res.* 41 (19), 4468–4478.
- Zhang, L., Loh, K.C., Zhang, J.X., Mao, L.W., Tong, Y.W., Wang, C.H., Dai, Y.J., 2019. Three-stage anaerobic co-digestion of food waste and waste activated sludge: identifying bacterial and methanogenic archaeal communities and their correlations with performance parameters. *Bioresour. Technol.* 285.
- Zhen, G.Y., Lu, X.Q., Kato, H., Zhao, Y.C., Li, Y.Y., 2017. Overview of pretreatment strategies for enhancing sewage sludge disintegration and subsequent anaerobic digestion: current advances, full-scale application and future perspectives. *Renew. Sustain. Energy Rev.* 69, 559–577.
- Zhou, H.D., Lv, S.F., Ying, Z.X., Wang, Y.Y., Liu, J.C., Liu, W.D., 2019. Characteristics of two-phase mesophilic anaerobic digestion of co-substrates consisting of waste activated sludge and corn silage based on modified ADM1. *Waste Manag. (Oxf.)* 91, 168–178.